Hypoxia-Inducible Factor -1 contributes to transcriptional regulation of Bcl2-adenovirus E1B 19KDa -interacting protein in hypoxic cortical neurons

By

Samira Atoui

A Thesis submitted to the Faculty of Graduate Studies of

The University of Manitoba

in partial fulfilment of the requirements for the degree of

MASTER OF SCIENCE

Department of Pharmacology and Therapeutics

Faculty of Medicine

University of Manitoba

This thesis is dedicated to my beloved family, especially my father Samir Atoui and my mother Ibtissam Wizani, and to the memory of my grand-father Amine Wizani.

Mom and dad, thank you for all the love, care, and support you have given me throughout my entire life.

Grandpa, it has already been 16 months since you have passed away. I miss you so much. You have always been an inspiration for me. Seeing you suffering from the long term disabilities of stroke and dying from stroke was the key for my interest and success in this thesis project. May your soul rest in peace.

Abstract

PARP-1 has been identified as a major player in apoptotic pathways. Its excessive activation causes mitochondrial dysfunction, permeability, and AIF mitochondrion-to-nucleus translocation. It has been suggested that PARP-1 interacts indirectly with Bnip3, a mitochondrial pro-apoptotic factor. However, the mechanistic linkage is still not well understood. Our lab has shown that cytosolic/nuclear NAD^+ depletion is a hallmark for PARP-1 over activation and inhibition of sirtuin activity. Specifically in my project, we think that PARP-1 induced- NAD^+ depletion and sirtuin inhibition causes hyperacetylation of the α subunit of the transcription factor HIF-1 allowing increased HIF-1 binding to Bnip3 upstream promoter, and increased Bnip3 expression. Indeed, our PARP-1 Knock out neurons, MNNG and PJ34 treatment, chromatin immunoprecipitation, and HIF-1α loss of function studies strongly confirmed the necessity of HIF-1 to increase Bnip3 expression in hypoxia. Overall, our research suggests a role for HIF-1 in increasing PARP-1 dependent Bnip3 expression in hypoxic models.

Acknowledgments

In the name of **Allah**, most Gracious, most Compassionate.

I would like to extend my deepest gratitude, and special thanks and appreciation to the following people who in one way or another have contributed to make this thesis a reality:

My graduate supervisor, Dr. Chris Anderson, for all the help, guidance, support, encouragement, and outstanding mentorship he has given me over the past 3 years. Thank you for giving me the opportunity to learn from you how to think and grow as a researcher and instructor.

My thesis committee members, Dr. Grant Hatch and Dr. Jiming Kong, and the ex officio member Dr. Paul Fernyhough, for their thoughtful ideas, and invaluable feedback and support on this project.

The Chris Anderson lab group including Dr. June Shao, Dr. Ping Lu, **Dr. Lingling Lu, and Adam Hogan-Cann**. Thank you for making the lab a peaceful place to work at. **Dr. Ping Lu**, special thanks to you for all the guidance and invaluable assistance you have given me.

My mom Ibtissam Wizani, my dad Samir Atoui, and my brothers Rida and Sami Atoui, for their constant care, love, support, and encouragement that strengthened me during tough times.

All other pharmacology students and faculty who offered me their assistance whenever needed and who made the lab environment more enjoyable to work at.

I have also been fortunate to receive financial support over the course of my studies, and I would like to thank:

- Research Manitoba
- University of Manitoba, including the
    - Faculty of Graduate Studies of Faculty of Medicine
    - Department of Pharmacology & Therapeutics

Table of Contents

List of figures

List of Abbreviations

AIF – apoptosis inducing factor

Akt – protein kinase B

AMD – auto-modification domain

AMPA – α-amino-3-hydroxy-5-methyl-4-isoxazolepropionic acid

AMPAR – α-amino-3-hydroxy-5-methyl-4-isoxazolepropionic acid receptor

AP – apurinic/apyrimidinic

APAF-1 – apoptotic Peptidase Activating Factor 1

APC/C – anaphase-promoting complex / cyclosome

APE1 – apurininc/apyrimidinic endonuclease 1

ATP – adenosine triphosphate

Bad – Bcl-2-associated death promoter

Bax – Bcl-2-associated X protein

BCA – binchoninic acid

BER – base excision repair

Bid – BH3 interacting-domain

Bnip3 – BCL2/adenovirus E1B 19 kd-interacting protein 3

BRCT – BRCA1 C terminus

Ca^{2+} - calcium ion

CAD – caspase activated DNase

CAKβ – calcium-sensitive tyrosine kinase β

CAMKII – Ca^{2+}/calmodulin-dependent protein kinase II

cAMP – cyclic adenosine monophosphate

CBF – cerebral blood flow

Cdc42 – cell division control protein 42

CHD4 – chromatin helicase DNA binding protein 4

CHIP – chromatin immunoprecipitation

CNS – central nervous system

CREB – cAMP response element-binding protein

Cyt *c* – cytochrome *c*

Cx43 – connexin 43

DAG – diacylglycerol

DAPK1 – death-associated protein kinase 1

DBD – DNA-binding domain

DIV – day *in vitro*

DNA – Deoxyribonucleic acid

DNA-PK – DNA dependent protein kinase

Drp – deoxyribosephosphate

DSB – double strand break

DSC – death signal complex

DSI – depolarization-induced suppression of inhibition

EAAC1 – excitatory amino-acid carrier 1

EDTA – ethylenediaminetetraacetic acid

Endo G – endonuclease G

EPSP – excitatory postsynaptic potential

ER – endoplasmic reticulum

FAD – flavin adenine dinucleotide

FBS – fetal bovine serum

FOXO – forkhead box O

GABA – gamma-aminobutyric acid

GAPDH – glyceraldehydes-3-phosphate dehydrogenase

GFP – green fluorescence protein

GLAST – glutamate aspartate transporter

GLT-1 – glutamate transporter 1

GluR-(1-4) – glutamate receptor (1-4)

HDAC – histone deacetylase

HIF – hypoxia inducible factor

H_2O_2 – hydrogen peroxide

HPLC – high-performance liquid chromatography

HR – homologous recombination

HRE – hypoxia response element

IAP – inhibitor-of-apoptosis protein

IP_3 – inositol triphosphate

IP_3R – inositol triphosphate receptor

IRAP – insulin-responsive aminopeptidase

JNK – c-Jun N-terminal kinase

K^+ - potassium ion

LTD – long term depression

LTP – long term potentiation

mART – mono(ADP-ribose) transferase

Mg^{2+} - magnesium ion

mGluR – metabotropic glutamate receptor

MKK3 – mitogen-activated protein kinase kinase 3

MNNG – methylnitronitrosoguanidine

MOI – multiplicity of infection

MOMP – mitochondrial outer membrane permeability

MPT – mitochondrial permeability transition

mPTP – mitochondrial permeability transition pore

MPTP – 1-methyl-4-phenyl-1,2,3,6-tetrahydropyridine

mRNA – messenger RNA

Mre11 – Meiotic Recombination 11

MSG – monosodium glutamate

MST1 – macrophage stimulating 1

MTEP – 3-[(2-methyl-1,3-thiazol-4-yl)ethynyl]pyridine

mTOR – mechanistic target of rapamycin

Na^{+} - sodium ion

NaCl – sodium chloride

NAD^{+} / NADH – nicotinamide adenine dinucleotide

NAF – sodium fluoride

NAM – nicotinamide

NMDA – N-methyl-D-aspartate

NMDAR – N-methyl-D-aspartate receptor

NO – nitric oxide

NOS – nitric oxide synthase

nNOS – neuronal nitric oxide synthase

NOS1AP – nitric oxide synthase 1 adaptor protein

NR1 – N-methyl-D-aspartate receptor 1

NR2 (A-D) – N-methyl-D-aspartate receptor 2 (A-D)

NR3 – N-methyl-D-aspartate receptor 3

$O^{\cdot -}_2$ – superoxide free radical

O_2 – oxygen

$ONOO^-$ - peroxynitrite free radical

PAR – ADP-ribose polymer

PARG – poly(ADP-ribose) glycohydrolase

PARP – poly(ADP-ribose) polymerase

PBM – PAR-mediated binding linear motifs

PBS – phosphate-buffered saline

P38 –38-kDa protein

P38MAPK – p38 mitogen-activated protein kinase

P53 – tumor protein 53

PcG – polycomb group

PCR – polymerase chain reaction

PHD – prolyl hydroxylase

PIP_2 – phosphatidylinositol biphosphate

PJ34 – *N*-(6-oxo-5, 6-dihydrophenanthridin-2-yl)-*N*, *N*-dimethylacetamide HCl

PKC – protein kinase C

PLC – phospholipase C

PSD-95 – postsynaptic density protein-95

PTP – permeability transition pore

PUMA – p53 upregulated modulator of apoptosis

PVDF – polyvinylidene fluoride

Q – glutamine residue

R – arginine residue

rCBF – regional cerebral blood flow

RIPA – radioimmunoprecipitation assay

RNA – ribonucleic acid

ROS – reactive oxygen species

RT-PCR – real time PCR

SDS – sodium dodecyl sulfate

SEM – standard error of the mean

SER – smooth endoplasmic reticulum

shRNA – small hairpin RNA

Sir – silent information regulator

Sirt – sirtuin

SLC – solute carrier

SSBR – single strand break repair

SSC – synaptic survival complex

t-Bid – truncated BH3 interacting-domain

TBS – tris-buffered saline

TBST – tris-buffered saline with tween 20

TCA – tricarboxylic acid

TCDD - 2,3,7,8-Tetrachlorodibenzo-*p*-dioxin

TRF – telomere repeat factor

TSA – trichostatin A

VRAC – volume regulated anion channel

XIAP – X-linked inhibitor of apoptosis protein

XRCC1 – X-ray repair cross-complementing protein 1

Chapter 1: Introduction

1.0 Stroke

Stroke is the fourth leading cause of death in North America (McIntosh, 2016), the major cause of acute hospitalization in the United States (Fang and Alderman, 2001), and leads to serious long term disabilities in many cases that are not fatal (Rothwell, 2001). Stroke threatens all ages but dominantly affects those above the age of 50 years due to development of many age-related risk factors over the course of life (Suwanwela and Koroshetz, 2007). Although age is the primary risk factor for stroke, there are also many risk factors such as smoking, hypertension, diabetes, obesity and others that result from unhealthy lifestyle choices or poverty. Fixed risk factors include gender, race, ethnicity, and heredity (Allen and Bayraktutan, 2008). Men are more predisposed to experience a stroke than women, with 19% greater risk under the age of 65 (Holroyd-Leduc et al., 2000). In contrast, women are more likely to die from stroke than men. All reasons for this are not known but could include longer time to treatment after stroke symptoms or longer life expectancy of women (Persky et al., 2010). Prevalence of stroke is 4.0% in non-Hispanic blacks or African Americans, 2.6% in Hispanics, 6% among American Indians, and 2.3% among non-Hispanic whites (Cruz-Flores et al., 2011). This racial difference is mostly relevant to younger adults and seems to decrease with age. Similarly, the risk of death from stroke is higher in non-whites than in whites and is greatest in non-Hispanic blacks or African Americans. It is not clear yet whether these differences are due to genetic variations or environmental differences, but it is very likely to be a combination (Cruz-Flores et al., 2011).

Types of stroke

Stroke causes brain tissue death resulting from disturbances in cerebral blood flow (CBF) and subsequent neurotoxic signaling cascades. CBF disturbances can be caused by rupture of blood vessels (haemorrhage) or by interruption of blood flow after narrowing or blockage of a blood supply vessel (ischemia). Ischemic strokes are more common and account for more than 80% of stroke cases (Peralta-Leal et al., 2009). Cells that are normally nourished by affected vessels become deficient in glucose and oxygen, reducing glycolysis and oxidative phosphorylation. ATP depletion results, inhibiting energy-requiring cellular processes, degrading normal transmembrane ion gradients, and leading to depolarization-induced release of excitatory amino acids, intracellular Ca^{2+} accumulation, and increased oxidative stress (Besancon et al., 2008). All together, these factors produce a deleterious cascade of events that lead to neuron death and cerebral tissue loss (infarction).

Ischemic stroke

Ischemic stroke results from occlusion of large arteries supplying the brain or smaller regional intracerebral arteries, and can occur in two ways. Thrombotic ischemic stroke occurs when cholesterol-rich plaques attach to the inner arterial walls to narrow or block the artery. Embolic stroke results when an embolus travels to the brain through the bloodstream, where it occludes brain blood flow (Suwanwela and Koroshetz, 2007). Ischemic stroke produces 3 defined areas of cellular metabolic deficits, dictated by the severity of nutrient loss: benign oligemia, penumbra, and core. In the region of benign oligemia, the occlusion causes a drop in perfusion pressure but does not alter brain tissue metabolic requirements or function. In this region, dilation of distal vasculature creates a low resistance path to attract CBF via a web of

neighbouring vessels known as leptomeningeal collaterals. This can maintain normal delivery flows back to the affected brain region (Suwanwela and Koroshetz, 2007). The penumbra is the outermost layer of cerebral tissue that experiences metabolic decline due to reduction of regional cerebral blood flow (rCBF) (25-50% of normal rCBF) (Lee et al., 2005b). Resulting ATP loss blocks synaptic activity, disrupting neuronal function. If blood flow is restored quickly (earlier than ~1 hour) after the onset of ischemia, penumbral tissue may be rescued. This is the theoretical basis behind most stroke neuroprotective therapeutic development. Recovery after reperfusion is time-dependent and must proceed as soon as possible in order to realize a reduction in infarct size. Reperfusion beyond 2-3 hours after ischemia is unlikely to be beneficial in rat models and may cause further harm by enhancing oxidative stress (Nagahiro et al., 1998). The stroke core is the innermost layer of dead tissue most severely affected by loss of blood flow (rCBF = 5-20% of normal rCBF) (Ginsberg, 2003). ATP declines to levels unable to meet cell requirements (Muir et al., 2006), leading to large-scale neuronal depolarization and toxic release of excitatory amino acid neurotransmitters. High extracellular concentrations of glutamate lead to intracellular Ca^{2+} overload, which triggers a cascade of molecular and biochemical events resulting in neuron death (Mark et al., 2001).

1.1 Glutamate

Glutamate is a non-essential proteinogenic amino acid first identified as the major excitatory neurotransmitter in 1960s (Curtis et al., 1960). Glutamate is normally stored in axon terminals and released at synapses to initiate an excitatory response. Under normal conditions, glutamate levels in the synapse are regulated by uptake in astrocytes via electrogenic ATP-dependent Na^{+}/glutamate co-transporters of the solute carrier (SLC) gene family (Palmer et al., 2003, Anderson and Swanson, 2000) including SLC1A1-3 encoding EAAC1, GLT-1, and

GLAST respectively (Hediger et al., 2013). These carriers are however inhibited by ATP-depletion, reducing glutamate clearance. They can also reverse direction with ischemic accumulation of intracellular Na^+ caused by Na^+/K^+ ATPase inhibition, resulting in large scale glutamate release. In addition, glutamate can egress from cells through large organic anion channels (VRACs) and connexin hemichannels (Cx43) activated in ischemia (Jiang et al., 2011, Orellana et al., 2009) (Sabirov and Okada, 2009), and can be exchanged for extracellular cysteine, further enhancing extracellular glutamate levels (Warr et al., 1999). Dramatically elevated extracellular glutamate levels are known to be a major contributor to neuron death in stroke by a process known as excitotoxicity. The excitotoxic effects of glutamate were first observed in 1950s when subcutaneous monosodium glutamate produced degeneration of the inner retinal layers (Lucas and Newhouse, 1957). The term "glutamate excitotoxicity" was later coined by J.W. Olney to describe brain lesions formed after subcutaneous injections of glutamate (Olney, 1969) or monosodium glutamate (MSG) in infant and adult mice (Jorgensen and Diemer, 1982). Glutamate excitotoxicity is dependent on activation of ionotropic glutamate receptors known as N-methyl-D-aspartate receptors (NMDARs). Competitive NMDAR antagonists reduce cortical edema (Steinberg et al., 1989) and infarct size (Steinberg et al., 1993, Steinberg et al., 1989, Chen et al., 1991, Roman et al., 1989) in pre-clinical animal focal ischemia models of stroke.

1.2 Glutamate Receptors

Glutamate activates 3 major families of receptors: (1) N-methyl-D-aspartate receptor (NMDAR), (2) AMPA/Kainate receptors, and (3) metabotropic glutamate receptors (mGluR). NMDA and AMPA/Kainate receptors are ionotropic, meaning that glutamate binding induces a conformational change to allow ion flow across the neuronal membrane; mGluRs are G-protein coupled receptors (Hara and Snyder, 2007).

NMDARs are heterotetrameric ligand-gated ion channels. All NMDA receptors possess two 938 amino acid NR1 subunits that have co-agonist binding sites for glycine or D-serine (Lau and Tymianski, 2010). The most extensively characterized NMDARs are neuronal, expressing two NR1 and two NR2 subunits containing glutamate binding sites. There are four NR2 subunits (NR2A-D). In neuronal NMDARs, NR2B is expressed mostly in extrasynaptic forebrain regions, whereas the NR2A subunit is mostly synaptic (Monyer et al., 1994, Steigerwald et al., 2000, Martel et al., 2009). The NR3 subunit has two isoforms: NR3A is expressed throughout the CNS in all areas of the isocortex, and parts of the amygdaloid nuclei, hippocampus, thalamus, hypothalamus, brainstem, and spinal cord neurons as well as in glia (Wong et al., 2002). NR3B is expressed primarily in motor neurons (Chatterton et al., 2002). NMDAR channels are blocked by magnesium ion (Mg^{2+}) at resting membrane potential. Therefore channel conductance requires not only glutamate binding but also membrane depolarization to displace Mg^{2+}. In normal neurotransmission, this depolarizing impulse is achieved when glutamate binds AMPA receptors (Blanke and VanDongen, 2009). Binding of two glutamate molecules allow extracellular Na^{+} influx sufficient to depolarize the neuronal membrane, facilitating displacement of Mg^{2+} from NMDAR channels. NMDA channels then allow influx of Na^{+} and Ca^{2+} and efflux of K^{+} (Lau and Tymianski, 2010) (Fig.1). Subsequent Ca^{2+} influx causes activation of many

Ca^{2+}-dependent enzymes that can either promote cell survival or cell death. In physiological conditions, NMDAR-induced Ca^{2+} influx regulates synaptic plasticity (k Zito, 2009) and memory function (Bliss and Collingridge, 1993). NMDARs mediate long term potentiation (LTP) and long term depression (LTD), which are processes that regulate the strength of synaptic transmission (Bliss and Collingridge, 1993) and may be responsible for learning and memory (Martin et al., 2000, Sanes and Lichtman, 1999). In addition to its role in synaptic plasticity, learning, and memory, NMDAR activity regulates brain development at the neuronal level by causing dendritic development mediated by the RhoGTPases, Rac and Cdc42, and inhibiting RhoA. Rac and Cdc42 are 2 small RhoGTPases that promote growth and refinement of dendritic arbors, and their orientation towards the barrel centre (Cline., 2009). In contrast, in pathological conditions characterized by dramatically elevated glutamate levels, including ischemia, NMDAR activity causes cell death.

Whether NMDARs contribute to cell death has been attributed to glutamate levels (Hardingham and Bading, 2003, Lipton and Kater, 1989), neuronal localization (extrasynaptic or synaptic) (Hardingham and Bading, 2010), and subunit composition. In normal conditions, extracellular glutamate is maintained at homeostatic levels by astrocytes, keeping NMDAR activity at physiologically low levels (Sabirov and Okada, 2009, Warr et al., 1999). In ischemic glutamate elevations, there is evidence of a dichotomous role of synaptic vs. extrasynaptic NMDARs. Synaptic NMDARs may be neuroprotective while extrasynaptic NMDARs may produce ischemic neuron death. In vitro, flow of equal concentrations of Ca^{2+} through synaptic and extrasynaptic hippocampal NMDARs induced different responses (Hardingham et al., 2002). Ca^{2+} flow through synaptic NMDARs induced expression of survival genes that promote mitochondrial health, anti-oxidant and anti-apoptotic effects (Zhang et al., 2007a, Zhang et al.,

2009). For example, synaptic NMDARs suppress the activity or expression of pro-apoptotic transcription factors, including *Puma* (Leveille et al., 2010), forkhead box O (FOXO) (Dick and Bading, 2010), and *p53* (Lau and Bading, 2009). In contrast, extrasynaptic NMDARs appear to contribute to cell death by shutting-off the neuroprotective CREB pathway (k Zito, 2009), activating FOXO (Dick and Bading, 2010), and activating calpains and the p38 stress pathway (Xu et al., 2009, Li et al., 2013). The NMDAR role in cell survival or cell death has also been defined based on differentiated NR2 subunit expression. NR2B-containing NMDARs are more likely to lead to neuron death, compared to those containing other NR2 subunits. The most popular explanation is the interaction of NR2B C terminus with the neuronal nitric oxide synthase (nNOS) via PDZ domain of the scaffolding protein PSD-95 (Sheng, 2001). nNOS generates nitric oxide (NO) to a level that is lower than the threshold for regulation of most NO targets, but which still contributes to cell dysfunction. More likely nNOS damages the cells via its interaction with nitric oxide synthase 1 adaptor protein (NOS1AP) which together form a complex with p38 mitogen-activated protein kinase (p38MAPK) activator, mitogen-activated protein kinase kinase 3 (MKK3), and activate the p38 stress pathway causing cell death (Li et al., 2013). Recently, Ca^{2+} flow though NR2B-containing NMDARs was reported to activate death-associated protein kinase 1 (DAPK1), a specific NMDAR "cell death signal" at extrasynaptic sites (Tu et al., 2010), suggesting not only a new mechanism of NMDAR-induced cell death, but also the possibility that NR2B-containing NMDARs are highly expressed at extrasynaptic sites. The autophosphrylated DAPK1 binds and phosphorylates NR2B to form a complex that recruits death signal complex (DSC) which in turn shuts off the neuronal synaptic survival complex (SSC) activity and causes neuronal death (Martin and Wang, 2010).

AMPA receptors are also heterotetrameric ligand-gated ion channels consisting of 4 subunits, GluR1-4, and only require glutamate binding for activation. They are located mostly on postsynaptic membranes (Castillo et al., 1997) but have also been found on presynaptic membranes (Chittajallu et al., 1996). Binding of two glutamate molecules allows extracellular Na^+ influx and intracellular K^+ efflux. AMPA receptors are also permeable to Ca^{2+} only if they contain GluR1, 3, or 4 subunits while the presence of GluR2 subunit removes calcium permeability (Burnashev et al., 1995). Hippocampal type I neurons (Iino et al., 1990) and neocortical layer V pyramidal neurons (Jonas et al., 1994) have low relative Ca^{2+} permeability associated with high relative abundance of GluR2 mRNA , thus more GluR2 – containing AMPARs. This low Ca^{2+} permeability of GluR2 is attributable to pre-mRNA stage RNA editing of glutamine (Q) residue with a positively charged arginine (R) residue in the pore forming segment and it affects at least 99% of GluR2 mRNA in embryonic, neonatal, and adult rat brain (Burnashev et al., 1992). Thereby, unlike NMDARs, Na^+ and K^+ are the main ions gated by AMPARs which might suggest the role of GluR2 containing AMPARs in protecting cells against excitotoxicity by prevention of calcium entry (Kim et al., 2001). By preventing Ca^{2+} entry into cells, Ca^{2+} -dependent CaMKII phosphorylation of AMPAR is inhibited, thus repressing upregulation of membranous AMPARs and inhibiting long lasting increase in excitatory postsynaptic potential (EPSP) size underlying LTP and single-channel conductance (Maren et al., 1993).

Kainate receptors are ligand-gated ion channels similar to AMPARs in that activation requires binding to two glutamate molecules. They are comprised of kainate receptor subunits GluR5-7 (Gluk1-3) and KA1-2 (Gluk 4-5). Kainate receptors are both localized in both presynaptic and postsynaptic membranes (Lau and Tymianski, 2010) where they are found to

play a role in synaptic plasticity (Mayer, 2005). Postsynaptically, they are excitatory, driving Na^+ influx and K^+ efflux, depolarizing neurons sufficiently to displace Mg^{2+} from NMDAR and mediate fast excitatory neurotransmission (Dingledine et al., 1999). Presynaptically, they partially regulate neurotransmitter release. At glutamatergic synapses, they were shown to drive excitotoxic glutamate release (Chittajallu et al., 1999).

mGluRs are single-peptide seven-transmembrane domain proteins linked to intracellular G proteins. They are classified into three main groups based on sequence homology and intracellular signal transduction pathways (Neugebauer, 2001). Group I includes mGluR 1 and 5, which are coupled to excitatory Gq proteins that activate phospholipase C to produce Inositol triphosphate (IP_3) and increase Ca^{2+} release from smooth endoplasmic reticulum (SER). Most of Group I mGluRs are located on postsynaptic membranes and act as ionotropic channels. Group II and III mGluRs are primarily located on presynaptic membranes, where they usually regulate neurotransmitter release (Alagarsamy et al., 1999). Group II and III mGluRs are coupled to Gi proteins and inhibit the activity of adenylyl cylcase, reducing cAMP levels (Bruno et al., 1995a). NMDAR and mGluR functional linkage has been reported, as Group I mGluR can be physically linked to the C-terminus of the NMDAR NR2B subunit by anchoring protein complexes such as Shank–GKAP–PSD-95 (Tu et al., 1999). This interaction allows NMDAR to dephosphorylate mGluR5 at sites responsible for protein kinase C (PKC)-dependent desensitization (Alagarsamy et al., 2002) and to potentiate mGluR5-mediated responses (Alagarsamy et al., 2005). Blocking mGluR5 with a nonselective mGluR antagonist LY341495; (Harney et al., 2006) and its antagonists 2-Methyl-6-(phenylethynyl)pyridine (MPEP) and 3-((2-Methyl-4-thiazolyl)ethynyl)pyridine (MTEP) abrogates NMDAR-mediated hippocampal LTP (Kwag and Paulsen, 2012) and LTD (Harney et al., 2006) without altering NMDAR function, suggesting

that NMDAR-induced LTP/LTD is influenced by mGluR5. There is evidence that mGluR5 activation facilitates LTP/LTD induction by potentiating NMDAR–mediated Ca^{2+} influx (Bruno et al., 1995b), where IP_3R- mediated Ca^{2+} release from intracellular stores stimulates PKC, and activates CAKβ, non-receptor tyrosine kinase to relieve autoinhibition of Src tyrosine kinases. The PKC/CAKβ/Src cascade enhances peak NMDA evoked currents and induces a long lasting enhancement of excitatory synaptic transmission (Kotecha et al., 2003). Whether it induces LTP or LTD depends on intracellular Ca^{2+} elevations evoked by either strong or weak membrane depolarization and Ca^{2+} influx. High intracellular Ca^{2+} elevations cause LTP while smaller Ca^{2+} elevations cause LTD (Artola and Singer, 1993, Lisman, 1989). More recent reports suggest that mGluR5 activation enhance depolarization-induced suppression of inhibition (DSI) and endocannabinoid release, reducing $GABA_A$ receptors-induced inhibition which facilitates the induction of NMDAR-LTP (Kwag and Paulsen, 2012). Whether or not NMDAR-induced LTP is mGluR5-dependent is however still debatable.

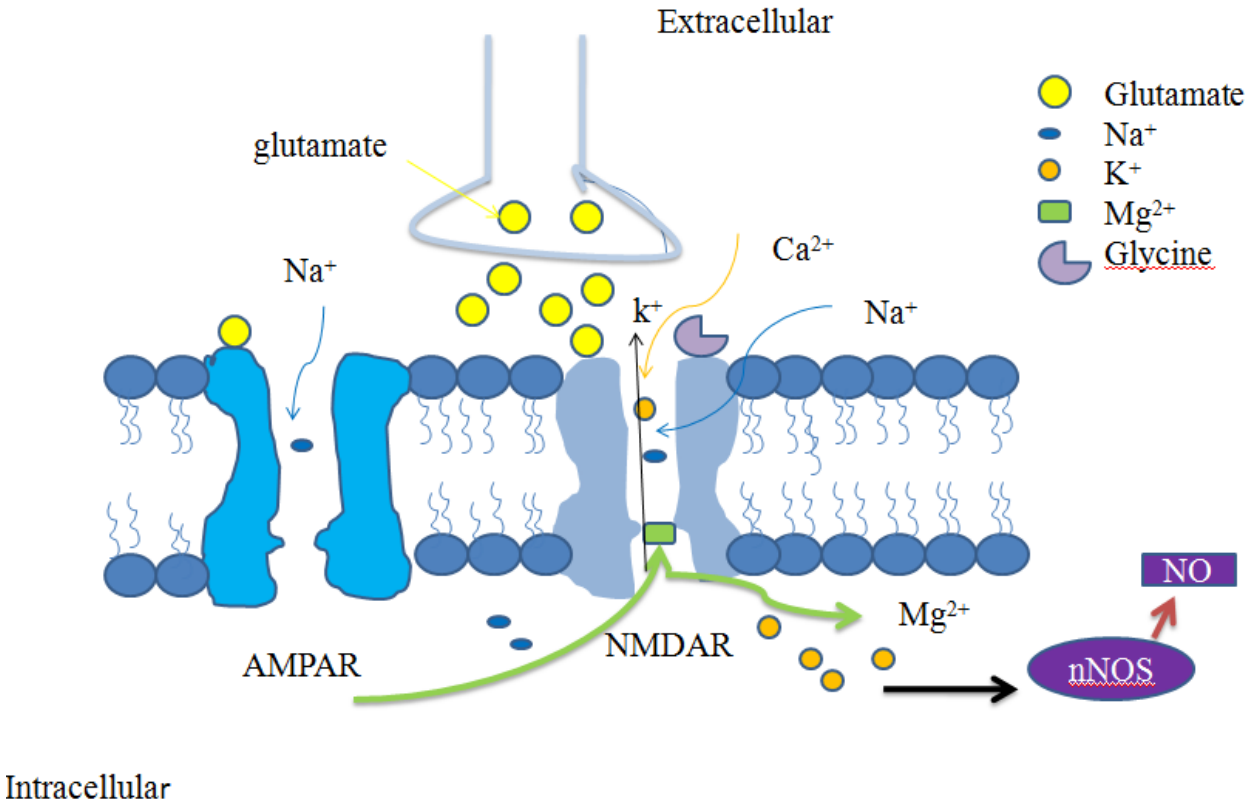

Figure 1: AMPAR and NMDAR cooperation to drive glutamate excitatory response.

Glutamate binding to AMPAR drives Na^+ influx triggering membrane depolarization that will help displacing Mg^{2+} from NMDAR intracellular site. Along with the removal of NMDAR blockade, the binding of the co-agonist glycine and the agonist glutamate to NMDAR drives the influx of Na^+ and Ca^{2+} as well as the efflux of K^+.

1.3 Glutamate excitotoxicity

Excitotoxicity refers to a process by which excessive extracellular excitatory neurotransmitter levels induce cell death in neurons (Olney et al., 1974). Neuron death in multiple ischemia/stroke models in vitro and in vivo results from glutamate excitotoxicity, in a manner reduced by pharmacological blockade of NMDAR (Choi, 1992). It is likely that excitotoxic NMDARs are extrasynaptic (Besancon et al., 2008) and contain the NR2B subunit (Kemp and McKernan, 2002), as selectively blocking NR2B in brain ischemia models with antagonists such as Ifenprodil and RO63-1908 resulted in neuroprotection (Hara and Snyder, 2007). NR2A is reported to promote cell survival, as the relatively NR2A-selective antagonist, NVP-AAM077, blocked cell survival mechanisms that act against apoptosis (Liu et al., 2007). Once activated by excitotoxic glutamate levels, NMDAR gates entry of excessive extracellular Ca^{2+}. ATP-dependent mechanisms normally active to keep Ca^{2+} low are inhibited by ATP depletion and thus intracellular Ca^{2+} accumulates (Thayer and Wang, 1995, Wang and Thayer, 1996). Overall, injury of cultured cortical neurons by glutamate can be considered in two temporal phases. First, AMPA, Kainate, and NMDA receptors cause increased Na^{+} influx and immediate neuronal swelling. Delayed cell degeneration follows, mediated by NMDA-receptor mediated influx of excessive Ca^{2+} (Choi, 1992).

1.3.1 Ca^{2+} as a mediator of glutamate excitotoxicity

To address how Ca^{2+} leads to cell death after its accumulation in the cell, two hypotheses have been suggested. The calcium overload hypothesis is that Ca^{2+} excitotoxicity results from intracellular Ca^{2+} exceeding a threshold level (Kawamata and Manfredi, 2010, Pivovarova et al., 2004). Alternatively there is a source-specificity hypothesis that contends that excitotoxicity

depends on the concentration of intracellular Ca^{2+} and its route of entry, coupled with the secondary messenger pathways it activates (Tymianski et al., 1993). The latter idea appears to be important as Ca^{2+} entry through NMDAR but not voltage-gated Ca^{2+} channels led to cell death in excitotoxicity from ischemia, trauma, and other neurological disorders models (Sattler and Tymianski, 2000). High levels of glutamate cause sustained activation of neuronal NMDA receptors, which cause increased Ca^{2+} influx. When NMDAR activation is intense enough to cause lethal accumulation of intracellular calcium, excitotoxicity will be triggered. If activation is insufficient, amplification is needed. This can be provided by release of Ca^{2+} from intracellular endoplasmic reticulum (ER) stores. Group I mGluR-mediated phospholipase C (PLC) activation cleaves membranous phosphatidylinositol bisphosphate (PIP_2) causing release of diacylglycerol (DAG) and IP_3. IP_3 binds to ER receptors (IP_3Rs) to liberate intracellular Ca^{2+} stores (Ozawa et al., 1998, Berridge, 1995). When lethal calcium overload is achieved, enzymes such as calpains, phospholipases, endonucleases, kinases, and caspases are activated, causing degradation of membrane lipids, DNA, and proteins (Lo et al., 2003). This can lead to necrotic cell death. There is also evidence that Ca^{2+}-dependent excitotoxicity leads to apoptotic cell death. Ca^{2+} release from the ER, Ca^{2+} influx through Ca^{2+} release-activated Ca^{2+}channels, and Ca^{2+} triggered activation of cell surface death receptors are all reportedly apoptogenic (Rizzuto and Pozzan, 2006). Whether cell death is by Ca^{2+} -dependent necrosis or apoptosis appears to depend on the intensity of glutamatergic activation. Severe excitotoxicity, as could occur in an ischemic core, for example, likely leads to necrosis. In contrast, when excitotoxicity is less severe (for example in the penumbra), neurons likely succumb by programmed cell death like apoptosis or autophagy (Yuan et al., 2003). High intracellular calcium concentrations and resulting free radicals can cause inner mitochondrial membrane permeabilization followed by outer membrane permeability

by activating mitochondrial permeability transition (MPT) pores (Sims and Muyderman, 2010). Ca^{2+} overload and ROS can also induce expression of pro-apoptotic proteins that belong to the Bcl-2 protein family including Bim, Bax, and Bad (Sims and Muyderman, 2010, Gao et al., 2005), which lead directly to mitochondrial outer membrane permeability (MOMP). MOMP facilitates release of pro-death factors from mitochondria, inducing caspase-dependent or caspase-independent apoptosis. Caspase-dependent apoptosis can be mediated by release of cytochrome *c* (cyt *c*). Cytosolic cyt *c* interacts with protein apoptotic peptidase activating factor-1 (Apaf-1) and dATP to form heptameric apoptosomes. Apoptosomes can then recruit, cleave, and activate the inactive pro-caspase-9 (Reubold et al., 2011). Initiator caspase 9 becomes active upon docking to the apoptosome which then cleaves and activates effector caspase 3 dimers (Mattson and Chan, 2003). Active caspase 3 is an executioner caspase that causes proteolysis of activating caspase activated DNase (CAD) which mediates oligonucleosomal DNA fragmentation (180-200 base pair DNA fragments) (Sims and Muyderman, 2010, Penninger and Kroemer, 2003). In addition, caspases are likely involved indirectly in enhanced MOMP. Caspase 8 can cleave BH3 interacting-domain death agonist, Bid, a member of the Bcl-2 protein family, into t-Bid, which translocates from the cytoplasm to mitochondria. t-Bid then increases release of mitochondrial apoptotic factors including cyt *c*, AIF and EndoG (Sims and Muyderman, 2010, Brustovetsky et al., 2003). Beside these players, it has been suggested that two intermembrane space proteins Smac/DIABLO and Omi/HtrA2 are able to induce caspase-dependent apoptosis by binding to and neutralizing the caspase inhibitor XIAP allowing amplified caspase activation (Martins et al., 2004, Okada et al., 2002, Jones et al., 2003). These 2 proteins bind to and block IAPs, a family of inhibitor-of-apoptosis proteins, preventing inhibitory effect on caspases 3, 7 and 9 (Sims and Muyderman, 2010). Under normal conditions, this

caspase-dependent apoptotic pathway regulates neuronal cell number during development and ensures proper connectivity between cells (Yuan et al., 2003). Under pathological conditions such as ischemic stroke, inhibition of these caspases has been shown to be neuro-protective (Cho and Toledo-Pereyra, 2008, Endres et al., 1998, Ma et al., 1998, Mouw et al., 2002).

Caspase-independent apoptosis is characterized by mitochondrial swelling and release of apoptosis inducing factor (AIF) and endonuclease G (Endo G) after MOMP and their translocation to nucleus where they induce chromatin condensation and large scale DNA fragmentation (Susin et al., 1999). Release of AIF has been found dependent on poly(ADP-ribose) polymerase -1 and inhibition of PARP activity blocked AIF mitochondrion-to-nucleus translocation (Hong SJ, 2000). (Will be discussed in details in section 1.4.5.1.)

1.3.2 ROS as mediators of glutamate excitotoxicity

Ca^{2+}-dependent neurotoxicity in ischemia is dominantly mediated by NMDA receptors (Zingarelli et al., 1996). NMDARs can be linked to N-terminus of nNOS via the scaffolding protein, PSD 95 (Rameau et al., 2003), and inhibition or deletion of nNOS limited NMDAR excitotoxicity, suggesting a key role for nitric oxide (NO) as well (Zhang et al., 1994, Zingarelli et al., 1996). NO can be destructive by reacting with superoxide free radical ($O^{\cdot -}_2$). Superoxide is normally formed by basal mitochondrial respiration and deactivated by superoxide dismutase into O_2 and hydrogen peroxide (H_2O_2). In glutamate excitotoxicity, mitochondrial permeability leads to enhanced cytoplasmic release of superoxide from mitochondria where it reacts with NO to form peroxynitrite ($ONOO^-$) free radicals (Zingarelli et al., 1996). Peroxynitrite causes enzyme inactivation by oxidation and nitration. Mitochondrial enzymes are vulnerable to this inactivation, leading to reduced ATP formation, opening of the permeability transition pore (PTP), and MOMP causing release of pro-death molecules, including cyt *c* and AIF (Pacher et

al., 2007). In turn, cyt *c* and AIF activate a series of downstream effectors that induce apoptotic cell death. In addition, peroxynitrite induces 8-hydroxyguanine (8-oxoG) residues mutations at G-C base pairs (Juedes and Wogan, 1996) resulting predominantly in single strand DNA breaks (Epe et al., 1996) which in turn activate the nuclear enzyme PARP-1 (Pacher and Szabo, 2008) causing a series of PARP-1-mediated events leading to cell death.

1.3.3 PARP-1 as a mediator of glutamate excitotoxicity

In addition to cerebral and cardiac ischemia, enormous PARP-1 activation is implicated in other pathological conditions such as 1-methyl-4-phenyl-1, 2, 3, 6-tetrahydropyridine-induced (MPTP) Parkinsonism, traumatic spinal cord injury, and streptozotocin-induced diabetes (Skaper, 2003). In ischemic stroke, $ONOO^-$ initiates a number of DNA base modifications (Pacher et al., 2007). In response to DNA damage, PARP-1 catalytic activity increases, enhancing the synthesis of target-bound ADP-ribose polymers (PARs) using nicotinamide adenine dinucleotide (NAD^+) as a substrate. This increases toxic PAR levels and depletes NAD^+ to critical levels, resulting in PARP-dependent neuron death (Kim et al., 2005).

1.4 PARP-1

The PARP family is a protein super family that consists of 18 putative proteins encoded by different genes (Ba and Garg, 2011). All have a conserved catalytic domain, but only PARP-1 and PARP-2 catalytic activity is DNA damage dependent (Ame et al., 2004). Members of this family have been classified in two different ways based on catalytic domain homology and enzymatic activity (Ba and Garg, 2011). The structural model classifies PARPs into 3 different classes (Lo et al., 2003): bona-fide PARPs 1-5 possess a conserved glutamate residue identified in PARP-1 and found to be important for PARP catalytic activity; the mono(ADP-ribose)

transferase (mART) PARPs 6-8, 10-12, and 14-16 have this catalytic glutamate replaced by isoleucine (Kleine et al., 2008). PARPs 9 and 13 lack the key NAD^+ binding residues and the catalytic glutamate residue (Krishnakumar and Kraus, 2010). PARPs are also classified by function: PARP-1 and PARP-2 are DNA-dependent poly(ADP-ribose) polymerases; Tankyrases 1 and 2, PARP-12, PARP-13 and tiPARP are zinc finger CCCH domain–containing PARPs; PARP-9/BAL1, PARP-14/BAL2, CoaSt6 and PARP-15 are macro poly(ADP-ribosyl) transferases; the functions of PARP-3, 4, and 10 are poorly understood (Schreiber et al., 2006). PARP-1 and PARP-2 are DNA-damage-dependent PARPs, likely induced in excitotoxic neuron death after oxidative DNA damage. They sense DNA breaks and help in spatial and temporal organization of DNA repair by poly(ADP-ribosyl)ating partner proteins in a process that normally regulates chromatin structure and DNA resynthesis (Schreiber et al., 2006). PARP-3 has been identified as a core component of the centrosome, where it interacts with PARP-1 to maintain centromeric heterochromatin integrity and centrosome function (Kanai et al., 2003). Mammalian vaults are eukaryotic organelles and large barrel-shaped complexes of ribonucleoproteins found in the cytoplasm and involved in intracellular transport. They consist of a small ribonucleic acid and three proteins of 100, 193, and 240 kDa in size. P193 has been identified as a new PARP protein and is known as VPARP or PARP4 (Kickhoefer et al., 1999). PARP-4 plays a role in cellular transport and has poly(ADP-ribosyl)transferase catalytic activity, but its N-terminal DNA binding domain is missing. Thus, this protein cannot bind DNA directly and co-activators are required for its catalytic activity. PARPs-5a and b are known as tankyrases 1 and 2. Both interact with the same set of proteins and are involved in maintaining telomere homeostasis and glucose transporter glut-4 containing vesicle trafficking. They co-localize with telomere repeat factor -1 (TRF-1), poly(ADP- ribosylate) TRF-1 and release it from telomeres,

allowing telomeres to be in a conformation that is easy to access by telomerases (Smith et al., 1998). In addition, tankyrases regulate insulin-responsive aminopeptidase (IRAP) via poly(ADP-ribosyl)ation, allowing the translocation of both IRAP and glut-4 from endosomal compartments to the plasma membrane (Chiang et al., 2008). PARP-7 (tiPARP) is a 2,3,7,8-tetrachlorodibenzo-*p*-dioxin (TCDD)-inducible poly(ADP-ribose) polymerase that appears to be involved in T-cell function and promotion of tumor growth if induced by TCDD (Ame et al., 2004). Other isoforms including PARPs 6, 8, and 16 have been discovered, but are poorly understood.

1.4.1 PARP-1 structure

Although investigation of other PARP isoforms is growing, PARP-1 has been studied most extensively (Ba and Garg, 2011, Smith, 2001). PARP-1 is a large protein composed of 1014 amino acids divided into 3 main functional domains (Fig 2): a 42KDa-N–terminal DNA binding domain that consists of 3 zinc finger structures (Zn1, Zn2, and Zn3) essential for sensing and binding DNA breaks, chromatin compaction, and protein-protein interaction. Zn1 and Zn2 recognize DNA and guide PARP-1 binding to damaged DNA while Zn3 facilitates inter-domain contact and assembly of DNA-activated conformation of PARP-1 (Ba and Garg, 2011). This domain also contains a nuclear localization sequence which acts as a caspase cleavage site. Adjacent to the Zn finger motifs is a 16 KDa central auto-modification (AMD) domain, with 15 conserved glutamate residues believed to be target for self-poly(ADP-ribosylation). The AMD also contains a BRCA1 C Terminus (BRCT) domain common to proteins associated with DNA-damage repair. BRCT domains are implicated in DNA binding, phosphorylation–independent protein interactions and ADP-ribose polymer (PAR) binding (Ame et al., 2004, Krishnakumar and Kraus, 2010). This domain is followed by a 55 KDa C-terminal catalytic domain. This is the most conserved part of PARP family (Ba and Garg, 2011), and contains a WGR domain which is

named after the most conserved amino acid sequence in its motif (Trp, Gly, Arg), and an active NAD^+ binding site. This site binds NAD^+ and mediates the ADP-ribosyl transferase activity that allows synthesis of PARs through the 50-amino acid PARP signature sequence located at the C-terminus of the catalytic domain (Yu et al., 2003, Wang et al., 2009, Virag et al., 2013).

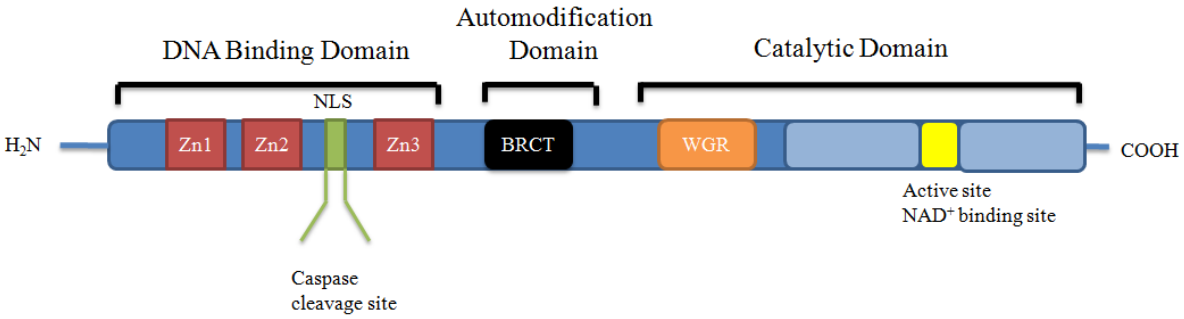

Figure 2: PARP-1 structure.
PARP-1 is a 116 kDa monomeric nuclear protein that consists of 3 domains: (1) an N-terminal double zinc finger DNA-binding domain (DBD), (2) a central automodification domain, and (3) a catalytic C-terminal NAD binding domain.

1.4.2 PARP-1 and DNA repair

PARP-1 is a nuclear enzyme involved in regulation of DNA repair, preservation of genomic integrity, proper assembly and regulation of mitotic apparatus, regulation of replication and transcription, as well as cell differentiation and proliferation (Yu et al., 2003, Chen et al., 2004). PARP-1 accounts for approximately 85% of maximally activated PARP activity (Virag et al., 2013). With low levels of DNA damage, PARP-1 is present at every ~1000 DNA base pairs (Hong et al., 2004) and acts as a survival factor that detects damaged DNA. It recognizes DNA strand breaks and participates in different types of DNA repair mechanisms.

Base-excision repair (BER) pathway

BER is an important DNA repair pathway resulting in excision of damaged bases. Small, oxidized, alkylated, or deaminated non-helix-distorting base lesions are recognized by DNA glycosylase, which catalyzes hydrolysis of the N-glycosidic bond of damaged deoxynucleosides and converts them to an intermediate product of BER, called an apurinic/apyrimidinic (AP) site. AP sites are then recognized by apurinic/apyrimidinic endonuclease 1 (APE1), which cleaves the 5'-phosphodiester bond, yielding a DNA nick with 3' hydroxyl group adjacent to 5' deoxyribosephosphate (dRP). PARP-1 is ubiquitously found at the sites of BER recognizing nicked regions of DNA at zinc fingers that define DNA-break-sensing motifs (Schreiber et al., 2006). PARP-1 binds nicked regions and uses NAD^+ as substrate to catalyze PAR formation. PARs are composed of 50-200 ADP ribose moieties attached covalently by o-glycosidic ribose-ribose bonds (Krishnakumar and Kraus, 2010). Negatively charged PARs are then reversibly bound covalently via ester linkages to glutamate residues of a variety of nuclear acceptor proteins including histones (H1, H2A, and H2B), topoisomerases, DNA helicases, and DNA

repair factors such as p53 (Krishnakumar and Kraus, 2010, Wang et al., 2009). When PARs bind histone zinc finger motifs, they promote relaxation of the surrounding chromatin and increase accessibility of repair proteins to damage sites (D'Amours et al., 1999). PARP-1 does not only repair DNA by facilitating chromatin remodelling, but it also interacts physically and functionally with various DNA-repair proteins to recruit them to damage sites (Kim et al., 2005). In BER, PARP-1 recruits BER repair factors including X-ray repair cross-complementing protein 1 (XRCC1), DNA polymerase β, and DNA ligase III to complete repair. More precisely, PARP-1 recruits XRCC1 by PAR-mediated binding linear motifs (PBMs) (Tallis et al., 2014). In turn, XRCC1 recruits Polymerase β, DNA ligase III, and other components of single strand break repair (SSBR) machinery (Zharkov, 2008). Recently, it was reported that XRCC1 interacts not only with PARP-1, but also with Condensin I, a chromosome-organizing complex. Condensin I interacts with both XRCC1 and PARP-1 in response to base damage and helps in allowing more efficient BER by modifying local chromatin and structural organization of DNA (Heale et al., 2006). To allow BER factors to complete repair, PARP-1 is autoPARylated. Auto-parylation triggers release from the chromatin (Krishnakumar and Kraus, 2010, Zharkov, 2008). Once the damage is repaired, *poly (ADP-ribose) glycohydrolase* (PARG) binds PARs and cleaves them from chromatin, allowing chromatin compaction (Zharkov, 2008).

DNA repair by non-homologous end joining

In non-homologous recombination, DNA double-strand breaks (DSBs) are corrected by ligation of two cleaved DNA ends. This process is initiated by Ku70/Ku80 heterodimer that consists of subunits Ku70 (70 kDa) and Ku80 (86 kDa). Ku70/Ku80 recruitment to damaged DNA recruits and activates the protein kinase DNA-PK (Shibata and Jeggo, 2014). PARP-1 and ku80 compete for damaged DNA and interact with a variety of proteins including the DNA-

dependent protein kinase (DNA-PK) to recruit and activate DNA polymerase and DNA ligase IV (Shibata and Jeggo, 2014).

DNA repair by homologous recombination

Homologous recombination is another PARP-1 associated dsDNA breaks repair pathway that uses the sister chromatid sequence of damaged DNA as a template. It starts by production of 3'-ssDNA overhangs. PARP-1 detects disrupted replication forks and attracts Mre11, a nuclear protein that has both 3' to 5' endonuclease and exonuclease activity. Mre11 forms a complex with DNA repair factors Rad50-NSB1 (MRN complex), causes non-homologous joining of DNA, and restarts the replication forks (Hartlerode and Scully, 2009). Nuclear PARP-1 foci co-localize with replication foci throughout S phase suggesting a possible physical interaction between PARP-1 and replication forks (Sugimura et al., 2008). It has also been reported that instead PARP-1 controls the number of nuclear homologous recombination (HR) sites and is not involved in the molecular part of this repair pathway. These HR sites have a stable component known as Rad51 foci in which several proteins involved in HR localize. PARP-1 does not localize to Rad51 and therefore is believed to not be involved in the HR event (Schultz et al., 2003). Thus, the mechanism through which PARP-1 is involved in HR DNA repair is still controversial and requires further study.

1.4.3 Additional roles of PARP-1

In response to DNA damage, it is important to limit transcription. PARP-1 plays a role in transcriptional regulation through modulation of chromatin structure or control of transcriptional machinery. In the presence of DNA breaks, PARP-1 preferentially binds and PARylates histone H1. This removes histones from chromatin, exposing it for transcription. In the absence of NAD^+ - the substrate for PARP catalytic activity - PARP-1 negatively regulates this process by binding

to nucleosomes and recruiting other components to compact the chromatin and make it inaccessible for transcription (Krishnakumar and Kraus, 2010). Chromatin helicase DNA binding protein 4 (CHD4) is a helicase family protein that participates in transcriptional repression. Recruitment of CHD4 to DNA damage sites is dependent on PARP-1 mediated PARylation (Tallis et al., 2014). Other repressors are Polycomb group (PcG) proteins (PRC1 and PRC2) and p53; these also require PARylation for recruitment and activity. Under genotoxic stress, PARP-1 and PARP-2 become hyperactive and their activity increases ~10-500 fold (Rouleau et al., 2010). Alternatively, PARP-1 binds to upstream promoter regions of many actively transcribed genes where it acts as a co-regulator, an enhancer-binding factor, or a regulator of insulators and insulator-binding factors (Krishnakumar and Kraus, 2010). As a co-regulator, PARP-1 regulates components of the transcription complex with or without its poly(ADP-ribosyl)ation activity. One example is PARP-1 binding to the promoter region of DNA methyltransferase, Dnmt1, silencing Dnmt1-mediated methylation in a PAR-dependent manner. Blockade of poly(ADP-ribosyl)ation induced *in vivo* DNA hyper-methylation and repressed gene expression, whereas cells with hyperactive PARP-1 exhibited dramatically reduced DNA methylation (Zardo et al., 2002).

Another potential physiological role of PARP- is regulation of cell division. Accurate segregation of chromosomes during cell division requires a functional mitotic apparatus. This apparatus contains PARP-1 as well as PARP-2, PARP-3, VPARP, tankyrase1, and tankyrase2 (Kim et al., 2005). PARP-2 is localized in the centromeres where it interacts with kinetochore proteins (Saxena et al., 2002a, Saxena et al., 2002b) and PARP-3 and tankyrases are associated with the centrosomes. PARP-1 is found in both regions and appears to be involved in capturing microtubules from mitotic spindles and centrosome organization. PARG, the PAR catabolizing

enzyme, localizes to the mitotic spindle, further suggesting that PAR dynamics are important for control of mitotic function. It has been proposed that PAR plays an important role in assembly and structure of bipolar spindles during mitosis. This was further supported when addition of PARG or PAR antibodies caused rapid breakdown of the spindle structure (Yelamos et al., 2011).

Telomeres are ribonucleoprotein complexes that cap the end of chromosomes and ensure chromosome integrity. Telomeres consist of double stranded tandem repeats of DNA rich in guanine bases and bound by a protective protein complex (shelterin/telosome) (Donate and Blasco, 2011). Both PARP-1 and PARP-2 regulate telomeres by interacting with telomeric repeat binding factor 2 (TRF2). TRF2 ensures telomere protection by interacting with DNA-damage signaling and repair factors. PARP-1 and PARP-2 control binding of TRF2 to DNA covalently by modifying its dimerization domain and non-covalently by attaching PAR polymers to its DNA binding domain. These two regulation mechanisms allow opening of the t-loop structure in response to DNA damage and make the chromatin accessible to DNA repair factors (Yelamos et al., 2011).

Finally PARP-1 and PARP-2 are important for chromosome segregation. They preserve the structure of centromeric heterochromatin and the integrity of mitotic spindles. PARP-1 interacts with 8 of 12 proteins that form the Anaphase–Promoting Complex or Cyclosome (APC/C) involved in chromatic separation. PARP-1 binds centromeric-pericentromeric heterochromatic regions while PARP-2 binds outer kinetochore at centromeres in prometaphase and metaphase cells (Sugimura et al., 2008, Poirier et al., 1982). Chromosomal miss-segregation seen in *parp2*$^{-/-}$ male mice was suggested to be caused by DNA-damage induced kinetochore defects and defects in centromeric heterochromatin.

1.4.4 PARP-1 and cell death in brain injury

Under genotoxic stress and extensive DNA damage, PARP-1 catalytic activity increases by up to 500 fold. Despite its protective role in DNA repair and cell survival, over-activation leads to cell death (D'Amours et al., 1999) (Fig3). In neurons, PARP-1 hyperactivity results from glutamate excitotoxicity and DNA oxidative damage, and can produce necrosis, caspase-independent apoptosis, or autophagy. Necrosis is ATP-independent, causing cell death by swelling and degradation of intracellular organelles and initiation of inflammatory response (Danial and Korsmeyer, 2004). In brain ischemia, necrosis happens early, theoretically when PARP-1-induced NAD^+ depletion causes reduction in ATP synthesis, mitochondrial dysfunction, and inhibition of energy-dependent processes. Although a PARP-1-dependent bioenergetic suicide theory has been forwarded (Sims et al., 1983), there is little direct evidence that PARP-dependent ATP depletion accounts for necrosis and it remains unclear how much ATP depletion in ischemia depends on PARP-1 activity and how much simply results from interruption of glycolysis by ischemia. Apoptosis is an active non-inflammatory process of cell death that requires energy in the form of ATP and causes chromatin condensation, nuclear pyknosis, cell rounding, DNA fragmentation, and membrane blebbing. In brain ischemia, PARP-1 induced apoptosis is caused by nuclear translocation of mitochondrial Apoptosis Inducing Factor (AIF) and cell death in a caspase-independent manner. Autophagy is a highly regulated cell death process that involves engulfment of cytoplasmic cellular proteins and intracellular organelles with double-membrane vesicles called autophagosomes (Nikoletopoulou et al., 2013). Autophagosomes then fuse with lysosomes to form autolysosomes, where specific acid hydrolases degrade engulfed material (Levine and Kroemer, 2008). Autophagy depends on a number of factors including PARP-1, AIF, caspases, Bcl-2 family proapoptotic proteins and

others (Lau and Tymianski, 2010). Interestingly, activation of this pathway has been associated with perturbations in mitochondrial function. Mitochondrial damage is known to result in activation of mitophagy, a specific type of autophagy that eliminates dysfunctional mitochondria under normal and pathological conditions including cerebral ischemia (Baek et al., 2014). PARP-1-induced energy collapse likely stimulates sequential inactivation of Akt protein kinase and key autophagy regulator, mTOR (Munoz-Gamez et al., 2009).

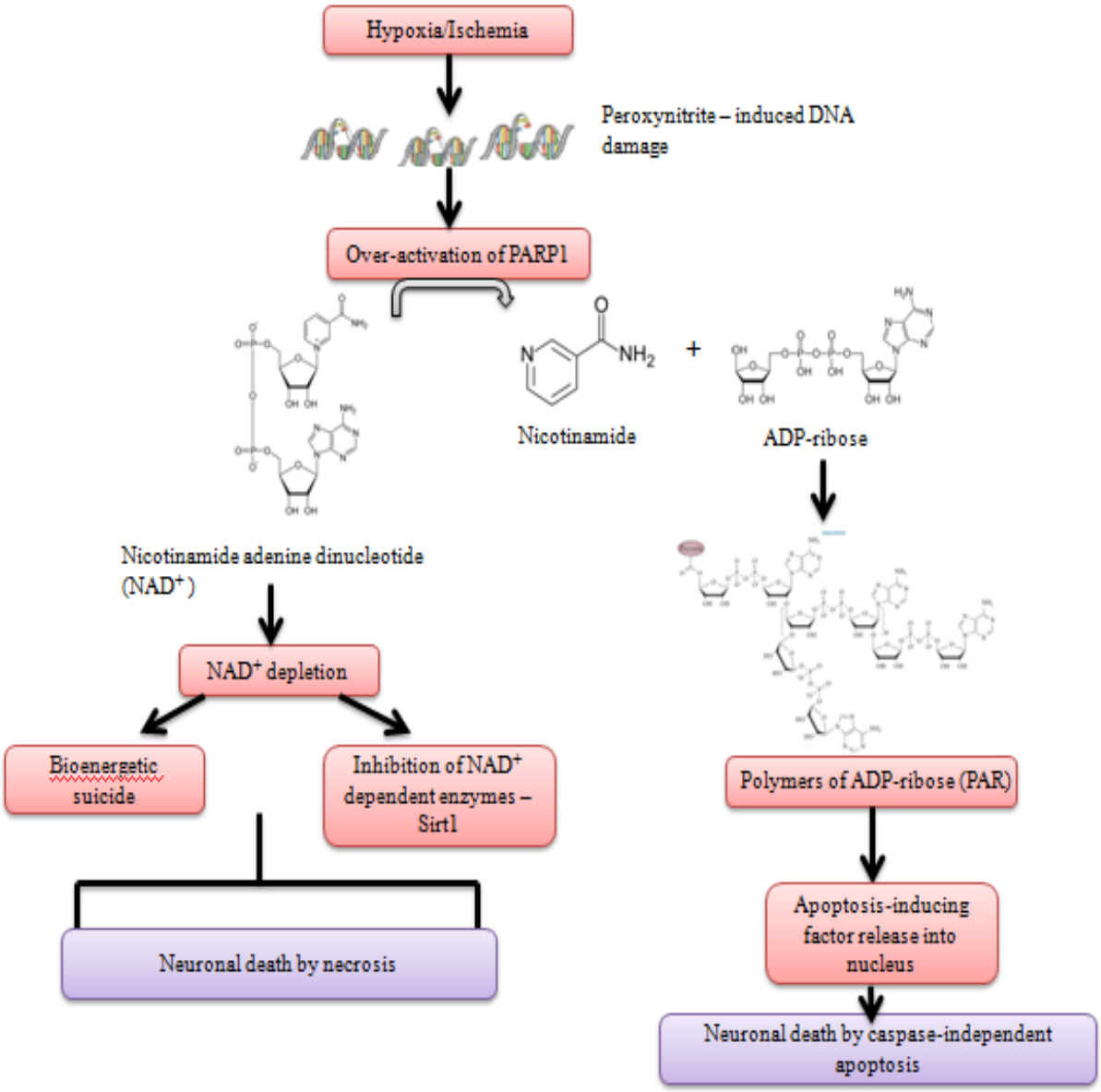

Figure 3: PARP-1-mediated cell death in ischemia.

PARP-1-mediated cell death in ischemia. Under genotoxic stress, PARP-1 gets over-activated and synthesizes polymers of ADP-ribose using NAD^+ as a substrate. PARP-1 causes necrotic cell death by depleting NAD^+ and ATP as well as it causes caspase-independent apoptotic neuronal death by inducing AIF mitochondrion-nucleus translocation.

1.4.5 Mechanisms of PARP1 mediated cell death

1.4.5.1 Caspase-independent neuron death

Pathological PARP-1 activity can induce programmed cell death that is caspase-independent. In a process referred to as Parthanatos, PARs formed by PARP-1, and cleaved from targets by PARG, lead to depolarization of mitochondrial membranes, MPT, and permeability to AIF by direct AIF chaperoning to the nucleus from mitochondria (Baek et al., 2013, Dawson and Dawson, 2004). Mammalian AIF is a 67-kDa conserved mitochondrial protein composed of three domains: : (1) an amino-terminal mitochondrial localization sequence, (2) a spacer sequence, and (3) a carboxyterminal oxidoreductase domain with flavin adenine dinucleotide (FAD) and nicotinamide adenine dinucleotide (NAD) binding sites (Daugas et al., 2000). The FAD-binding domain is similar to bacterial oxidoreductases (Wang et al., 2009). Structurally, it has been reported from liver preparations that most mitochondrial AIFs are localized within intermembrane space while only 30% are loosely associated with the outer mitochondrial membrane facing the cytosolic side (Yu et al., 2003). Physiologically, AIF maintains the integrity of mitochondrial structure and acts as NADH oxidase involved in oxidative phosphorylation (Wang et al., 2009, Virag et al., 2013). Lack of a functional AIF gene has been correlated to decrease in complex I activity in the electron transport chain as well as to death during embryonic development (Koh et al., 2005) suggesting an important role of AIF in cell survival. However, under pathological conditions, including ischemia, AIF has been shown to be involved in programmed cell death (Yu et al., 2003, Wang et al., 2009, Andrabi et al., 2008). Mitochondrial membrane depolarization leads to release of AIF and nuclear translocation (Cao et al., 2007). In the nucleus, AIF causes nuclear condensation, degradation of DNA into large scale (50 Kb) fragments that are larger than those seen after activation of caspase-3 and phosphatidyl-

serine exposure (Moubarak et al., 2007, Koh et al., 2005). AIF itself does not have a DNAse activity. Once AIF binds DNA, it recruits DNAses including Endonuclease G (Endo G). Similarly to AIF, this protein is located in the intermembrane space and can translocate to the nucleus under many conditions including temporary and permanent brain ischemia in absence of caspase activation (Sims and Muyderman, 2010, Cho and Toledo-Pereyra, 2008, Penninger and Kroemer, 2003, Li et al., 2001). Unlike AIF, Endo G can induce DNA fragmentation on its own (Cho and Toledo-Pereyra, 2008, Penninger and Kroemer, 2003). Co-immunprecipitation and immunohistochemistry studies revealed that AIF and Endo G interact physically in the nucleus at about the same time following focal cerebral ischemia (Lee et al., 2005a). Silencing the expression of Bnip3 has been shown to prevent AIF and EndoG mitochondrion-to-nucleus translocation as well as DNA fragmentation in stroke and ischemic cardiomyocytes models (Zhang et al., 2011a). Bnip3 induces Endo G release and Endo G dependent high molecular weight DNA fragmentation, suggesting that this type of DNA fragmentation detected after Bnip3 activation in hypoxia is driven by Endo G (Li et al., 2001, Zhang et al., 2007b, Zhao et al., 2009). Notwithstanding these assertions, it is important to note that other studies are contradictory on the role of Endo G in AIF-induced DNA fragmentation (Lee et al., 2005a) following Bnip3 activation. Further work is required to identify the endonuclease/s responsible for AIF nuclear effects (Wang et al., 2009). The neurotoxic effect of AIF seems to be associated with its translocation to the nucleus and not to its loss from the mitochondrion (Cheung et al., 2006) suggesting that AIF is active in nucleus and not in mitochondrion.

While PAR is reported to cause parthanatos dependent on AIF, PARP-1 also appears to liberate AIF from mitochondria by inducing MOMP in other ways (Vande Velde et al., 2000, Ba and Garg, 2011). There are several reports that NAD^+ depletion by PARP-1 hyperactivity is

necessary for AIF release (Vande Velde et al., 2000, Ba and Garg, 2011, Alano et al., 2010), including a recent report from our lab showing that NAD^+ depletion leads to enhanced expression of the pro-death Bcl-2 family member, Bnip3, and associated MPT (Lu et al., 2014). Under normal conditions, Bnip3 is expressed at low levels in neurons. This changes during prolonged hypoxic conditions, when Bnip3 expression is dramatically increased (Zhang et al., 2007b). Bnip3 expression has been suggested to induce cell death mainly via mitochondrial dysfunction and opening of the mitochondrial permeability transition pore (mPTP) (Vande Velde et al., 2000). Upon activation, homodimeric Bnip3 integrates into the outer membrane of the mitochondria, increasing permeability and triggering release of AIF Endo G apoptotic factors (Nakamura et al., 2012). Over-expression of Bnip3 in neurons induces death while silencing is neuroprotective in rat models of ischemic stroke (Graham and Chen, 2001, Cho and Toledo-Pereyra, 2008).

1.4.5.1a NAD^+ depletion in caspase-independent cell death

PARP-1 consumes NAD^+ through adenosine 5'-diphosphate (ADP-ribosyl)ation of nuclear-associated proteins. This in turn leads to ATP depletion by inhibition of NADH-dependent ATP synthesis, and by enhanced ATP consumption by phosphoribosyl pyrophosphate synthetase and nicotinamide mononucleotide adenylyltransferase during attempted NAD^+ replenishment (4 ATP needed to synthesize 1 NAD^+) (Virag et al., 2013). Reduced synthesis of NADH/ATP involves PARP-1 consumption of cytoplasmic NAD^+ and glycolytic inhibition. Depletion of NAD^+ acts as a cofactor for the glyceraldehyde-3-phosphate dehydrogenase (GAPDH) step of glycolysis (Fig.3). Thus, depletion of NAD^+ inhibits the activity of GAPDH and glycolysis (Ying et al., 2003). A lethal bioenergetic cycle was hypothesized in the 1980s (Berger, 1985), but whether bioenergetic depletion kills directly or by triggering autophagy has not completely been defined.

The evidence is stronger that NAD^+ depletion is responsible for increasing MPT (Alano et al., 2004, Ying et al., 2005) and AIF-dependent cell death (Alano et al., 2010, Alano et al., 2004, Schreiber et al., 2006). Our lab recently reported that NAD^+ depletion is sufficient to inhibit sirtuin activity and drive transcription of the pro-death Bcl-2 family member Bnip3 (Lu et al., 2014) in the first comprehensive description of how this might happen. Understanding this pathway is important to develop therapeutics for an effective treatment of stroke. However, these therapeutics might be beneficial only for males since the stroke-induced cell death mechanisms are sexually dimorphic. Although PARP-1 caspase-independent pathway is activated in both sexes, emerging data show that PARP, nNOS, and AIF deletions reduce infarct size in male animals only (Manwani and McCullough, 2011), suggesting that this pathway induces cell death only in males. Females' cell death has rather been reported to be caspase-dependent (Siegel et al., 2010, Manwani and McCullough, 2011). Thus, sex-specific therapies may be necessary for the effective treatment of stroke. Signaling mechanisms responsible for those differences remain unclear, but might be related to NAD^+ levels. Baseline NAD^+ levels are higher in males than females. In ischemia, NAD^+ depletion is detected in males and ovariectomized females but not in intact females (Siegel and McCullough, 2013), suggesting that hormones such as estrogens are somehow neuroprotective in animal models of stroke (Hurn and Macrae, 2000, Alkayed et al., 1998, Simpkins et al., 1997). Deletion of PARP-1 prevents stroke induced NAD^+ loss in males but worsens NAD^+ loss in females (Siegel and McCullough, 2013), suggesting sex specific NAD^+ changes in WT or PARP-1 KO mice.

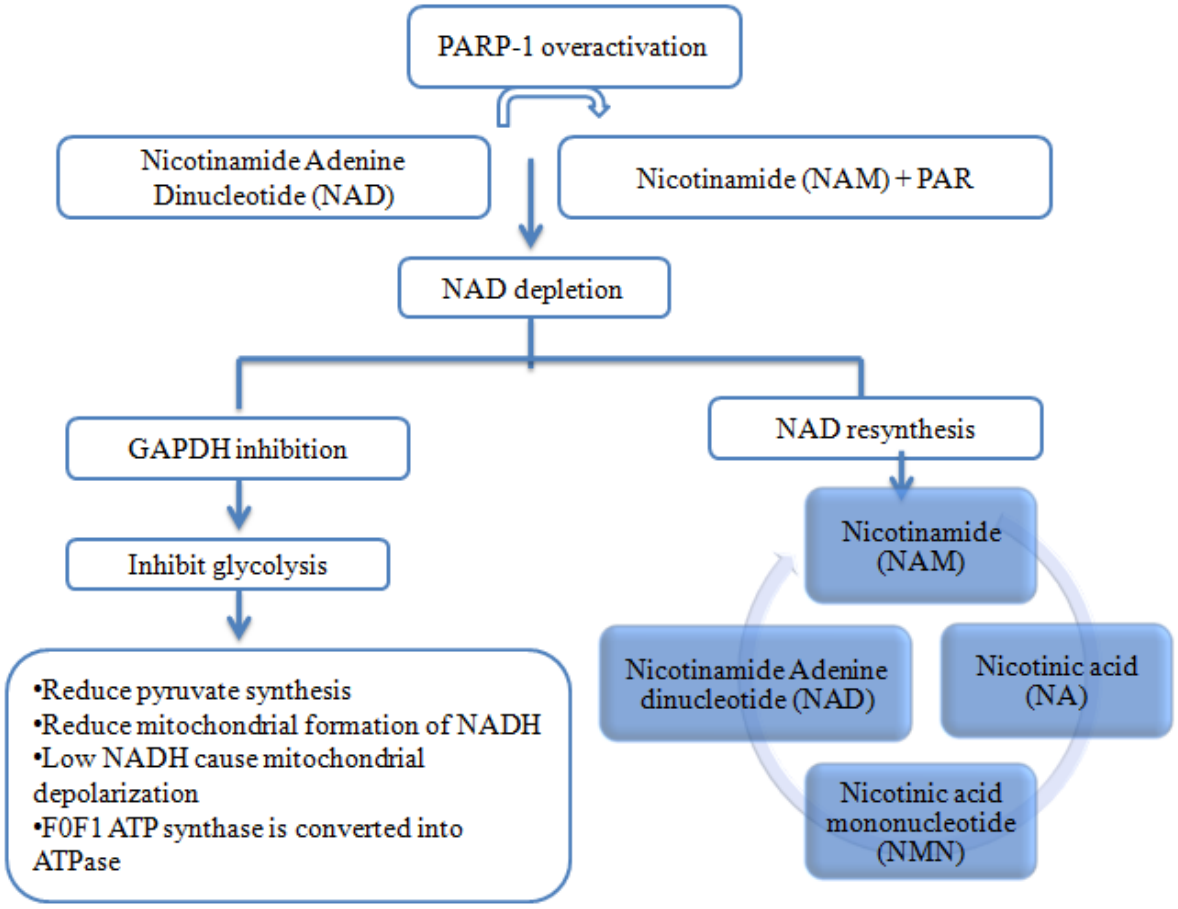

Figure 4: Bioenergetic suicide.

PARP-1 over activation depletes NAD leading to inhibition of glyceraldehyde 3-phosphate dehydrogenase (GAPDH) step of glycolysis. This inhibition triggers sequential shut down of glycolysis, TCA cycle, and oxidative phosphorylation. To counteract this fatal depletion of NAD, cells initiate the ATP-consuming salvage pathway to re-synthesize NAD. Both processes end up depleting ATP.

1.4.5.1b NAD^+ and Sirtuins

Sirtuins are NAD^+ dependent class III histone deacetylases, which are mammalian homologs of Sir-2 (Silent Information Regulator), which act as aging regulators in yeast (Guarente, 2000). This family consists of seven proteins, Sirt1-7. Sirt-1, Sirt-6, and Sirt-7 localize to the nucleus while Sirt-2 is mainly the cytoplasm, and Sirt-3-5 are mitochondrial (Michishita et al., 2005). There is functional variability, as Sirt-1 and Sirt-5 are primarily protein deacetylases, Sirt-4 and Sirt-6 are mono(ADP)-ribosyltransferases, and Sirt-2 and Sirt-3 each have both enzymatic activities. The activity of Sirt-7 is not well understood (Luna et al., 2013). Sirt-1 hydrolyzes NAD^+ to remove the acetyl group from substrates with acetyl-lysine to generate the deacetylated substrate, nicotinamide (NAM), and 2'-O-Acetyl-ADP-Ribose.

PARP-1 and Sirt-1 both depend on NAD^+ and share the same contiguous cytoplasmic/nuclear NAD^+ pool (Luna et al., 2013). Under physiological conditions, when DNA damage is limited, the interplay between Sirt-1 and PARP-1 seems to be positive. Mild activation of PARP-1/PARP-2 leads to mild formation of PAR and inhibits Sirt-1-mediated deacteylation of histones, causing chromatin decondensation and gene expression (Schreiber et al., 2006). However, under pathological conditions where DNA damage is excessive, the interplay is negative and contributes to cell death (Brooks and Gu, 2009, Michan and Sinclair, 2007).

1.4.5.1c Sirt-1deacetylase activity-regulation of transcription factors

Sirt-1 deacetylase activity regulates several important transcription factors that bind to upstream promoter regions of pro-apoptotic factors, including Bnip3. Increased PARP-1 activity depletes NAD^+ and inhibits Sirt-1 deacetylase activity, which increases acetylated levels of transcription factors including FOXO3 (Brunet et al., 2004) and HIF-1 (Lim et al., 2010). Hyper-

acetylation causes these factors to bind to respective Bnip3 promoter response elements, leading to enhancement of Bnip3 expression (Lu et al., 2014, Giaccia et al., 2003). FOXO3 is an inactive cytosolic transcription factor under normal conditions. In oxidative stress, c-Jun N-terminal kinase (JNK) or macrophage stimulating 1 (MST1) protein directly phosphorylates FOXO3 causing dissociation from its binding partner 14-3-3, facilitating translocation and accumulation into nucleus, where it enhances transcription of several pro-apoptotic targets including Bnip3, Bim, HIF-1, the dynamin-related protein Drp1, and survivin (Hagenbuchner and Ausserlechner, 2013, Tran et al., 2002, Lu et al., 2014). Sirt-1 deacetylation activity also plays a role in maintaining FOXO3 cytosolic localization (Giannakou and Partridge, 2004). When FOXO3 is deacetylated it is inactive, but when Sirt-1 activity declines, it becomes hyperacetylated and moves to the nucleus (Hagenbuchner and Ausserlechner, 2013). It was shown that FOXO3 can drive Bnip3 expression in skeletal muscle (Mammucari et al., 2007) and our lab recently showed that genotoxic stress causes PARP-1 mediated NAD^+ depletion, inhibits sirtuin, increases FOXO3 acetylation, FOXO3 binding to Bnip3 upstream promoter region, and enhances Bnip3 expression (Lu et al., 2014).

HIF-1 is another transcription factor that activates over 80 genes that are part of the cellular response to hypoxia and is deacetylated by Sirt-1 (Lim et al., 2010). HIF-1 is a heterodimer transcription factor composed of α and β subunit (aryl hydrocarbon receptor nuclear translocator ARNT). The α subunit is oxygen-dependent whereas the β subunit is constitutively expressed. Under normal conditions, α is expressed at low levels whereas it is upregulated in hypoxic conditions. This depends on the hydroxylase activity of prolyl hydroxylase (PHD) which hydroxylates α subunit at normal conditions, allowing the von Hippel-Lindau protein to ubiquitinate and the proteosome to subsequently degrade the α subunit. In hypoxia however, the

hydroxylation is inhibited allowing HIF-1α induction, stabilization, dimerization with the β subunit and translocation from cytoplasm into nucleus (Muz et al., 2009, Martinez-Romero et al., 2009) where functional HIF-1 regulates transcription of a variety of target genes that carry the Hypoxia Response Element (HRE) in their upstream promoter regions. HIF-1 activity depends on α subunit expression level and plays a role in hypoxia-mediated apoptosis in myocardial infarctions and most solid tumors (Stroka et al., 2001). To date, HIF-1α has been shown to do this in two ways: one way is through interaction with p53. It has been suggested that HIF-1α regulates p53-mediated function by binding directly to Mdm2, the product of a p53-inducible gene. Mdm2 has been shown to play a role in stabilizing p53, exporting it from nucleus and inducing programmed cell death via regulation of Bax or growth arrest (Chen et al., 2003, Sermeus and Michiels, 2011). Another way is through HIF-1 binding to HREs associated with Bnip3 and enhancing its expression. Bnip3 has been identified as a hypoxia-inducible gene that is regulated by HIF-1 (Giaccia et al., 2003). Since HIF-1α is regulated by Sirt-1, PARP-1-mediated NAD^+ depletion might lead to HIF-1α hyperacetylation and Bnip3 transcription. Acetylated HIF-1α combines with the β subunit to form the functional HIF-1 core. The core then binds the HRE in Bnip3 upstream promoter and increase Bnip3 expression. Cells lacking HIF-1α cannot produce large amounts of Bnip3 and their cell death rate is reduced (Greijer and van der Wall, 2004). PARP-1 and Bnip3 both lead to hypoxic/ischemic mitochondrial permeability, AIF release, and caspase-independent cell death (Yu et al., 2002, Alano et al., 2004), suggesting common pathways. Our lab showed that pharmacological inhibition and genetic deletion of PARP-1 reduced Bnip3 expression and Bnip3-induced neuron death in cortical neurons in hypoxia (Lu et al., 2014). We then showed that FOXO3 plays an important role in PARP-1 regulation of Bnip3. Since HIF-1α is also regulated by Sirt-1/NAD^+, the major objective of the

current project is to understand how HIF-1α contributes to Bnip3 expression when PARP-1 is pathologically activated.

1.5 Objectives

The objective is to determine how PARP-1 activation leads to mitochondrial dysfunction, permeability, and AIF-dependent neuron death in hypoxia.

1.6 Hypothesis

PARP-1 mediated NAD^+ depletion leads to sirtuin inhibition, HIF-1α hyper-acetylation and increased HIF-1-mediated Bnip3 transcription.

1.7 Thesis Rationale and Objectives

Our focus is to determine whether PARP-1 mediated HIF-1α post-translational acetylation caused by sirtuin inhibition leads to Bnip3 expression, mitochondrial permeability, and AIF-dependent cell death. This interest came from data our lab collected that showed hypoxia produces PARP-1-dependent depletion of NAD^+ and inhibition of the NAD^+ dependent sirtuin deacetylase activity (Lu et al., 2014). This in turn, caused hyperacetylation of the transcription factor FOXO3a, enhanced binding of FOXO3a to Bnip3 upstream promoter, increased levels of Bnip3 transcript, and elevated mitochondrial dysfunction. Similar to FOXO3a, HIF-1α is deacetylated by Sirt-1 and HIF-1 is a transcription factor that binds upstream the Bnip3 promoter region at hypoxia response elements (HRE). Therefore, we set out to test whether PARP-1 influences Bnip3 in a manner requiring HIF-1α in hypoxic conditions. We used cultured primary cortical neurons as a model system. Cells were exposed to nominal anoxia to investigate the effects of extreme hypoxia in cerebral ischemia. Cells were also exposed, in select experiments, to the DNA alkylator, MNNG. This model causes cell death by causing DNA strand breaks and therefore by more directly activating PARP-1. This allows more effective isolation of PARP-1-dependent pathways for study. In response, we assessed NAD^+ levels, sirtuin activity, acetylation

of HIF-1α, HIF-1 binding at Bnip3 HREs, and Bnip3 expression. To determine the role of specific intermediates along this pathway, we used *parp-1*$^{-/-}$ neurons and lentiviral shRNA to achieve PARP-1 and HIF-1α loss of function, respectively. Various pharmacological approaches were also used, as indicated.

Chapter 2. Materials and Methods

2.1 Chemicals and reagents

N-(6-oxo-5, 6-dihydrophenanthridin-2-yl)-*N*, *N*-dimethylacetamide HCl (PJ34) was purchased from Calbiochem. β-Nicotinamide Adenine Dinucleotide hydrate (NAD^+) and *N*-methyl-*N*-nitro-*N* nitrosoguanidine (MNNG) were purchased from Sigma-Aldrich. Protein inhibitor cocktail tablets and bicinchoninic acid (BCA) protein assay kits were obtained from Roche Diagnostics GmbH and Thermo Scientific, respectively.

2.2 Mouse Primary neuron cultures and treatments

Mouse primary neuron cultures were prepared as previously described (Lu et al., 2014). Briefly, they are prepared from embryonic day 14 (for shRNA transfection experiments) and day 15/16 (for all other experiments) CD1 and *parp1*$^{-/-}$ mouse cortices from either sex in accordance with the guidelines of the Canadian Council on Animal Care. Cells were plated on poly-D-lysine-coated plates in Neurobasal medium (NB) with B27 supplement (Invitrogen), 1.2 mM glutamine, and 5% fetal bovine serum (FBS; Hyclone). FBS was removed the following day (day 1) and replaced with NB/B27/glutamine. Cultures were maintained at 37°C/5% CO_2 and given a partial media change on day 6. Cultures were used on day 9–10 post-culture for all experiments. Neurons were exposed to hypoxia or to MNNG. For hypoxia, cultured neurons were placed in a hypoxic chamber (Billups-Rothenberg, Inc) humidified by placing a petri dish containing sterile water and filled with 5% CO_2/95% N2 gas mixture. These cells were then incubated at 37°C, 5% CO_2 in a normoxic conventional incubator for 2, 6, 12, or 24hr. Control cultures were also incubated at 37°C, 5% CO_2 in same incubator as hypoxia treated cells for the same period of time. To induce DNA damage and activate PARP-1, cortical neurons were exposed to MNNG (50 μM, 30 min) and then rescued in NB medium for 4hr. Media was changed after MNNG

exposure. NAD^+ (3 mM) and PJ34 (10 μM) were added before the addition of MNNG or the initiation of hypoxia and readded after the medium exchange following MNNG exposure.

2.3 Real time PCR

Total RNA was extracted by using an RNeasy kit (Qiagen). Real-time RT-PCR was performed using an iTaq™ universal SYBR®Green One-Step RTPCR Kit (Bio-Rad) with Applied Biosystems 7300 RT-PCR system. Primers for mouse HIF-1α, Bnip3, and β-actin are as follows:

HIF-1α forward: 5'-AGACAGACAAAGCTCATCCAAGG-3'; HIF-1α reverse: 5'-GCGAAGCTATTGTCTTTGGGTTTAA-3'; Bnip3 forward: 5'-GTAGAACTGCACTTCAGCAATGG-3'; Bnip3 reverse: 5'-GGGCTGTCACAGTGAGAACTC-3'; β-actin forward: 5'-GGGCTATGCTCTCCCTCACG-3'; β-actin reverse: 5'-GTCACGCACGATTTCCCTCTC-3'. PCR parameters were as follows: 50°C for 10 min, 95°C for 1 min, followed by 45 cycles of PCR at 95°C for 15 s and 60°C for 1min. Standard curves were generated, and the relative amount of target gene mRNA was normalized to β-actin mRNA. Specificity was verified by melt curve analysis.

2.4 Western blot analysis

Tissue culture plates were washed with ice-cold-PBS pH 7.4 and cells were gently scraped off and collected in ice-cold PBS. Collected cells were then centrifuged at 2500 x g for 10 min (4°C). Pellets were resuspended in 100 μl RIPA lysis buffer (50mM Tris-HCl, 150 mM NaCl, 0.1% SDS, 50mM NaF, and 1% Triton X-100, with protease inhibitor cocktail, pH 8.0) and the lysates were incubated on ice for 30 minutes. Lysates were then sonicated and incubated for an additional 30 minutes before centrifugation at 10,000x g for 10 minutes (4°C). Pellets were discarded and supernatants collected into 1.5 ml microtubes. Protein concentrations were

determined using Pierce BCA protein assay kit. Total cell homogenates (20 µg) were separated on 7.5% polyacrylamide gels and transferred to PVDF membranes according to standard procedures. A blocking buffer of 5% nonfat powdered milk in TBS with 0.1% Tween 20 was used for all incubations. Membranes were washed, and the ECL Plus Chemiluminescence Kit (GE Healthcare) was used to visualize immunoreactive bands with a Chemi-Doc Imager (Bio-Rad). Primary antibodies were anti-HIF1-α antibody (1:1000; Novus Biologicals), anti-Bnip3 antibody (1:1000; Cell Signaling), and anti-β-actin antibody (1:4000; Sigma-Aldrich). Densitometry analysis was performed using Image J (National Institutes of Health). Values for each lane were normalized to protein loading markers (Precision Plus Protein^{TM} Dual Color Standards; Bio-Rad).

2.5 Chromatin immunoprecipitation

Cortical neurons (about $2.5x10^6$) were cross-linked with 1% formaldehyde (Sigma-Aldrich) at 37°C for 10 min, rinsed twice with PBS, and harvested in 500 µl PBS to be then centrifuged at 2500 x g for 10 min (4°C). Supernatant was discarded and the pellet was suspended in 100 µl diluted 10 x lysis buffer (50mM Tris-HCl, 5mM $CaCl_2$, pH 7.9) at room temperature, 1 ul BSA and digested by micrococcal nuclease (New England Biolabs) into fragments ranging in size from 150 to 900 bp. Lysates were incubated for 20 min at 37°C. Digestion was then stopped by adding 10 µl of 0.5 M EDTA and incubation on ice for 1 min. Nuclei were pelleted by centrifugation at 13,000 x g at 4°C for 1 min. Supernatant was discarded and the pellet resupsended in 150 µl 1x CHIP buffer (150mM NaCl, 20 mM Tris-HCl, 0.1% SDS, and 0.5% Triton X-100, pH 8.1) and 7.5 µl probe with protease inhibitor mixture (Roche Applied Science), incubated on ice for 10 min and sonicated with three 10 s pulses. Samples were either incubated with 5 µg secondary antibody (anti-rabbit IgG, HRP-linked antibody, cell signaling) to

act as immunoprecipitation control or incubated with 5 µg anti-HIF-1α antibody (1:1000, Abcam) to act as immunoprecipitation sample overnight with rotation at 4°C. On the next day, 20 µl of protein A/G ultra Resin agarose beads (Thermo scientific) were added to each sample and incubated for 3 hours with rotation at 4°C. Beads with binding partners were then washed with 1x CHIP buffer and TE buffer (10 mM Tris-HCl, pH 8.0, and 1 mM EDTA) consecutively. Complexes were eluted from beads with elution buffer (1% SDS, 0.1 M $NaHCO_3$) at 65°C for 30 min then stored overnight at -20°C. NaCl (0.33 M) was added to reverse cross-linking at 65°C for 4 hours. Immunoprecipitated and input DNA were then purified by treatment with RNaseA and proteinase K (0.1mg/ml, Sigma Aldrich) and recovered using Chip DNA Clean & Concentrator kit (Zymo Research). Real-time quantitative PCR was performed with primers designed to amplify a 265 bp region of the mouse Bnip3 upstream promoter region flanking HRE, a putative HIF-1α binding element (5'RCGTG-3'). Primers were forward 5'-CCAACTCGCCATTGATGCTG -3' and reverse 5'-CGGTTGACCCATAGTTCCCC-3'.

2.6 Lentiviral shRNA treatment of neuron cultures

Cortical neurons were infected with either control sequences or high-titer lentiviral preparations expressing HIF1-α shRNA lentishort hairpin RNA (shRNA) in the pLKO.1 plasmid backbone (TRCN0000054450), obtained from GE Healthcare and prepared by the Lentiviral Core Platform of the University of Manitoba. Neurons were infected at 1 d *in vitro* (DIV) with a multiplicity of infection (MOI) of 2 for 6hr. Medium was replaced with fresh neurobasal medium. Total cell RNAs and proteins were isolated at 4 DIV, and HIF1-α knockdown and Bnip3 mRNA and protein levels were quantified by RT- PCR and Western blotting at 7 DIV.

2.7 Intracellular NAD^+ determinations

Adherent cortical neurons (about $2.5x10^6$) were harvested by scraping into ice-cold phosphate-buffered saline (pH 7.2), followed by centrifugation at 2500 x g for 10 min at 4°C. The cell pellet was then resuspended in Perchloric acid (0.5 N) and extracts were neutralized with 1 N potassium hydroxide. The supernatant was then collected and used for NAD^+ quantification using high-performance liquid chromatography (HPLC). Separations were performed on a Microsorb C18 4.6×100 mm column (particle size, 3 µm; pore size, 100 Å; Rainin Instrument Company) at a flow rate of 0.5 ml/min through a photodiode array detector, utilizing a Waters 600E Multisolvent Delivery System (Waters, Mississauga, ON, Canada) as described previously (Lu et al., 2014). A flow rate of 0.5 ml/min was used throughout. To determine NAD^+ levels, absorbance change at 254 nm was measured. The results were normalized to total protein, measured by BSA standards and Pierce BCA protein assay.

2.8 SIRT activity assay

SIRT Direct Fluorescent Screening Assay Kit (Cayman Chemical Company) was used to determine Sirtuin activity. Cortical neurons (about 6×10^4 cells/well) were plated on 96-well plates and 25 µl of assay buffer (50 mM Tris-HCl, 137 mM NaCl, 2.7 mM KCl, and 1 mM $MgCl_2$, pH 8.0) was added. To initiate the reactions, 15 ul of substrate solution, containing the p53 deacetylation target sequence Arg-His-Lys-Lys (ε-acetyl)-aminomethylcoumarin and the HDAC I/II inhibitor trichostatin A, was added and covered plates were incubated on a shaker for 45 min at room temperature. 50 µl of Stop/Developing solution with 2mM Nicotinamide was added and plates were incubated at room temperature for 30 min to convert Arg-His-Lys-Lys-aminomethylcoumarin into Arg-His-Lys-Lys and the fluorescent product aminomethylcoumarin.

Relative sample fluorescence was determined by reading plates in a fluorometer with an excitation wavelength of 355 nm and an emission wavelength of 460 nm.

2.9 Acetylated-Lysine HIF-1α quantification

$5x10^6$ neuronal cultures were lysed in 150 µl ND-Lysis buffer, 7.5 µl protease cocktail inhibitor 20xs, 5 µM TSA, and 5 mM nicotinamide. Lysates were then sonicated and left on orbital rotor for 30 min at 4ºC followed by centrifugation at 12000 x g for 10 min. Pellets were discarded and supernatants collected into 1.5 ml microtubes. Protein assay and western blotting were performed as described in section 2.4. Blots were first probed with anti-acetylated-lysine antibody (1:1000; Millipore and Cell signaling) anti-β-actin antibody (1:4000; Sigma-Aldrich) to detect the acetylated lysine and β-actin protein bands. Blots were then stripped with Restore Western Blot Stripping Buffer (Thermo Fisher Scientific) at 37°C for 30 min followed by 5 min wash in TBST and incubation with anti-rabbit IgG, HRP-linked antibody (1:1000 Cell Signaling) for 1 hr 30 min at room temperature to verify effective removal of anti-acetylated-lysine primary antibody. Once verified, blots were blocked with blocking buffer of 5% nonfat powdered milk in TBS with 0.1% Tween 20 for 1 hour at room temperature, then probed with polyclonal anti-HIF-1α (3µl; Novus Biologicals) at 4ºC with rotation. On the next day, membranes were washed and incubated in secondary antibody as previously mentioned. ECL Plus Chemiluminescence Kit (GE Healthcare) was used to visualize immunoreactive bands with a Chemi-Doc Imager (Bio-Rad). Adobe Photoshop CS6 software was used to overlay the acetylated-lysine HIF-1α band.

2.10 Statistics

Data are presented as the mean ± standard error of the mean (SEM). For all experimental readouts 3 or more experimental replicates were used. Each replicate represented at least 2 duplicate culture measurements and was sampled from distinct pools of animal tissue. GraphPad Prism software (version 5.0) was used for statistical analyses. One-way ANOVA with Student-Newman Keuls *post hoc* multiple comparison test was utilized to compare > 2 groups with one variable. Two-way ANOVA with Bonferroni's test was used to compare > 2 groups with more than two variables. $p < 0.05$ was considered as statistically significant unless otherwise noted. Asterisks are used herein to denote significance according to the following scheme: $^{*} = p < 0.05$; $^{**} = p < 0.01$

Chapter 3. Results

3.1 Effects of hypoxia on HIF-1α expression

Since our hypothesis requires isolation of HIF-1α post-translation modification as a causal factor in Bnip3 induction, we first endeavored to understand whether our extreme nominal anoxia model of hypoxia affects HIF-1α expression. Wild type and *parp-1*$^{-/-}$ neuron cultures (day 9 *in vitro*) were exposed to 95% N_2/5% CO_2 for 2, 6, or 24 hr. At each time point, HIF-1α mRNA levels were normalized to housekeeping β-actin message by real-time qPCR, and the effects of hypoxia expressed relative to normoxic respective genotypic controls (wildtype or *parp-1*$^{-/-}$). Neither hypoxia nor *parp-1* deletion had any significant effects on HIF-1α mRNA (Fig. 5). Total cell homogenate HIF-1α antigen levels were also assessed using a western blotting approach at each time point. Band intensities were quantified using densitometry, relative to β-actin standards for each sample. Consistent with PCR data, hypoxia produced no significant changes in total HIF-1α protein expression (Fig. 6). Although other studies have reported a significant increase in HIF-1α protein levels in hypoxia, we have not been able to detect that increase possibly because our cells were nominally exposed to 0% oxygen.

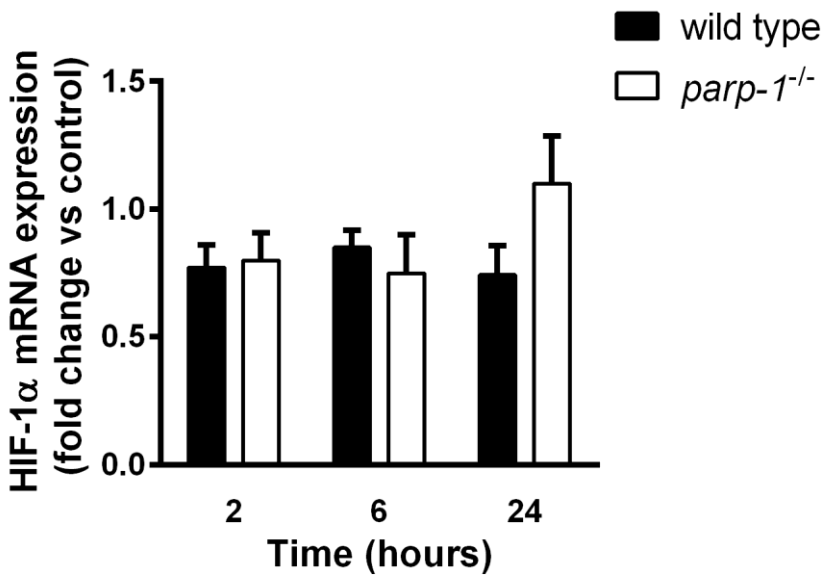

Figure 5: HIF-1α mRNA levels are PARP-1 independent and do not change in severe hypoxia.

Cortical neurons were exposed to 2, 6, and 24 hr hypoxia. Total RNA was isolated using RNeasy Plus Mini Kit (Qiagen). The real-time RT-PCR assay was performed using iScript™ One-Step RT-PCR Kit (Bio-Rad). Significant differences were not detected at any time point and were not seen between the different groups. All data are reported as mean ± SEM; n = 4-6 and were analyzed using two–way ANOVA with the Bonferroni *post hoc* test.

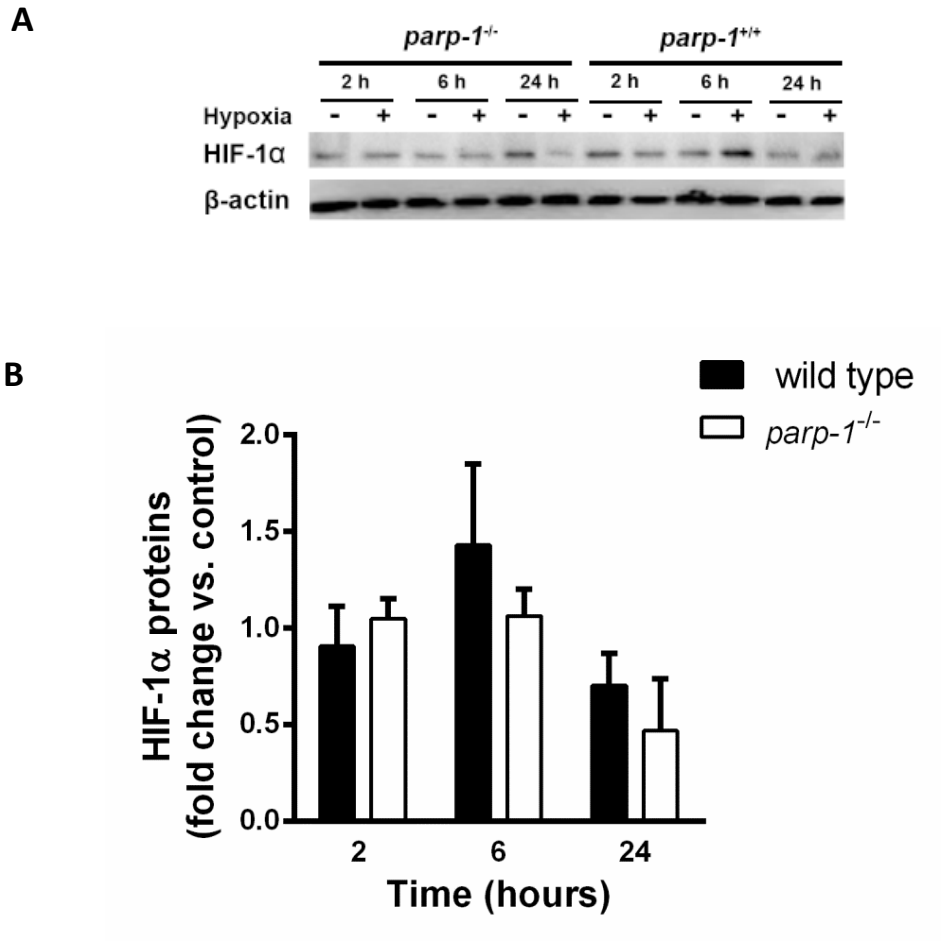

Figure 6: Total HIF-1α protein levels are PARP-1 independent and do not change significantly in severe hypoxia.

Cortical neurons were exposed to 2, 6, and 24 hr hypoxia. Total cell lysates were then isolated and 120 Kda HIF-1α and 42 Kda β-actin proteins were quantified. ***A***, Immunoblotting (IB) with an anti-HIF-1α antibody (Abcam) and anti-β-actin antibody (Sigma-Aldrich). ***B***, Significant differences were not detected at any time point and were not seen between the different groups. All data are reported as mean ± SEM; n = 3-4 and were analyzed using two–way ANOVA with the Bonferroni *post hoc* test.

3.2 Hypoxic Bnip3 expression is PARP-1 dependent

To determine the effect of hypoxia and PARP-1 on expression of the pro-death Bcl-2 family member protein, Bnip3, total RNA was isolated and real-time PCR performed to quantify relative changes in Bnip3 mRNA levels. Bnip3 mRNA increased to 1.5 ± 0.6, 5.7 ± 0.7 and 19.4 ± 5.0 relative to normoxic controls at 2, 6 and 24 hours of hypoxia (Fig. 7A-C), respectively. Non-selective pharmacological inhibition of PARP-1 and PARP-2 with PJ34 (10 μM) significantly attenuated hypoxic Bnip3 induction at all times points, indicating that hypoxic enhancement of Bnip3 mRNA levels is dependent on the ADP-ribosylation activity of PARP family members. The same experiment was performed using cortical neurons cultured from *parp-1*$^{-/-}$ mice. PARP-1 deletion reduced hypoxic Bnip3 mRNA enhancement from 15.8 ± 2.9 to 6.6 ± 1.4 ($p<0.01$; Fig 7D) at 24 hours of hypoxia, supporting a specific role for the PARP-1 isoform in this process. Support for our hypothesis requires that PARP-1 activity reduces cellular NAD^+ levels sufficiently to inhibit Bnip3 expression. We therefore tested whether exogenous NAD^+ supplementation could limit hypoxic increases in Bnip3 mRNA. Given during the 2, 6 and 24 hour hypoxic periods, NAD^+ (3 mM) reduced hypoxic Bnip3 mRNA levels to values not statistically different than normoxic controls (Fig. 7A-C). This experiment suggests that hypoxic Bnip3 increases known to be PARP-1-dependent also require depletion of cellular NAD^+ levels.

In addition to determining the effects of PARP-1 activity and NAD^+ supplementation on Bnip3 mRNA levels, we also investigated total Bnip3 protein levels using quantitative western blotting. Unlike Bnip3 mRNA levels, there was no significant change in total Bnip3 protein at the 2 hour hypoxia time point (Fig. 8A); however in agreement with mRNA data, the 6 and 24 hour time points were accompanied by significant increases in Bnip3 protein levels of 3.1 ± 0.36

fold and 3.5 ± 0.7-fold relative to normoxic controls (Fig. 8B, C; $p<0.01$). At both of these time points, hypoxic increases in Bnip3 protein were significantly mitigated both PJ34 (10 μM, $p<0.05$) and exogenous NAD^+ (3 mM, $p<0.05$), providing further support for the conclusion that hypoxic Bnip3 induction is PARP and NAD^+-dependent. Also in agreement with Bnip3 mRNA data in Fig. 7, hypoxic Bnip3 protein increases were much weaker in *parp-1*$^{-/-}$ neurons than in wildtype cells (Fig. 8D, $p<0.01$), strengthening the assertion that hypoxic effects on Bnip3 expression are related specifically to the PARP-1 isoform.

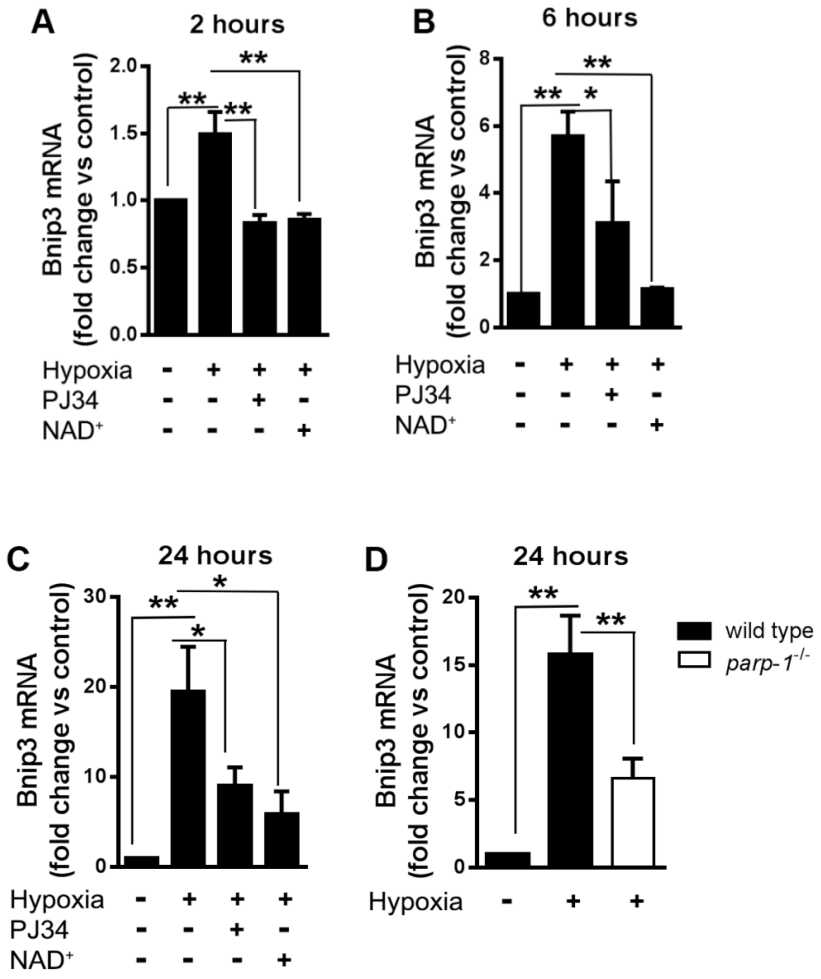

Figure 7: Hypoxia increases Bnip3 mRNA levels in a PARP-1 and NAD$^+$ sensitive manner. Cortical neurons were either exposed to 2, 6, or 24 hr hypoxia. Total cell Bnip3 mRNA levels were significantly increased at all times after exposure to hypoxia. ***A-C,*** Pharmacological inhibition of PARP-1 with 10 μM PJ34 as well as supplementation of cells with 3 mM exogenous NAD$^+$ reduced hypoxic Bnip3 mRNA levels to values not statistically different than normoxic controls. ***D***, PARP-1 deletion reduced Bnip3 mRNA hypoxic increase to a level not statistically different from wild type normoxia supporting the effect of PARP-1 on Bnip3 expression. $^*p<0.05$ and $^{**}p<0.01$. Data are all reported as the mean ± SEM (*n* = 5-8 for **A**, n = 3 for **B**, n = 8-9 for **C**, n = 4 for **D,** n = 4-6. All data are analyzed using one-way ANOVA with Student-Newman-Keuls *post hoc* test.

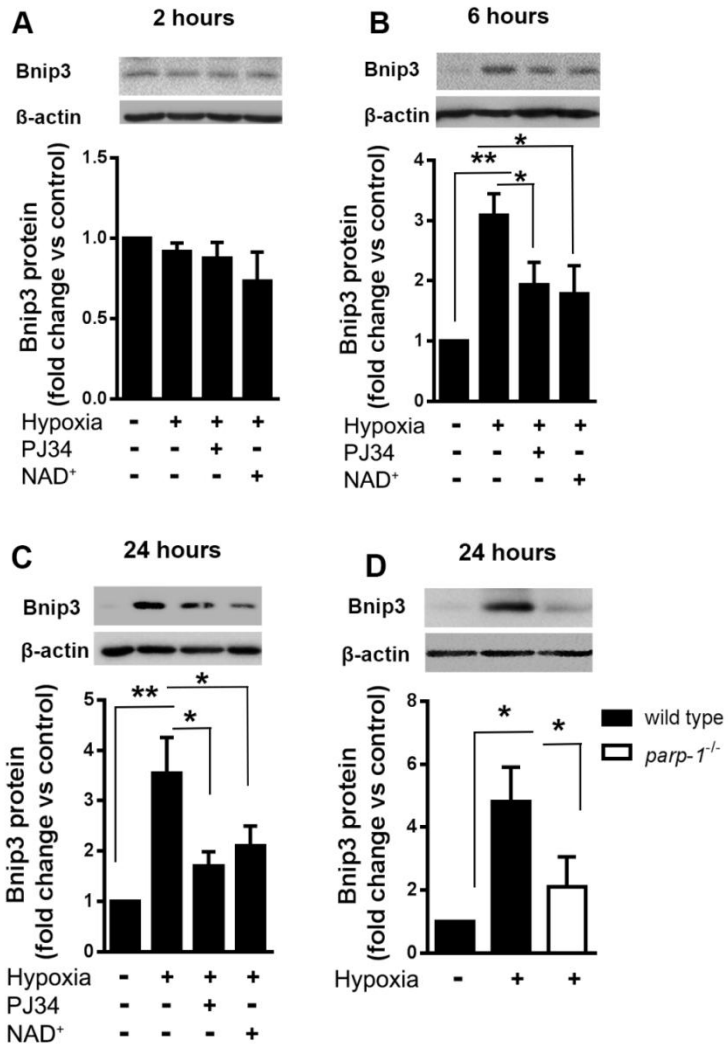

Figure 8: Hypoxia increases Bnip3 protein expression in a PARP-1 and NAD$^+$-sensitive manner.

Cortical neurons were exposed to 2, 6, or 24 hr hypoxia. Total cell Bnip3 protein levels were increased at 6 and 24 hours, but not at 2 hours, after exposure to hypoxia**.** ***A-C,*** Pharmacological inhibition of PARP-1 with 10 µM PJ34 as well as supplementation of cells with 3 mM exogenous NAD^+ reduced hypoxic Bnip3 protein levels to values not statistically different than normoxic controls. ***D***, PARP-1 deletion reduced hypoxic Bnip3 protein to a level not statistically different from wild type normoxia supporting the effect of PARP-1 on Bnip3 protein levels. $^*p<0.05$ and $^{**}p<0.01$. Data are all reported as the mean ± SEM (n=3-6). All data are analyzed using one-way ANOVA with Student-Newman-Keuls *post hoc* test.

3.3 Hypoxia causes PARP-1-dependent NAD^+ depletion and sirtuin deacetylase inhibition

Both PARP-1 ADP-ribosylation and sirtuin deacetylase activities use NAD^+ as a substrate. We next tested whether dramatic increases in PARP-1 activity in hypoxia are sufficient to cause a noticeable decline in cell NAD^+ levels and a commensurate reduction in sirtuin deacetylase activity. Hypoxia reduced NAD^+ levels from 1.2 ± 0.096 to 0.72 ± 0.016 nmol/mg protein ($p<0.01$) in cortical neuron cultures after 6 hours, and from 1.1 ± 0.13 to 0.52 ± 0.057 nmol/mg protein ($p<0.01$) after 24 hours (Fig. 9A). In accordance with these data, NAD^+-dependent sirtuin deacetylase activity also declined significantly at 6 and 24 hours of hypoxia (Fig. 9B, $p<0.01$). Re-establishment of NAD^+ by exogenous supplementation (3 mM) restored normal deacetylase activity to levels indistinguishable from normoxic controls ($p>0.05$), suggesting that NAD^+ depletion is a driving force behind sirtuin inhibition. Moreover, PARP inhibition by PJ34 (10 μM) curtailed loss of both NAD^+ (Fig. 9A) and sirtuin activity (Fig. 9B), suggesting that PARP-1 is a contributor to NAD^+ depletion to an extent sufficient to cause sirtuin inhibition.

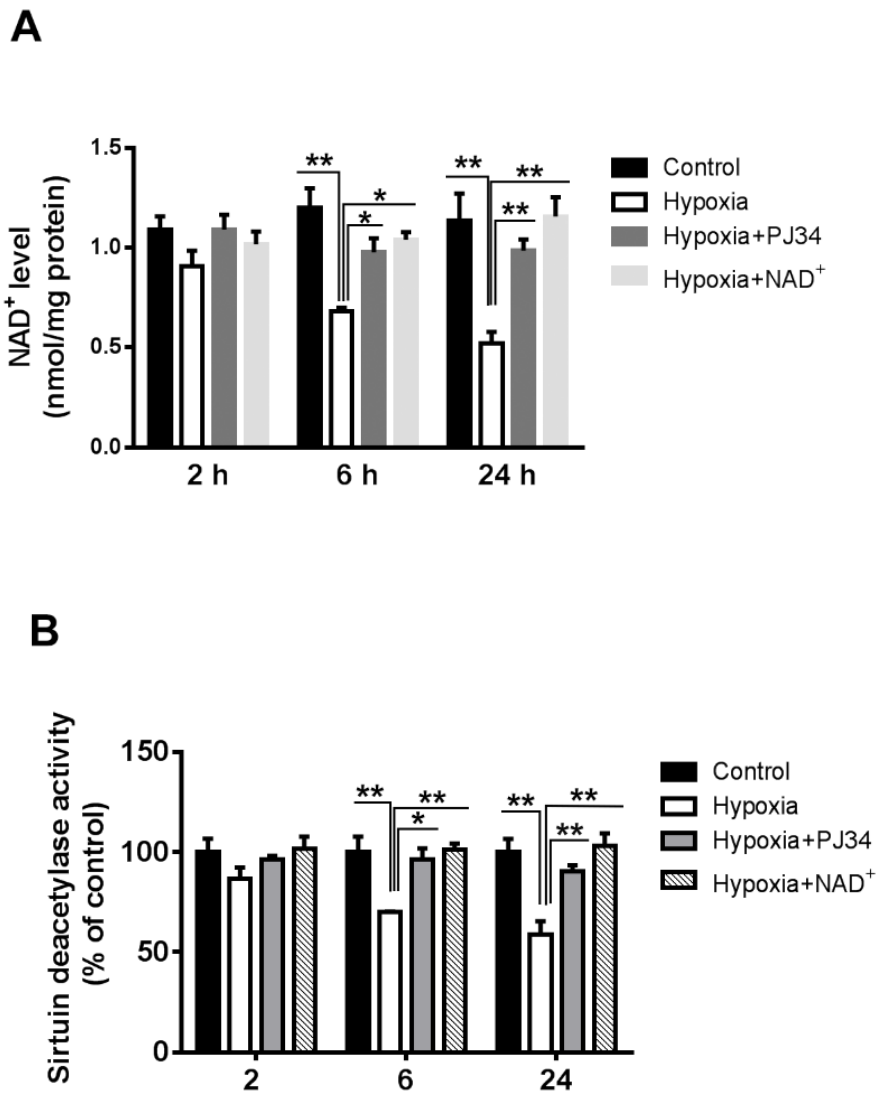

Figure 9: Hypoxia causes PARP-1 dependent NAD^+ depletion and sirtuin inhibition

A, Exposure of cortical neurons to 6 and 24 hr, but not as early as 2 hr of hypoxia reduced total cell NAD^+ measured by high-performance liquid chromatography (HPLC). $^{**}p < 0.01$ compared with the normoxic control group. NAD^+ loss was rescued at both 6 and 24 hr by the PARP inhibitor, PJ34 (10 μM) and the exogenous NAD^+ (3 mM) replacement. $^{*}p < 0.05$ and $^{**}p < 0.01$, compared with the hypoxic group. ***B***, Sirtuin deacetylase activity, measured using SIRT Direct Fluorescent Screening Assay Kit, was reduced by 6 and 24 hr hypoxia. $^{**}p < 0.01$ compared with the normoxic control group. Sirtuin deacetylase activity was rescued by the PARP-1 inhibitor, PJ34 (10 μM) and the exogenous NAD^+ (3 mM) replacement at both 6 and 24 hr hypoxia. $^{*}p < 0.05$ and $^{**}p < 0.01$, compared with the hypoxic group. All data are reported as the mean ± SEM and were analyzed using two-way ANOVA with the Bonferroni *post hoc* test.

3.4 Hypoxia induces PARP-1 dependent HIF-1α hyper-acetylation

Sirtuins interact physically with the α subunit of the transcription factor HIF-1 to cause deacetylation (Laemmle et al., 2012). We hypothesized that PARP-1 mediated inhibition of sirtuin deacetylase activity in hypoxia leads to enhanced HIF-1α acetylation. Total cell homogenates were separated by polyacrylamide gel electrophoresis and immunoblotted using an anti-acetyl-lysine antibody after exposing cortical neurons to either 6 hr or 24 hr of hypoxia. Many bands were detected, including one at the expected site of HIF-1α (Fig. 10A; 120 KDa, red frame). Acetylation level was enhanced in hypoxia in comparison with normoxia. Hypoxic increases in lysine-residue acetylation levels were mitigated by both PJ34 (10 μM) and exogenous NAD^+ (3 mM) (Fig. 10A). Blots were then stripped (Fig. 10B) and re-probed with anti-HIF-1α. This produced the expected 120 KDa HIF-1α band (Fig. 10 C, red frame). HIF-1α protein levels did not vary a lot between the different treatment groups (Fig. 10C) confirming that HIF-1α protein stability is PARP-1 independent as previously shown in Fig. 6. Pseudo-coloured images indicate that the putative acetylated HIF-1α band (Fig. 10D, green) and the HIF-1α band (Fig. 10D, red) overlay precisely at the same molecular weight (Fig. 10D, yellow), suggesting both antibodies are detecting the same protein (HIF-1α). We then quantified ratios of acetylated HIF-1α (Fig. 10A) to total HIF-1α. At both 6 (Fig. 10E) and 24 (Fig. 10F) hours of hypoxia, acetylated HIF-1α levels were significantly increased 1.6 ± 0.19 fold and 1.6 ± 0.28 fold, respectively ($p<0.01$ and $p<0.05$). This effect was eliminated to levels not different than normoxic controls at 6 and 24 hours respectively by PJ34 (10 μM) (0.69 ± 0.21 fold, $p<0.01$ and 1.1 ± 0.08 fold, $p<0.05$) and PARP-1 deletion (0.59 ± 0.11 fold, $p<0.01$ and 0.88 ± 0.11 fold, $p<0.05$), indicating acetylation is PARP-1-dependent. Supplementation of media with NAD^+ (3 mM) also

eliminated HIF-1α hyperacetylation at both 6 and 24 hours to 0.67 ± 0.21 fold, $p<0.01$ and 0.93 ± 0.08, $p<0.05$ fold respectively, indicating an NAD^+-dependent process.

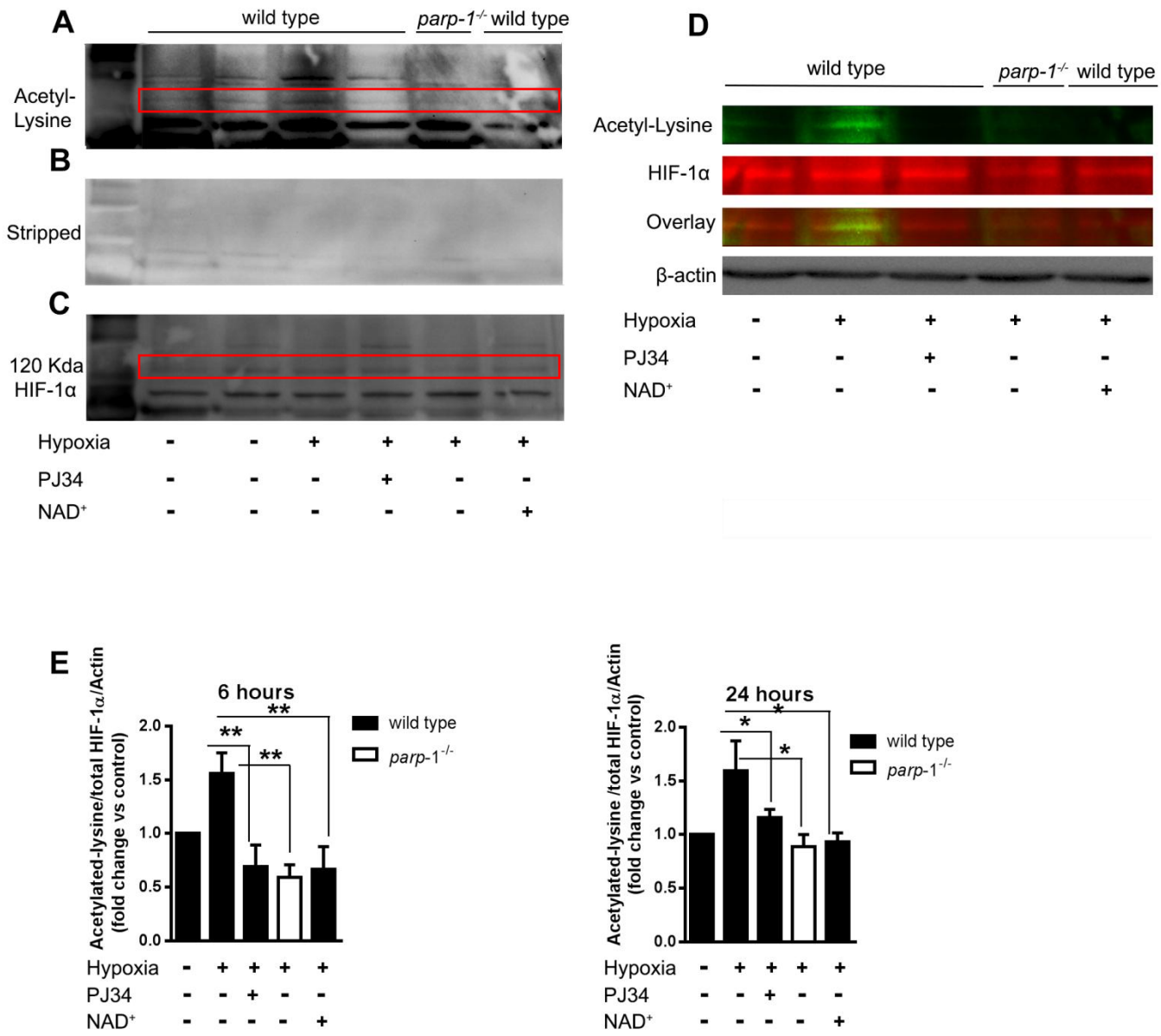

Figure 10: Hypoxia enhances PARP-1-dependent HIF-1α acetylation.

Cortical neurons were exposed to 6 and 24 hr hypoxia. ***A,*** Acetyl-lysine proteins detected by quantitative immunoblotting. Hypoxia increases acetylation in a manner reversed by 10 μM PJ34 (PARP inhibitor), PARP-1 deletion, and 3 mM NAD^+ supplementation. ***B***, Blot stripped with Restore Western Blot Stripping buffer (Thermo Fisher Scientific) at 37°C for 30 min followed by 5 min wash in TBST and incubation with anti-rabbit IgG, HRP-linked antibody (1:1000 Cell Signaling) for 1 hr 30 min at room temperature verifying effective removal of anti-acetyl-lysine primary antibody. ***C***, Hypoxic 120 KDa HIF-1α protein levels are not significantly different from normoxic levels and are not affected by neither PARP-1 inhibition/deletion nor by NAD^+ supplementation. ***D,*** ~120 KDa anti-acetyl-lysine band (green) merged with 120 KDa HIF-1α band (red) shows successful overlay of the 2 bands allowing quantification of anti-acetyl-lysine

HIF-1α (yellow) at 6 and 24 hr hypoxia in ***E-F,*** respectively. Hypoxia significantly increases acetylation of HIF-1α at both time points This increase was attenuated by PARP-1 inhibition and deletion as well as by NAD^+ supplementation, **$p<0.01$ and *$p<0.05$. Data are all reported as the mean ± SEM (n=5-7). All data are analyzed using one-way ANOVA with Student-Newman-Keuls *post hoc* test.

3.5 Hypoxia increases HIF-1α binding to the Bnip3 upstream promoter region

Hyper-acetylated HIF-1α promotes HIF-1 assembly and transcriptional regulation by HIF-1. To determine whether PARP-1-mediated sirtuin inhibition and HIF-1α hyper-acetylation influences Bnip3 transcription, we used a chromatin immunoprecipitation approach, followed by qPCR, to assess physical association of HIF-1α with a specific HRE consensus sequence in the Bnip3 upstream promoter region. Fragmented nuclear DNA was immunoprecipitated with an anti-HIF-1α antibody. Recovered DNA was then analyzed by real-time qPCR using HRE-flanking primers to produce a 265-bp amplicon that served as a quantifiable indicator of DNA associated with HIF-1α binding (Fig. 11A). Hypoxia significantly enhanced levels of the HIF-1α-associated DNA amplicon, relative to normoxic controls, at 6 hours (Fig. 11B; 1.9 ± 0.4-fold, $p<0.05$) and 24 hours (Fig. 11C; 2.5 ± 0.2-fold, $p<0.01$). This indicates enhanced Bnip3 HIF-1/HRE binding in hypoxia. At both time points, this effect was significantly attenuated by PJ34 (10 μM, $p<0.01$) and PARP-1 deletion ($p<0.05$, 6 hr; $p<0.01$, 24 hr) to levels not distinguishable from normoxic controls, indicating dependence on PARP-1. Replenishment of NAD^+ levels (3 mM) had a similar effect ($p<0.01$), supporting the conclusion that loss of NAD^+ is required to support hypoxic HIF-1/HRE interaction in the Bnip3 promoter region.

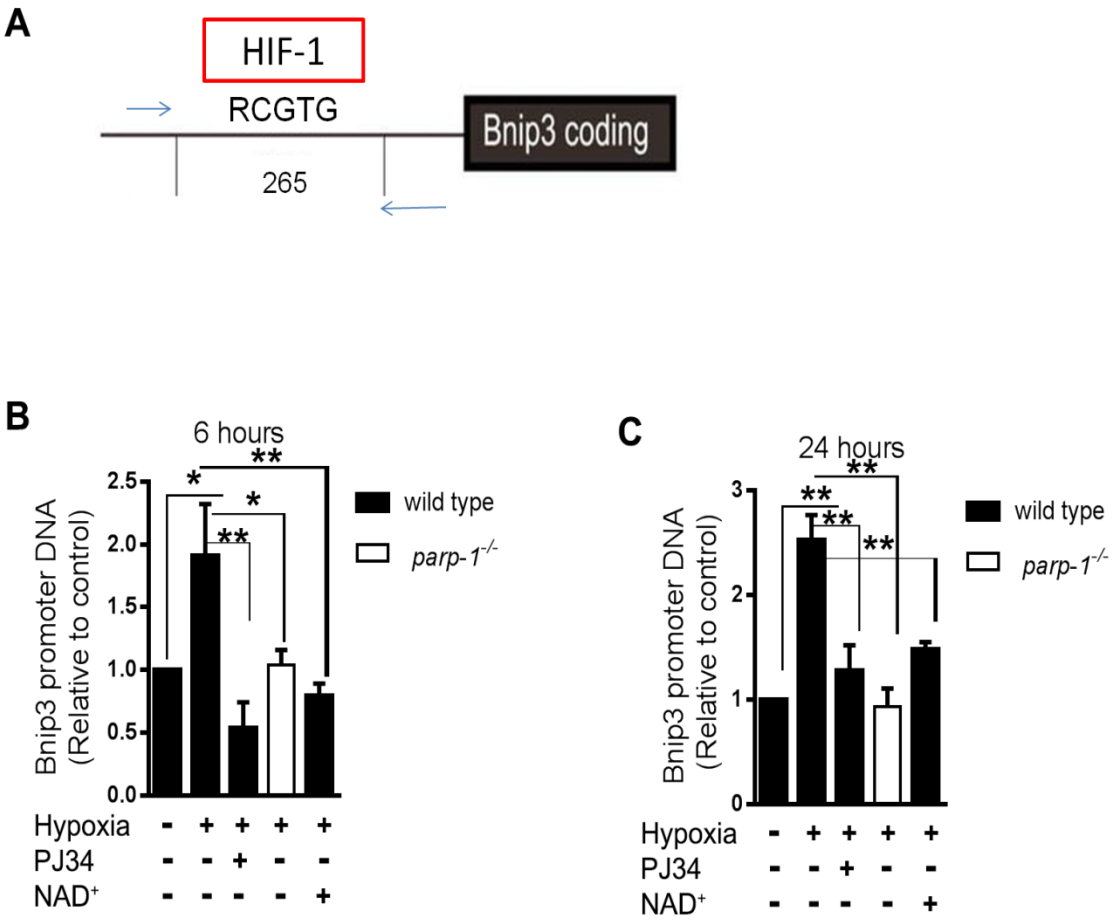

Figure 11: Hypoxia causes PARP-1 dependent interaction of HIF-1α with HREs in the Bnip3 upstream promoter region.

A, Chromatin immunoprecipitation with an anti-HIF-1α antibody (Abcam), followed by real-time qPCR using primers flanking a putative Hypoxia response element (HRE), produced a 265 bp fragment. This DNA fragment was quantified in hypoxia to determine relative extent of HIF-1/HRE binding as a surrogate for HIF-1-induced Bnip3 transcription. ***B***, Hypoxia induces significant increase in HIF-1 binding to the Bnip3 upstream promoter region at 6 hr ($^{*}p < 0.05$) and 24 hr ($^{**}p < 0.01$). Enhanced interaction was mitigated with the PARP-1 inhibitor PJ34 (10 μM) at both time points ($^{**}p < 0.01$), PARP-1 deletion ($^{*}p < 0.05$), and NAD^{+} (3 mM) supplementation ($^{*}p < 0.05$). All data are reported as mean ± SEM (n = 3-6 at 6 hr, n = 5-7 at 24 hr) using ANOVA with the Student-Newman-Keuls *post hoc* test.

3.6 Hypoxic Bnip3 expression is HIF-1α dependent

We have demonstrated that HIF-1α and Bnip3 are both affected by hypoxia in a way that supports a cause and effect relationship governed by transcriptional regulation of Bnip3 by HIF-1. The next step was to strengthen these findings by providing direct evidence of cause and effect. To achieve this, we generated lentiviral particles expressing shRNA directed against mouse HIF-1α. Cortical neuron cultures were exposed to shRNA or one of two negative control shRNA sequences (scramble shRNA or GFP sequence shRNA) for 72 hours at a multiplicity of infection of 2.0. This approach resulted in HIF-1α mRNA silencing to 13 ± 2% control values (Fig. 12A, $p<0.01$), and HIF-1α protein silencing to 36 ± 7% control (Fig. 12B, $p<0.01$). After verification of significant silencing, cultures with scrambled or HIF-1α shRNA were exposed to hypoxia and Bnip3 mRNA and total protein levels assessed. Relative to the normoxic control, shRNA reduced hypoxic Bnip3 mRNA level increases from 9.4 ± 0.6-fold for the scrambled shRNA sequence to 2.3 ± 0.2-fold (Fig. 12C, $p<0.01$). Similarly, shRNA reduced hypoxic Bnip3 protein expression increases from 3.3 ± 0.82-fold for the scrambled shRNA sequence to 0.6 ± 0.1-fold (Fig. 12D, $p<0.01$). In no cases, neither normoxic nor hypoxic, were control shRNA sequences significantly different than control without lentiviral treatment. These data collectively demonstrate that hypoxic increases in Bnip3 expression can be mediated by the activity of HIF-1α.

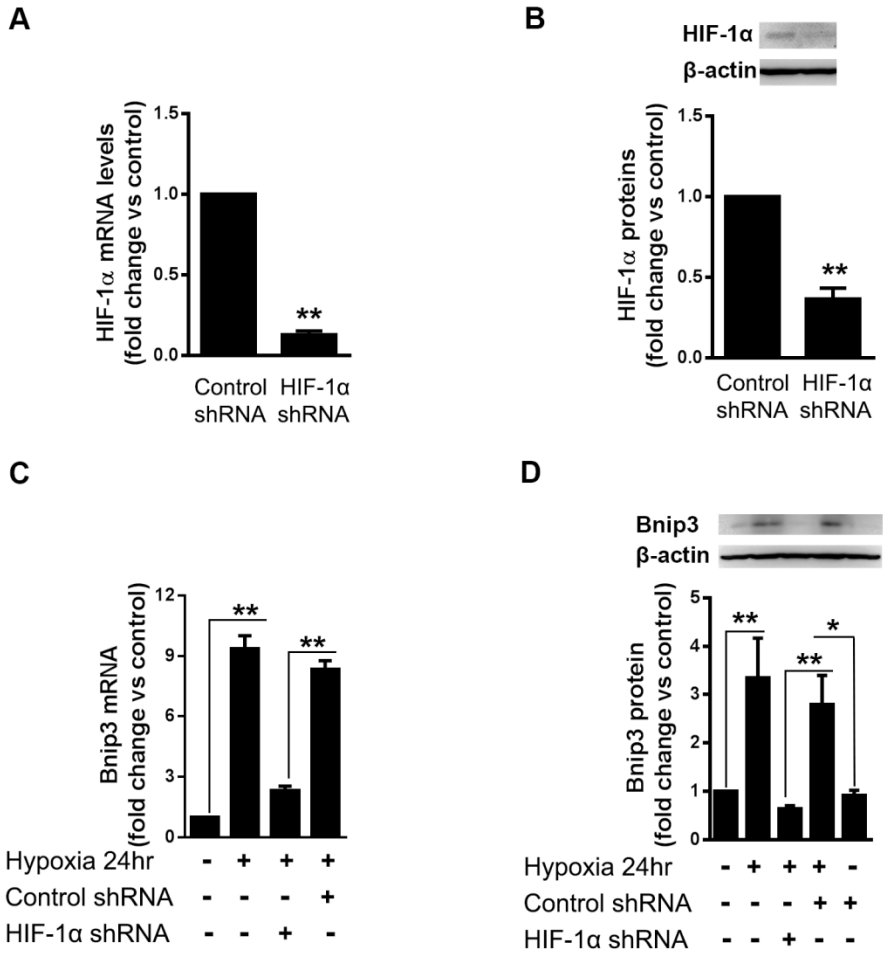

Figure 12: HIF-1α silencing reduces hypoxic Bnip3 expression.

Cortical neuron cultures were treated with lentiviral particles expressing either scrambled shRNA as a control or shRNA directed to reduce transcription of HIF-1α. Real time PCR (***A***) and western blotting (***B***) indicated a dramatic reduction of HIF-1α mRNA and protein levels respectively, thus supporting successful partial HIF-1α silencing ($^{**}p<0.01$). ***C-D,*** Hypoxia (24 hr) enhanced Bnip3 mRNA and protein levels ($^{**}p<0.01$) in a manner significantly attenuated by HIF-1α shRNA ($^{**}p<0.01$ and $^{*}p<0.05$ respectively). All data are reported as mean ± SEM (n = 5-7) using ANOVA with the Student-Newman-Keuls *post hoc* test.

3.7 Genotoxic PARP-1 activation induces HIF-1-dependent Bnip3 expression

Experiments to this point have shown linkage of PARP-1 to each part of the hypoxic pathway from NAD^+ depletion to Bnip3 expression using loss of function tools. However, common involvement of PARP-1 at each step does not equate to a demonstration that PARP-1 activation can be the pivotal starting point for this hypoxic cascade. It remains possible that a plethora of other perturbations caused by hypoxia leads to the endpoints we have observed, with or without PARP-1 dependence. To address this, we used an *N*-methyl-*N*`-nitro-*N*-nitrosoguanidine (MNNG) genotoxicity model that is employed extensively to activate PARP-1 more selectively that hypoxia is expected to (Chiu et al., 2011, Xu et al., 2006). This better isolates the consequences of PARP-1 activation so that we can determine whether the HIF-1α/Bnip3 cascade can be initiated by PARP-1 activity. Cortical neuron cultures were exposed to MNNG (50 μM, 30 min) and then rescued into normal culture medium. Similar to hypoxia, MNNG increased Bnip3 mRNA levels by 1.8 ± 0.17-fold 4 hours after rescue (Fig. 13A, $p<0.01$). Bnip3 induction was sensitive to both PJ34 (10 μM) and NAD^+ (3 mM). Again in accordance with hypoxia findings, MNNG also caused a significant decline in NAD^+ levels, from 1.6 ± 0.08 to 0.5 ± 0.1 nmol/mg protein ($p<0.01$), which was attenuated by the PARP-1 inhibitor, PJ34 (Fig 13B, $p<0.01$).

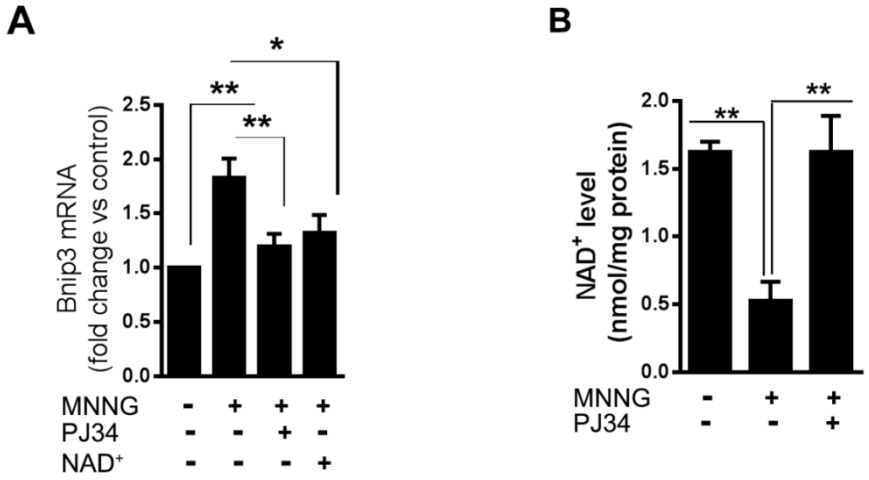

Figure 13: Direct PARP-1 activation by DNA damage induces Bnip3 expression and NAD^+ depletion.

Cortical neurons were exposed to the DNA alkylating agent (50 µM; 30 min) to cause pathological activation of PARP-1. ***A***, Total cell Bnip3 mRNA levels were significantly increased 4 hrs after MNNG removal ($^{**}p<0.01$), in a manner reversed by addition of 10 µM of the PARP-1 inhibitor, PJ34, ($^{**}p<0.01$), and 3 mM NAD^+ supplementation ($^{*}p<0.05$). ***B***, NAD^+ levels were reduced 4 hrs after MNNG removal, compared to control cells ($^{**}p<0.01$); PJ34 treatment preserved NAD^+ to control levels ($^{**}p<0.01$). All data are reported as mean ± SEM (n = 5-9) using ANOVA with the Student-Newman-Keuls *post hoc* test.

To further illustrate the role of direct PARP-1 activation in the sirtuin/HIF-1α/Bnip3 cascade, we performed HIF-1α chromatin immunoprecipitation, followed by Bnip3 HRE real-time qPCR. MNNG increased HIF-1α-associated amplicon levels by 2.1 ± 0.5-fold 4 hours after rescue (Fig. 14A, $p<0.01$). This effect was statistically eliminated by both PJ34 ($p<0.01$) and NAD^+ ($p<0.01$) replacement. Finally, we determined that normoxic MNNG treatment is sufficient to produce enhanced Bnip3 mRNA levels (Fig. 14B, $p<0.01$) and that this effect is at least partially dependent on HIF-1α, as shRNA for HIF-1α but not scrambled shRNA dramatically reduced that effect of MNNG ($p<0.01$). Taken together, these data show that direct activation of PARP-1 by MNNG is capable of phenocopying NAD^+ and HIF-1α-dependent Bnip3 induction, independent of hypoxia.

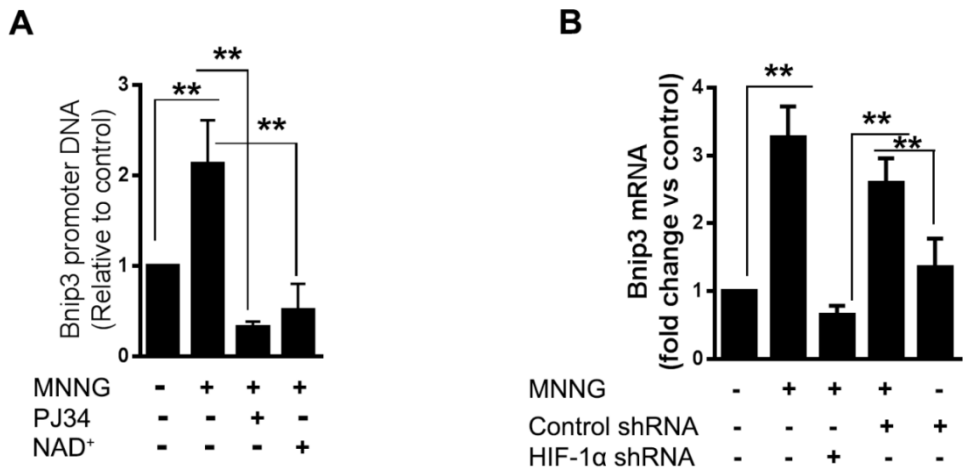

Figure 14: Direct PARP-1 activation by DNA damage enhances HIF-1-Bnip3 interaction causing increased HIF-1-dependent Bnip3 expression.

A, Chromatin immunoprecipitation with anti-HIF-1α antibody (Abcam), followed by real-time qPCR using primers flanking a putative HIF-1α response element (HRE). MNNG-induced PARP-1 activation caused a significant increase in Bnip3 promoter DNA binding HIF-1 in a manner reduced by 10 μM PJ34 addition or 3 mM NAD^+ supplementation ($^{**}p<0.01$). ***B***, Similar to hypoxia, 50 μM MNNG (30 min) induced increases in Bnip3 mRNA levels were attenuated by treating cortical neurons with HIF-1α, but not control (scramble) shRNA, ($^{**}p<0.01$). All data are reported as the mean ± SEM (n = 4-6) and compared using one way ANOVA with the Student-Newman-Keuls *post hoc* test.

Chapter 4: Discussion

The results of this thesis support a novel signaling pathway for hypoxic neuronal expression of the pro-death factor Bnip3, mediated by excessive DNA damage-induced PARP-1 overactivation. There is significant evidence from the literature that Bnip3 leads to caspase-independent neuronal death in hypoxia/ischemia models by causing mitochondrial permeability (Zhang et al., 2011b, Diwan et al., 2007, Regula et al., 2002, Lu et al., 2014). Our previous results showed increased expression of total cell Bnip3 transcript and protein within 24 hours of hypoxia. Therefore, our objective was to gain insight into the mechanism and develop concepts about how to limit Bnip3 expression for therapeutic gain. We originally postulated that PARP-1 is a logical candidate mediator of Bnip3 induction largely because PARP-1 and Bnip3 were both observed to cause mitochondrial-dependent and caspase-independent programmed cell death in ischemic stroke models (Yu et al., 2002, Virag et al., 1998, Desagher and Martinou, 2000). Current results support this idea by showing that enhanced Bnip3 expression in hypoxia is dependent on PARP-1 activity, and by identifying a novel signaling pathway leading from PARP-1 activity to Bnip3 expression. Previously, we showed that the transcription factor FOXO3a acts as a link between PARP-1 and Bnip3. PARP1 influenced Bnip3 production by depleting cytosolic NAD^+, inhibiting sirtuin deacetylase activity, and causing increased binding of FoxO3a to the Bnip3 upstream promoter region (Lu et al., 2014). We now show that sirtuin inhibition by hypoxic PARP-1 activity affects not only FOXO3a, but also HIF-1α, leading to HIF-1-driven Bnip3 transcript and protein elevations. Overall, results show that hypoxic PARP-1 activity leads to sequential depletion of intracellular NAD^+ levels, inhibition of NAD^+-dependent sirtuin deacetylase activity, hyper-acetylation of HIF-1α, and enhanced HIF-1-driven Bnip3 expression (Fig. 15). These results add to an important body of literature showing that

PARP-1-induced NAD^+ depletion leads to a network of harmful events that lead to neuronal death and support strategies aimed at enhancing NAD^+ or limiting HIF-1 activity as encouraging research directions.

Several observations support the conclusion that hypoxia leads to PARP-1-mediated HIF-1α modification and Bnip3 induction. We assessed six separate outcomes in response to 6 hours and 24 hours of hypoxia, each postulated as necessary sequential steps in our hypothetical PARP-1/HIF-1 signaling axis. We confirmed that PARP-1 induces NAD^+ depletion in hypoxia (Fig. 9A) and determined that this total cell depletion represented nuclear/cytosolic NAD^+ depletion sufficient to inhibit sirtuin deacetylase activity. Under normal conditions, endogenous sirtuin and HIF-1 co-immunoprecipitate allowing sirtuin decatylase to consume cytosolic/nuclear NAD^+ and deacetylate the alpha subunit of HIF-1. This reduces HIF-1 complex formation and inhibits expression of HIF-1-dependent genes (Laemmle et al., 2012). Therefore, we verified whether the PARP-1 induced loss of sirtuin activity in hypoxia leads to a hyperacetylation of HIF-1α. Our results showed increased acetylation in HIF-1α in hypoxic cells. HIF-1 is a transcription factor known to bind the Bnip3 upstream promoter region and regulate its expression (Greijer and van der Wall, 2004). Using a chromatin immunoprecipitation strategy, we also determined that PARP-1-induced HIF-1α hyper-acetylation corresponds with physical binding of HIF-1 to the Bnip3 upstream promoter region. Finally, in agreement with the other experiments, we also showed that hypoxia increases Bnip3 transcript and protein levels. Previously, our lab measured total cell Bnip3 mRNA at 0,20,40,60, and 80 hours of hypoxia, reporting a time-dependent increase starting at 12 hours and reaching its maximum at 80 hours (Lu et al., 2014). Consistently, we have shown a significant increase in Bnip3 mRNA and proteins starting at 12 hours of hypoxia. Although earlier studies have reported that Bnip3

expression happens in a delayed manner and is first detected at around 36 hours of hypoxia (Bruick, 2000), we and others reported an earlier increase in Bnip3 expression and protein levels (Walls et al., 2009, Regula et al., 2002). This could be explained by the fact that there are 2 isoforms of Bnip3 proteins with molecular weights of 30 kDa and 60 kDa. In neurons exposed to <36 hours of hypoxia, the 30 kDa isoform was the only detected form. However, exposure of cells to longer than 36 hours of hypoxia induced accumulation of both Bnip3 protein isoforms (Zhang et al., 2007b, Bruick, 2000) explaining the higher increase detected at later time points. All hypoxic effects, including NAD^+ depletion, sirtuin activity, HIF-1α acetylation, HIF-1/Bnip3 binding and expression levels, were mitigated by pharmacological and genomic PARP-1 silencing. These results strongly indicate that PARP-1 is a hypoxic mediator for all outcomes in our proposed PARP-1/Bnip3 signaling pathway.

In addition to showing that PARP-1 loss of function mitigates hypoxic HIF-1α modification and Bnip3 expression, we also demonstrated directly that HIF-1α is required for Bnip3 induction using a lentiviral shRNA approach. HIF-1α shRNA caused significant HIF-1α silencing and suppressed hypoxic enhancements of Bnip3 message and protein. This positively implicates HIF-1α in hypoxic Bnip3 induction but we recognized these experiments do not directly tell us whether PARP-1 is required in this pathway. There are two experiments that suggest to us that PARP-1 indeed does lead to Bnip3 induction by a mechanism dependent on HIF-1α. First, using chromatin immunoprecipitation we showed hypoxic increases in HIF-1 binding to HRE sequences specifically in the Bnip3 upstream promoter region in a manner that was reduced by PARP-1 inhibition and deletion. Second, involvement of PARP-1 was further supported by use of a second cell toxicity model (genotoxicity using MNNG). MNNG directly activates PARP-1 by creating DNA strand breaks (Chiu et al., 2011). MNNG-induced PARP-1

activity enhanced Bnip3 levels and this was mitigated by HIF-1α shRNA, directly supporting a role for PARP-1 inducing Bnip3 in a HIF-1α-dependent manner.

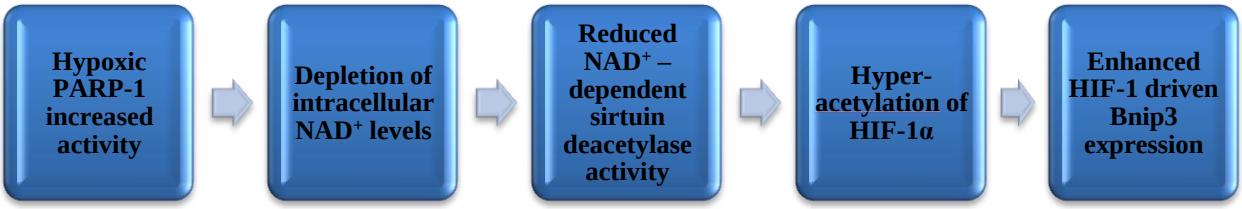

Figure 15: Novel PARP-1 cell death pathway - Major findings.

Increased PARP-1 activation in cerebral ischemia leads to depletion of nuclear and cytosolic NAD^+ levels to a point where NAD^+ are no longer available for the sirtuin deacetylase activity. This inhibits the lysine deacetylation of the alpha subunit of the proapoptotic transcription factor HIF-1 leading to HIF-1 activation, followed by increased expression of the proapoptotic mitochondrial protein, Bnip3.

Our data clearly support a role for PARP-1 in a post-translation modification of HIF-1α (acetylation) as a driving force for Bnip3 expression. It is important however to consider this in the context of other possible interactions between PARP-1 and HIF-1α. We considered the possibility that hypoxia could influence HIF-1α expression (Hatfield et al., 2010, Semenza, 1999) or that PARP-1 could bind directly to HIF-1α (Elser et al., 2008). We monitored HIF-1α transcript levels in response to hypoxia and saw no significant difference compared to normoxic cells. Hypoxic induction of HIF-1α is suggested to be seen at the protein level due to inhibition of oxygen-dependent prolyl hydroxylase enzymes, which in normoxia use O_2 to hydroxylate HIF-1α and induce its degradation by the ubiquitin-proteasome pathway (Greijer and van der Wall, 2004). We however saw no change in protein levels either. One possible explanation for why our results didn't show upregulation of HIF-1α protein in hypoxia is that in our severe hypoxia model of nominal anoxia (~0.02% O_2), there is increased accumulation of p53 (Sermeus and Michiels, 2011). p53 is known to bind HIF-1α and HIF-1α becomes unstable when bound to p53 (Ravi et al., 2000), thus reducing HIF-1α stability at nominal anoxia. HIF-1α proteins are however more stable under hypoxic conditions where O_2 levels are higher than 2% partially because p53 levels are not as high as in anoxia (Hammond et al., 2002). In addition, the same experiments (Figs. 5 and 6) showed no effect of the absence of PARP-1 on either HIF-1α mRNA or protein levels. A previous study found that HIF-1α accumulates more in wildtype than in *parp-1*$^{-/-}$ cortical neurons in hypoxia (Martinez-Romero et al., 2009). However the same group and others also reported that PARP-1 does not increase HIF-1α expression (Martinez-Romero et al., 2012, Elser et al., 2008). It also remains possible that PARP-1 and HIF-1α interact directly. PARP-1 was shown to coactivate HIF-1α-dependent gene expression by physically interacting and forming a complex with HIF-1α in K562 tumor cells (Elser et al., 2008). In other words,

expression of HIF-1-dependent genes required PARP-1 as a transcriptional co-activator. In agreement, our results showed that expression of Bnip3, a HIF-1-dependent gene, required PARP-1 to see an induction. Whether a physical interaction exists is not clear yet. We performed preliminary experiments suggesting that PARP-1 and HIF-1α co-immunoprecipitated (Fig. 16). This line of study will have to be developed further before conclusions can be drawn.

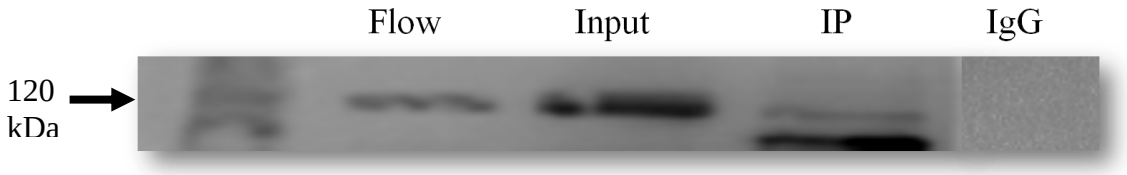

Figure 16: Co-immunoprecipitation of endogenous PARP-1-HIF-1α.

500 μg cortical neurons proteins extracts from CD-1 wild type mice were immunoprecipitated for PARP-1 using PARP-1 antibody (Abcam 9534). Samples were then probed for HIF-1α by Western blotting using 3 μg of HIF-1α antibody. IgG antibody was used as a negative control for immunoprecipitation. 30 μg of whole cell protein lysate was used as input.

The classic mechanism through which PARP-1-induced depletion of cytosolic NAD^+ causes cell death was -and still is by some- suggested to be by energy failure (Berger, 1985). The bioenergetics models suggests that NAD^+ levels are depleted to the point where cells starve for energy either due to consumption of ATP to resynthesize and replenish NAD^+ or to failed NAD^+-dependent steps of glycolysis and oxidative phosphorylation (Ying et al., 2003, Zong et al., 2004). In agreement with the bioenergetic suicide hypothesis, our previous results show that PARP-1 depletes NAD^+ levels to a point where it causes cell death and that supplementation of cells with exogenous NAD^+ can rescue cell survival (Lu et al., 2014). However, our results suggest a different NAD^+-dependent pathway of PARP-1 toxicity – that NAD^+ depletion inhibits sirtuins and leads to Bnip3 induction. In agreement with others findings, our results show that hypoxic/ischemic PARP-1 overactivation depletes cytosolic/nuclear NAD^+ pools (Lu et al., 2014, Alano et al., 2007). Supplementation of cells with exogenous NAD^+ significantly reduced hypoxic Bnip3 transcripts and proteins, rescued sirtuin deacetylase activity, and mitigated HIF-1α hyperacetylation and subsequent binding to Bnip3 upstream promoter regions. All of this indicates that increased HIF-1α activity and Bnip3 expression result from NAD^+ depletion. In turn, increased Bnip3 expression resulting from NAD^+ depletion induces mitochondrial dysfunction and cell death, both of which can be rescued with NAD^+ supplementation (Lu et al., 2014). The results of this thesis should be considered in combination with other laboratory data, collectively showing that there are severe consequences on sirtuin-controlled signaling that result from PARP-1-mediated NAD^+ depletion. In addition to current results showing a role for HIF-1α, the Anderson lab has also shown that FOXO3a (Lu et al., 2014) and PGC-1α are also affected by PARP-1-mediated sirtuin inhibition, leading to mitochondrial dysfunction and cell death by several pathways. It should be noted that there is an NAD^+-independent theory for how

PARP-1 causes hypoxic mitochondrial damage and cell death (called Parthanatos). ADP-ribose polymers (PAR) moieties have been suggested to act as mitochondrial AIF-releasing factors independent of NAD^+ (Yu et al., 2002) (Andrabi et al., 2006, Yu et al., 2006). The debate about the NAD^+ dependence of PARP-1-mediated neuronal death is still active and developing. It is likely that there are both NAD^+-dependent and NAD^+-independent mechanisms that play a role. Because there is significant evidence that NAD^+ depletion represents a critical step in PARP-1 induced neuron death, NAD^+ enhancement strategies may be beneficial potential therapeutic agents for degenerative diseases. NAD^+ repletion decreased PARP-1-mediated cell death by preventing glycolytic inhibition, restoring oxidative phosphorylation (Ying et al., 2003), and blocking AIF mitochondrion-to-nucleus translocation (Alano et al., 2004, Alano et al., 2010). Therefore, exogenous NAD^+ administration or overexpression of NAD^+ biosynthetic enzymes may decrease ischemic brain injury. Intranasal administration of 10 mg/kg NAD^+ 2 hours after ischemic onset significantly reduced infarct formation by 85% and mitigated ischemia-induced neuronal damage when assessed at 24-72 hours after ischemia (Ying et al., 2007). Protective effects of NAD^+ have also been found in multiple other diseases including myocardial infarction (Hsu et al., 2009), Parkinson's Disease and traumatic brain injury (Ying, 2007). In addition, inhibition of the NAD^+ catabolizing enzyme, CD38, was shown to enhance NAD^+ levels and reduced oxidative damage to fibroblasts, suggesting this may be an appropriate strategy to enhance NAD^+-driven sirtuin activity.

Understanding the mechanisms of genotoxic PARP-1 activity is important for future therapeutic development in several disorders underpinned by PARP-1 activity. Parthanatos and bioenergetic suicide represent distinct PARP-1-mediated neurotoxic pathways. Our findings do not argue for or against either of these theories specifically. Rather, cumulative data from our lab

support a new companion set of NAD^+-dependent PARP-1 death pathways dependent on sirtuins and downstream transcription of pro-death targets. Results from our studies identify several new targets downstream of PARP-1 with experimental therapeutic potential. Current results of this thesis support targeting HIF-1α and NAD^+ enhancement, adding to FOXO3a and PGC-1α, identified by other lab members.

Despite the importance of this PARP-1 induced caspase-independent cell death pathway in stroke, its major limitation is that it is sex-specific. Targeting this pathway might offer neuroprotection in males but not in females. Treatment with nicotinamide, NAD^+ precursor, protects male mice and PARP-1 knockout mice, but has minimal effects in wild-type female brain (Siegel and McCullough, 2013). This may be secondary to sexual differences in preservation of mitochondrial energy metabolism (Klaidman et al., 2003). Hence, this could be a limitation to the interpretation of data from the cell culture results. Future studies will be designed to further elucidate these pathways and how they might be targeted for therapeutic value in disorders characterized by PARP-1 over-activity. For example, mouse temporary global ischemia (TGI) might be used to determine whether HIF-1 contributes to Bnip3 expression *in vivo*. Bnip3 protein expression and transcripts will be quantified, PARP1/HIF-1 signaling pathways will be evaluated, hippocampal NAD^+ levels will be measured and Sirt1/HIF-1α co-IP, HIF-1α acetylation and HIF-1α CHIP of Bnip3 promoter sequences will be performed in hippocampal homogenates. Hippocampal neuron death will be quantified in frozen sections and animal behavior will be assessed using open field activity and Morris Water Maze test to identify locomoter differences that could bias the measures of learning and memory.

Chapter 5: References

ALAGARSAMY, S., MARINO, M. J., ROUSE, S. T., GEREAU, R. W. T., HEINEMANN, S. F. & CONN, P. J. 1999. Activation of NMDA receptors reverses desensitization of mGluR5 in native and recombinant systems. *Nat Neurosci,* 2**,** 234-40.

ALAGARSAMY, S., ROUSE, S. T., JUNGE, C., HUBERT, G. W., GUTMAN, D., SMITH, Y. & CONN, P. J. 2002. NMDA-induced phosphorylation and regulation of mGluR5. *Pharmacol Biochem Behav,* 73**,** 299-306.

ALAGARSAMY, S., SAUGSTAD, J., WARREN, L., MANSUY, I. M., GEREAU, R. W. T. & CONN, P. J. 2005. NMDA-induced potentiation of mGluR5 is mediated by activation of protein phosphatase 2B/calcineurin. *Neuropharmacology,* 49 Suppl 1**,** 135-45.

ALANO, C. C., GARNIER, P., YING, W., HIGASHI, Y., KAUPPINEN, T. M. & SWANSON, R. A. 2010. NAD+ depletion is necessary and sufficient for poly(ADP-ribose) polymerase-1-mediated neuronal death. *J Neurosci,* 30**,** 2967-78.

ALANO, C. C., TRAN, A., TAO, R., YING, W., KARLINER, J. S. & SWANSON, R. A. 2007. Differences among cell types in NAD(+) compartmentalization: a comparison of neurons, astrocytes, and cardiac myocytes. *J Neurosci Res,* 85**,** 3378-85.

ALANO, C. C., YING, W. & SWANSON, R. A. 2004. Poly(ADP-ribose) polymerase-1-mediated cell death in astrocytes requires NAD+ depletion and mitochondrial permeability transition. *J Biol Chem,* 279**,** 18895-902.

ALKAYED, N. J., HARUKUNI, I., KIMES, A. S., LONDON, E. D., TRAYSTMAN, R. J. & HURN, P. D. 1998. Gender-linked brain injury in experimental stroke. *Stroke,* 29**,** 159-65; discussion 166.

ALLEN, C. L. & BAYRAKTUTAN, U. 2008. Risk factors for ischaemic stroke. *Int J Stroke,* 3**,** 105-16.

AME, J. C., SPENLEHAUER, C. & DE MURCIA, G. 2004. The PARP superfamily. *Bioessays,* 26**,** 882-93.

ANDERSON, C. M. & SWANSON, R. A. 2000. Astrocyte glutamate transport: review of properties, regulation, and physiological functions. *Glia,* 32**,** 1-14.

ANDRABI, S. A., DAWSON, T. M. & DAWSON, V. L. 2008. Mitochondrial and nuclear cross talk in cell death: parthanatos. *Ann N Y Acad Sci,* 1147**,** 233-41.

ANDRABI, S. A., KIM, N. S., YU, S. W., WANG, H., KOH, D. W., SASAKI, M., KLAUS, J. A., OTSUKA, T., ZHANG, Z., KOEHLER, R. C., HURN, P. D., POIRIER, G. G., DAWSON, V. L. & DAWSON, T. M. 2006. Poly(ADP-ribose) (PAR) polymer is a death signal. *Proc Natl Acad Sci U S A,* 103**,** 18308-13.

ARTOLA, A. & SINGER, W. 1993. Long-term depression of excitatory synaptic transmission and its relationship to long-term potentiation. *Trends Neurosci,* 16**,** 480-7.

BA, X. & GARG, N. J. 2011. Signaling mechanism of poly(ADP-ribose) polymerase-1 (PARP-1) in inflammatory diseases. *Am J Pathol,* 178**,** 946-55.

BAEK, S. H., BAE, O. N., KIM, E. K. & YU, S. W. 2013. Induction of mitochondrial dysfunction by poly(ADP-ribose) polymer: implication for neuronal cell death. *Mol Cells,* 36**,** 258-66.

BAEK, S. H., NOH, A. R., KIM, K. A., AKRAM, M., SHIN, Y. J., KIM, E. S., YU, S. W., MAJID, A. & BAE, O. N. 2014. Modulation of mitochondrial function and autophagy mediates carnosine neuroprotection against ischemic brain damage. *Stroke,* 45**,** 2438-43.

BERGER, N. A. 1985. Poly(ADP-ribose) in the cellular response to DNA damage. *Radiat Res,* 101**,** 4-15.

BERRIDGE, M. J. 1995. Inositol trisphosphate and calcium signaling. *Ann N Y Acad Sci,* 766**,** 31-43.

BESANCON, E., GUO, S., LOK, J., TYMIANSKI, M. & LO, E. H. 2008. Beyond NMDA and AMPA glutamate receptors: emerging mechanisms for ionic imbalance and cell death in stroke. *Trends Pharmacol Sci,* 29**,** 268-75.

BLANKE, M. L. & VANDONGEN, A. M. J. 2009. Activation Mechanisms of the NMDA Receptor. *In:* VAN DONGEN, A. M. (ed.) *Biology of the NMDA Receptor*. Boca Raton (FL).

BLISS, T. V. & COLLINGRIDGE, G. L. 1993. A synaptic model of memory: long-term potentiation in the hippocampus. *Nature,* 361**,** 31-9.

BROOKS, C. L. & GU, W. 2009. How does SIRT1 affect metabolism, senescence and cancer? *Nat Rev Cancer,* 9**,** 123-8.

BRUICK, R. K. 2000. Expression of the gene encoding the proapoptotic Nip3 protein is induced by hypoxia. *Proc Natl Acad Sci U S A,* 97**,** 9082-7.

BRUNET, A., SWEENEY, L. B., STURGILL, J. F., CHUA, K. F., GREER, P. L., LIN, Y., TRAN, H., ROSS, S. E., MOSTOSLAVSKY, R., COHEN, H. Y., HU, L. S., CHENG, H. L., JEDRYCHOWSKI, M. P., GYGI, S. P., SINCLAIR, D. A., ALT, F. W. & GREENBERG, M. E. 2004. Stress-dependent regulation of FOXO transcription factors by the SIRT1 deacetylase. *Science,* 303**,** 2011-5.

BRUNO, V., BATTAGLIA, G., COPANI, A., GIFFARD, R. G., RACITI, G., RAFFAELE, R., SHINOZAKI, H. & NICOLETTI, F. 1995a. Activation of class II or III metabotropic

glutamate receptors protects cultured cortical neurons against excitotoxic degeneration. *Eur J Neurosci,* 7**,** 1906-13.

BRUNO, V., COPANI, A., KNOPFEL, T., KUHN, R., CASABONA, G., DELL'ALBANI, P., CONDORELLI, D. F. & NICOLETTI, F. 1995b. Activation of metabotropic glutamate receptors coupled to inositol phospholipid hydrolysis amplifies NMDA-induced neuronal degeneration in cultured cortical cells. *Neuropharmacology,* 34**,** 1089-98.

BRUSTOVETSKY, N., DUBINSKY, J. M., ANTONSSON, B. & JEMMERSON, R. 2003. Two pathways for tBID-induced cytochrome c release from rat brain mitochondria: BAK-versus BAX-dependence. *J Neurochem,* 84**,** 196-207.

BURNASHEV, N., MONYER, H., SEEBURG, P. H. & SAKMANN, B. 1992. Divalent ion permeability of AMPA receptor channels is dominated by the edited form of a single subunit. *Neuron,* 8**,** 189-98.

BURNASHEV, N., ZHOU, Z., NEHER, E. & SAKMANN, B. 1995. Fractional calcium currents through recombinant GluR channels of the NMDA, AMPA and kainate receptor subtypes. *J Physiol,* 485 (Pt 2)**,** 403-18.

CAO, G., XING, J., XIAO, X., LIOU, A. K., GAO, Y., YIN, X. M., CLARK, R. S., GRAHAM, S. H. & CHEN, J. 2007. Critical role of calpain I in mitochondrial release of apoptosis-inducing factor in ischemic neuronal injury. *J Neurosci,* 27**,** 9278-93.

CASTILLO, P. E., MALENKA, R. C. & NICOLL, R. A. 1997. Kainate receptors mediate a slow postsynaptic current in hippocampal CA3 neurons. *Nature,* 388**,** 182-6.

CHATTERTON, J. E., AWOBULUYI, M., PREMKUMAR, L. S., TAKAHASHI, H., TALANTOVA, M., SHIN, Y., CUI, J., TU, S., SEVARINO, K. A., NAKANISHI, N., TONG, G., LIPTON, S. A. & ZHANG, D. 2002. Excitatory glycine receptors containing the NR3 family of NMDA receptor subunits. *Nature,* 415**,** 793-8.

CHEN, D., LI, M., LUO, J. & GU, W. 2003. Direct interactions between HIF-1 alpha and Mdm2 modulate p53 function. *J Biol Chem,* 278**,** 13595-8.

CHEN, M., BULLOCK, R., GRAHAM, D. I., FREY, P., LOWE, D. & MCCULLOCH, J. 1991. Evaluation of a competitive NMDA antagonist (D-CPPene) in feline focal cerebral ischemia. *Ann Neurol,* 30**,** 62-70.

CHEN, M., ZSENGELLER, Z., XIAO, C. Y. & SZABO, C. 2004. Mitochondrial-to-nuclear translocation of apoptosis-inducing factor in cardiac myocytes during oxidant stress: potential role of poly(ADP-ribose) polymerase-1. *Cardiovasc Res,* 63**,** 682-8.

CHEUNG, E. C., JOZA, N., STEENAART, N. A., MCCLELLAN, K. A., NEUSPIEL, M., MCNAMARA, S., MACLAURIN, J. G., RIPPSTEIN, P., PARK, D. S., SHORE, G. C., MCBRIDE, H. M., PENNINGER, J. M. & SLACK, R. S. 2006. Dissociating the dual roles of apoptosis-inducing factor in maintaining mitochondrial structure and apoptosis. *EMBO J,* 25**,** 4061-73.

CHIANG, Y. J., HSIAO, S. J., YVER, D., CUSHMAN, S. W., TESSAROLLO, L., SMITH, S. & HODES, R. J. 2008. Tankyrase 1 and tankyrase 2 are essential but redundant for mouse embryonic development. *PLoS One,* 3**,** e2639.

CHITTAJALLU, R., BRAITHWAITE, S. P., CLARKE, V. R. & HENLEY, J. M. 1999. Kainate receptors: subunits, synaptic localization and function. *Trends Pharmacol Sci,* 20**,** 26-35.

CHITTAJALLU, R., VIGNES, M., DEV, K. K., BARNES, J. M., COLLINGRIDGE, G. L. & HENLEY, J. M. 1996. Regulation of glutamate release by presynaptic kainate receptors in the hippocampus. *Nature,* 379**,** 78-81.

CHIU, L. Y., HO, F. M., SHIAH, S. G., CHANG, Y. & LIN, W. W. 2011. Oxidative stress initiates DNA damager MNNG-induced poly(ADP-ribose)polymerase-1-dependent parthanatos cell death. *Biochem Pharmacol,* 81**,** 459-70.

CHO, B. B. & TOLEDO-PEREYRA, L. H. 2008. Caspase-independent programmed cell death following ischemic stroke. *J Invest Surg,* 21**,** 141-7.

CHOI, D. W. 1992. Excitotoxic cell death. *J Neurobiol,* 23**,** 1261-76.

CLINE., R. C. E. A. H. T. 2009. Biology of the NMDA Receptor. *In:* PRESS, C. (ed.).

CRUZ-FLORES, S., RABINSTEIN, A., BILLER, J., ELKIND, M. S., GRIFFITH, P., GORELICK, P. B., HOWARD, G., LEIRA, E. C., MORGENSTERN, L. B., OVBIAGELE, B., PETERSON, E., ROSAMOND, W., TRIMBLE, B., VALDERRAMA, A. L., AMERICAN HEART ASSOCIATION STROKE, C., COUNCIL ON CARDIOVASCULAR, N., COUNCIL ON, E., PREVENTION, COUNCIL ON QUALITY OF, C. & OUTCOMES, R. 2011. Racial-ethnic disparities in stroke care: the American experience: a statement for healthcare professionals from the American Heart Association/American Stroke Association. *Stroke,* 42**,** 2091-116.

CURTIS, D. R., PHILLIS, J. W. & WATKINS, J. C. 1960. The chemical excitation of spinal neurones by certain acidic amino acids. *J Physiol,* 150**,** 656-82.

D'AMOURS, D., DESNOYERS, S., D'SILVA, I. & POIRIER, G. G. 1999. Poly(ADP-ribosyl)ation reactions in the regulation of nuclear functions. *Biochem J,* 342 (Pt 2)**,** 249-68.

DANIAL, N. N. & KORSMEYER, S. J. 2004. Cell death: critical control points. *Cell,* 116**,** 205-19.

DAUGAS, E., NOCHY, D., RAVAGNAN, L., LOEFFLER, M., SUSIN, S. A., ZAMZAMI, N. & KROEMER, G. 2000. Apoptosis-inducing factor (AIF): a ubiquitous mitochondrial oxidoreductase involved in apoptosis. *FEBS Lett,* 476**,** 118-23.

DAWSON, V. L. & DAWSON, T. M. 2004. Deadly conversations: nuclear-mitochondrial cross-talk. *J Bioenerg Biomembr,* 36**,** 287-94.

DESAGHER, S. & MARTINOU, J. C. 2000. Mitochondria as the central control point of apoptosis. *Trends Cell Biol,* 10**,** 369-77.

DICK, O. & BADING, H. 2010. Synaptic activity and nuclear calcium signaling protect hippocampal neurons from death signal-associated nuclear translocation of FoxO3a induced by extrasynaptic N-methyl-D-aspartate receptors. *J Biol Chem,* 285**,** 19354-61.

DINGLEDINE, R., BORGES, K., BOWIE, D. & TRAYNELIS, S. F. 1999. The glutamate receptor ion channels. *Pharmacol Rev,* 51**,** 7-61.

DIWAN, A., KRENZ, M., SYED, F. M., WANSAPURA, J., REN, X., KOESTERS, A. G., LI, H., KIRSHENBAUM, L. A., HAHN, H. S., ROBBINS, J., JONES, W. K. & DORN, G. W. 2007. Inhibition of ischemic cardiomyocyte apoptosis through targeted ablation of Bnip3 restrains postinfarction remodeling in mice. *J Clin Invest,* 117**,** 2825-33.

DONATE, L. E. & BLASCO, M. A. 2011. Telomeres in cancer and ageing. *Philos Trans R Soc Lond B Biol Sci,* 366**,** 76-84.

ELSER, M., BORSIG, L., HASSA, P. O., ERENER, S., MESSNER, S., VALOVKA, T., KELLER, S., GASSMANN, M. & HOTTIGER, M. O. 2008. Poly(ADP-ribose) polymerase 1 promotes tumor cell survival by coactivating hypoxia-inducible factor-1-dependent gene expression. *Mol Cancer Res,* 6**,** 282-90.

ENDRES, M., NAMURA, S., SHIMIZU-SASAMATA, M., WAEBER, C., ZHANG, L., GOMEZ-ISLA, T., HYMAN, B. T. & MOSKOWITZ, M. A. 1998. Attenuation of delayed neuronal death after mild focal ischemia in mice by inhibition of the caspase family. *J Cereb Blood Flow Metab,* 18**,** 238-47.

EPE, B., BALLMAIER, D., ROUSSYN, I., BRIVIBA, K. & SIES, H. 1996. DNA damage by peroxynitrite characterized with DNA repair enzymes. *Nucleic Acids Res,* 24**,** 4105-10.

FANG, J. & ALDERMAN, M. H. 2001. Trend of stroke hospitalization, United States, 1988-1997. *Stroke,* 32**,** 2221-6.

GAO, Y., SIGNORE, A. P., YIN, W., CAO, G., YIN, X. M., SUN, F., LUO, Y., GRAHAM, S. H. & CHEN, J. 2005. Neuroprotection against focal ischemic brain injury by inhibition of c-Jun N-terminal kinase and attenuation of the mitochondrial apoptosis-signaling pathway. *J Cereb Blood Flow Metab,* 25**,** 694-712.

GIACCIA, A., SIIM, B. G. & JOHNSON, R. S. 2003. HIF-1 as a target for drug development. *Nat Rev Drug Discov,* 2**,** 803-11.

GIANNAKOU, M. E. & PARTRIDGE, L. 2004. The interaction between FOXO and SIRT1: tipping the balance towards survival. *Trends Cell Biol,* 14**,** 408-12.

GINSBERG, M. D. 2003. Adventures in the pathophysiology of brain ischemia: penumbra, gene expression, neuroprotection: the 2002 Thomas Willis Lecture. *Stroke,* 34**,** 214-23.

GRAHAM, S. H. & CHEN, J. 2001. Programmed cell death in cerebral ischemia. *J Cereb Blood Flow Metab,* 21**,** 99-109.

GREIJER, A. E. & VAN DER WALL, E. 2004. The role of hypoxia inducible factor 1 (HIF-1) in hypoxia induced apoptosis. *J Clin Pathol,* 57**,** 1009-14.

GUARENTE, L. 2000. Sir2 links chromatin silencing, metabolism, and aging. *Genes Dev,* 14**,** 1021-6.

HAGENBUCHNER, J. & AUSSERLECHNER, M. J. 2013. Mitochondria and FOXO3: breath or die. *Front Physiol,* 4**,** 147.

HAMMOND, E. M., DENKO, N. C., DORIE, M. J., ABRAHAM, R. T. & GIACCIA, A. J. 2002. Hypoxia links ATR and p53 through replication arrest. *Mol Cell Biol,* 22**,** 1834-43.

HARA, M. R. & SNYDER, S. H. 2007. Cell signaling and neuronal death. *Annu Rev Pharmacol Toxicol,* 47**,** 117-41.

HARDINGHAM, G. E. & BADING, H. 2003. The Yin and Yang of NMDA receptor signalling. *Trends Neurosci,* 26**,** 81-9.

HARDINGHAM, G. E. & BADING, H. 2010. Synaptic versus extrasynaptic NMDA receptor signalling: implications for neurodegenerative disorders. *Nat Rev Neurosci,* 11**,** 682-96.

HARDINGHAM, G. E., FUKUNAGA, Y. & BADING, H. 2002. Extrasynaptic NMDARs oppose synaptic NMDARs by triggering CREB shut-off and cell death pathways. *Nat Neurosci,* 5**,** 405-14.

HARNEY, S. C., ROWAN, M. & ANWYL, R. 2006. Long-term depression of NMDA receptor-mediated synaptic transmission is dependent on activation of metabotropic glutamate receptors and is altered to long-term potentiation by low intracellular calcium buffering. *J Neurosci,* 26**,** 1128-32.

HARTLERODE, A. J. & SCULLY, R. 2009. Mechanisms of double-strand break repair in somatic mammalian cells. *Biochem J,* 423**,** 157-68.

HATFIELD, K. J., BEDRINGSAAS, S. L., RYNINGEN, A., GJERTSEN, B. T. & BRUSERUD, O. 2010. Hypoxia increases HIF-1alpha expression and constitutive cytokine release by primary human acute myeloid leukaemia cells. *Eur Cytokine Netw,* 21**,** 154-64.

HEALE, J. T., BALL, A. R., JR., SCHMIESING, J. A., KIM, J. S., KONG, X., ZHOU, S., HUDSON, D. F., EARNSHAW, W. C. & YOKOMORI, K. 2006. Condensin I interacts

with the PARP-1-XRCC1 complex and functions in DNA single-strand break repair. *Mol Cell,* 21**,** 837-48.

HEDIGER, M. A., CLEMENCON, B., BURRIER, R. E. & BRUFORD, E. A. 2013. The ABCs of membrane transporters in health and disease (SLC series): introduction. *Mol Aspects Med,* 34**,** 95-107.

HOLROYD-LEDUC, J. M., KAPRAL, M. K., AUSTIN, P. C. & TU, J. V. 2000. Sex differences and similarities in the management and outcome of stroke patients. *Stroke,* 31**,** 1833-7.

HONG, S. J., DAWSON, T. M. & DAWSON, V. L. 2004. Nuclear and mitochondrial conversations in cell death: PARP-1 and AIF signaling. *Trends Pharmacol Sci,* 25**,** 259-64.

HONG SJ, D. T., DAWSON VL 2000. PARP and the Release of Apoptosis-Inducing Factor from Mitochondria. Austin (TX).

HSU, C. P., OKA, S., SHAO, D., HARIHARAN, N. & SADOSHIMA, J. 2009. Nicotinamide phosphoribosyltransferase regulates cell survival through NAD+ synthesis in cardiac myocytes. *Circ Res,* 105**,** 481-91.

HURN, P. D. & MACRAE, I. M. 2000. Estrogen as a neuroprotectant in stroke. *J Cereb Blood Flow Metab,* 20**,** 631-52.

IINO, M., OZAWA, S. & TSUZUKI, K. 1990. Permeation of calcium through excitatory amino acid receptor channels in cultured rat hippocampal neurones. *J Physiol,* 424**,** 151-65.

JIANG, S., YUAN, H., DUAN, L., CAO, R., GAO, B., XIONG, Y. F. & RAO, Z. R. 2011. Glutamate release through connexin 43 by cultured astrocytes in a stimulated hypertonicity model. *Brain Res,* 1392**,** 8-15.

JONAS, P., RACCA, C., SAKMANN, B., SEEBURG, P. H. & MONYER, H. 1994. Differences in Ca2+ permeability of AMPA-type glutamate receptor channels in neocortical neurons caused by differential GluR-B subunit expression. *Neuron,* 12**,** 1281-9.

JONES, J. M., DATTA, P., SRINIVASULA, S. M., JI, W., GUPTA, S., ZHANG, Z., DAVIES, E., HAJNOCZKY, G., SAUNDERS, T. L., VAN KEUREN, M. L., FERNANDES-ALNEMRI, T., MEISLER, M. H. & ALNEMRI, E. S. 2003. Loss of Omi mitochondrial protease activity causes the neuromuscular disorder of mnd2 mutant mice. *Nature,* 425**,** 721-7.

JORGENSEN, M. B. & DIEMER, N. H. 1982. Selective neuron loss after cerebral ischemia in the rat: possible role of transmitter glutamate. *Acta Neurol Scand,* 66**,** 536-46.

JUEDES, M. J. & WOGAN, G. N. 1996. Peroxynitrite-induced mutation spectra of pSP189 following replication in bacteria and in human cells. *Mutat Res,* 349**,** 51-61.

K ZITO, V. S. 2009. NMDA Receptor Function and Physiological Modulation.

KANAI, M., TONG, W. M., SUGIHARA, E., WANG, Z. Q., FUKASAWA, K. & MIWA, M. 2003. Involvement of poly(ADP-Ribose) polymerase 1 and poly(ADP-Ribosyl)ation in regulation of centrosome function. *Mol Cell Biol,* 23**,** 2451-62.

KAWAMATA, H. & MANFREDI, G. 2010. Mitochondrial dysfunction and intracellular calcium dysregulation in ALS. *Mech Ageing Dev,* 131**,** 517-26.

KEMP, J. A. & MCKERNAN, R. M. 2002. NMDA receptor pathways as drug targets. *Nat Neurosci,* 5 Suppl**,** 1039-42.

KICKHOEFER, V. A., SIVA, A. C., KEDERSHA, N. L., INMAN, E. M., RULAND, C., STREULI, M. & ROME, L. H. 1999. The 193-kD vault protein, VPARP, is a novel poly(ADP-ribose) polymerase. *J Cell Biol,* 146**,** 917-28.

KIM, D. Y., KIM, S. H., CHOI, H. B., MIN, C. & GWAG, B. J. 2001. High abundance of GluR1 mRNA and reduced Q/R editing of GluR2 mRNA in individual NADPH-diaphorase neurons. *Mol Cell Neurosci,* 17**,** 1025-33.

KIM, M. Y., ZHANG, T. & KRAUS, W. L. 2005. Poly(ADP-ribosyl)ation by PARP-1: 'PAR-laying' NAD+ into a nuclear signal. *Genes Dev,* 19**,** 1951-67.

KLAIDMAN, L., MORALES, M., KEM, S., YANG, J., CHANG, M. L. & ADAMS, J. D., JR. 2003. Nicotinamide offers multiple protective mechanisms in stroke as a precursor for NAD+, as a PARP inhibitor and by partial restoration of mitochondrial function. *Pharmacology,* 69**,** 150-7.

KLEINE, H., POREBA, E., LESNIEWICZ, K., HASSA, P. O., HOTTIGER, M. O., LITCHFIELD, D. W., SHILTON, B. H. & LUSCHER, B. 2008. Substrate-assisted catalysis by PARP10 limits its activity to mono-ADP-ribosylation. *Mol Cell,* 32**,** 57-69.

KOH, D. W., DAWSON, T. M. & DAWSON, V. L. 2005. Mediation of cell death by poly(ADP-ribose) polymerase-1. *Pharmacol Res,* 52**,** 5-14.

KOTECHA, S. A., JACKSON, M. F., AL-MAHROUKI, A., RODER, J. C., ORSER, B. A. & MACDONALD, J. F. 2003. Co-stimulation of mGluR5 and N-methyl-D-aspartate receptors is required for potentiation of excitatory synaptic transmission in hippocampal neurons. *J Biol Chem,* 278**,** 27742-9.

KRISHNAKUMAR, R. & KRAUS, W. L. 2010. The PARP side of the nucleus: molecular actions, physiological outcomes, and clinical targets. *Mol Cell,* 39**,** 8-24.

KWAG, J. & PAULSEN, O. 2012. Gating of NMDA receptor-mediated hippocampal spike timing-dependent potentiation by mGluR5. *Neuropharmacology,* 63**,** 701-9.

LAEMMLE, A., LECHLEITER, A., ROH, V., SCHWARZ, C., PORTMANN, S., FURER, C., KEOGH, A., TSCHAN, M. P., CANDINAS, D., VORBURGER, S. A. & STROKA, D. 2012. Inhibition of SIRT1 impairs the accumulation and transcriptional activity of HIF-1alpha protein under hypoxic conditions. *PLoS One,* 7**,** e33433.

LAU, A. & TYMIANSKI, M. 2010. Glutamate receptors, neurotoxicity and neurodegeneration. *Pflugers Arch,* 460**,** 525-42.

LAU, D. & BADING, H. 2009. Synaptic activity-mediated suppression of p53 and induction of nuclear calcium-regulated neuroprotective genes promote survival through inhibition of mitochondrial permeability transition. *J Neurosci,* 29**,** 4420-9.

LEE, B. I., LEE, D. J., CHO, K. J. & KIM, G. W. 2005a. Early nuclear translocation of endonuclease G and subsequent DNA fragmentation after transient focal cerebral ischemia in mice. *Neurosci Lett,* 386**,** 23-7.

LEE, D. H., KANG, D. W., AHN, J. S., CHOI, C. G., KIM, S. J. & SUH, D. C. 2005b. Imaging of the ischemic penumbra in acute stroke. *Korean J Radiol,* 6**,** 64-74.

LEVEILLE, F., PAPADIA, S., FRICKER, M., BELL, K. F., SORIANO, F. X., MARTEL, M. A., PUDDIFOOT, C., HABEL, M., WYLLIE, D. J., IKONOMIDOU, C., TOLKOVSKY, A. M. & HARDINGHAM, G. E. 2010. Suppression of the intrinsic apoptosis pathway by synaptic activity. *J Neurosci,* 30**,** 2623-35.

LEVINE, B. & KROEMER, G. 2008. Autophagy in the pathogenesis of disease. *Cell,* 132**,** 27-42.

LI, L. L., GINET, V., LIU, X., VERGUN, O., TUITTILA, M., MATHIEU, M., BONNY, C., PUYAL, J., TRUTTMANN, A. C. & COURTNEY, M. J. 2013. The nNOS-p38MAPK pathway is mediated by NOS1AP during neuronal death. *J Neurosci,* 33**,** 8185-201.

LI, L. Y., LUO, X. & WANG, X. 2001. Endonuclease G is an apoptotic DNase when released from mitochondria. *Nature,* 412**,** 95-9.

LIM, J. H., LEE, Y. M., CHUN, Y. S., CHEN, J., KIM, J. E. & PARK, J. W. 2010. Sirtuin 1 modulates cellular responses to hypoxia by deacetylating hypoxia-inducible factor 1alpha. *Mol Cell,* 38**,** 864-78.

LIPTON, S. A. & KATER, S. B. 1989. Neurotransmitter regulation of neuronal outgrowth, plasticity and survival. *Trends Neurosci,* 12**,** 265-70.

LISMAN, J. 1989. A mechanism for the Hebb and the anti-Hebb processes underlying learning and memory. *Proc Natl Acad Sci U S A,* 86**,** 9574-8.

LIU, Y., WONG, T. P., AARTS, M., ROOYAKKERS, A., LIU, L., LAI, T. W., WU, D. C., LU, J., TYMIANSKI, M., CRAIG, A. M. & WANG, Y. T. 2007. NMDA receptor subunits have differential roles in mediating excitotoxic neuronal death both in vitro and in vivo. *J Neurosci,* 27**,** 2846-57.

LO, E. H., DALKARA, T. & MOSKOWITZ, M. A. 2003. Mechanisms, challenges and opportunities in stroke. *Nat Rev Neurosci,* 4**,** 399-415.

LU, P., KAMBOJ, A., GIBSON, S. B. & ANDERSON, C. M. 2014. Poly(ADP-ribose) polymerase-1 causes mitochondrial damage and neuron death mediated by Bnip3. *J Neurosci,* 34**,** 15975-87.

LUCAS, D. R. & NEWHOUSE, J. P. 1957. The toxic effect of sodium L-glutamate on the inner layers of the retina. *AMA Arch Ophthalmol,* 58**,** 193-201.

LUNA, A., ALADJEM, M. I. & KOHN, K. W. 2013. SIRT1/PARP1 crosstalk: connecting DNA damage and metabolism. *Genome Integr,* 4**,** 6.

MA, J., ENDRES, M. & MOSKOWITZ, M. A. 1998. Synergistic effects of caspase inhibitors and MK-801 in brain injury after transient focal cerebral ischaemia in mice. *Br J Pharmacol,* 124**,** 756-62.

MAMMUCARI, C., MILAN, G., ROMANELLO, V., MASIERO, E., RUDOLF, R., DEL PICCOLO, P., BURDEN, S. J., DI LISI, R., SANDRI, C., ZHAO, J., GOLDBERG, A. L., SCHIAFFINO, S. & SANDRI, M. 2007. FoxO3 controls autophagy in skeletal muscle in vivo. *Cell Metab,* 6**,** 458-71.

MANWANI, B. & MCCULLOUGH, L. D. 2011. Sexual dimorphism in ischemic stroke: lessons from the laboratory. *Womens Health (Lond Engl),* 7**,** 319-39.

MAREN, S., TOCCO, G., STANDLEY, S., BAUDRY, M. & THOMPSON, R. F. 1993. Postsynaptic factors in the expression of long-term potentiation (LTP): increased glutamate receptor binding following LTP induction in vivo. *Proc Natl Acad Sci U S A,* 90**,** 9654-8.

MARK, L. P., PROST, R. W., ULMER, J. L., SMITH, M. M., DANIELS, D. L., STROTTMANN, J. M., BROWN, W. D. & HACEIN-BEY, L. 2001. Pictorial review of glutamate excitotoxicity: fundamental concepts for neuroimaging. *AJNR Am J Neuroradiol,* 22**,** 1813-24.

MARTEL, M. A., WYLLIE, D. J. & HARDINGHAM, G. E. 2009. In developing hippocampal neurons, NR2B-containing N-methyl-D-aspartate receptors (NMDARs) can mediate signaling to neuronal survival and synaptic potentiation, as well as neuronal death. *Neuroscience,* 158**,** 334-43.

MARTIN, H. G. & WANG, Y. T. 2010. Blocking the deadly effects of the NMDA receptor in stroke. *Cell,* 140**,** 174-6.

MARTIN, S. J., GRIMWOOD, P. D. & MORRIS, R. G. 2000. Synaptic plasticity and memory: an evaluation of the hypothesis. *Annu Rev Neurosci*, 23**,** 649-711.

MARTINEZ-ROMERO, R., CANUELO, A., MARTINEZ-LARA, E., JAVIER OLIVER, F., CARDENAS, S. & SILES, E. 2009. Poly(ADP-ribose) polymerase-1 modulation of in vivo response of brain hypoxia-inducible factor-1 to hypoxia/reoxygenation is mediated by nitric oxide and factor inhibiting HIF. *J Neurochem,* 111**,** 150-9.

MARTINEZ-ROMERO, R., CANUELO, A., SILES, E., OLIVER, F. J. & MARTINEZ-LARA, E. 2012. Nitric oxide modulates hypoxia-inducible factor-1 and poly(ADP-ribose) polymerase-1 cross talk in response to hypobaric hypoxia. *J Appl Physiol (1985),* 112**,** 816-23.

MARTINS, L. M., MORRISON, A., KLUPSCH, K., FEDELE, V., MOISOI, N., TEISMANN, P., ABUIN, A., GRAU, E., GEPPERT, M., LIVI, G. P., CREASY, C. L., MARTIN, A., HARGREAVES, I., HEALES, S. J., OKADA, H., BRANDNER, S., SCHULZ, J. B., MAK, T. & DOWNWARD, J. 2004. Neuroprotective role of the Reaper-related serine protease HtrA2/Omi revealed by targeted deletion in mice. *Mol Cell Biol,* 24**,** 9848-62.

MATTSON, M. P. & CHAN, S. L. 2003. Calcium orchestrates apoptosis. *Nat Cell Biol,* 5**,** 1041-3.

MAYER, M. L. 2005. Crystal structures of the GluR5 and GluR6 ligand binding cores: molecular mechanisms underlying kainate receptor selectivity. *Neuron,* 45**,** 539-52.

MCINTOSH, J. 2016. *Stroke: Causes, Symptoms, Diagnosis and Treatment* [Online]. MediLexicon International Ltd, Bexhill-on-Sea, UK. Available: http://www.medicalnewstoday.com/articles/7624.php 2016].

MICHAN, S. & SINCLAIR, D. 2007. Sirtuins in mammals: insights into their biological function. *Biochem J,* 404**,** 1-13.

MICHISHITA, E., PARK, J. Y., BURNESKIS, J. M., BARRETT, J. C. & HORIKAWA, I. 2005. Evolutionarily conserved and nonconserved cellular localizations and functions of human SIRT proteins. *Mol Biol Cell,* 16**,** 4623-35.

MONYER, H., BURNASHEV, N., LAURIE, D. J., SAKMANN, B. & SEEBURG, P. H. 1994. Developmental and regional expression in the rat brain and functional properties of four NMDA receptors. *Neuron,* 12**,** 529-40.

MOUBARAK, R. S., YUSTE, V. J., ARTUS, C., BOUHARROUR, A., GREER, P. A., MENISSIER-DE MURCIA, J. & SUSIN, S. A. 2007. Sequential activation of poly(ADP-ribose) polymerase 1, calpains, and Bax is essential in apoptosis-inducing factor-mediated programmed necrosis. *Mol Cell Biol,* 27**,** 4844-62.

MOUW, G., ZECHEL, J. L., ZHOU, Y., LUST, W. D., SELMAN, W. R. & RATCHESON, R. A. 2002. Caspase-9 inhibition after focal cerebral ischemia improves outcome following reversible focal ischemia. *Metab Brain Dis,* 17**,** 143-51.

MUIR, K. W., BUCHAN, A., VON KUMMER, R., ROTHER, J. & BARON, J. C. 2006. Imaging of acute stroke. *Lancet Neurol,* 5**,** 755-68.

MUNOZ-GAMEZ, J. A., RODRIGUEZ-VARGAS, J. M., QUILES-PEREZ, R., AGUILAR-QUESADA, R., MARTIN-OLIVA, D., DE MURCIA, G., MENISSIER DE MURCIA, J., ALMENDROS, A., RUIZ DE ALMODOVAR, M. & OLIVER, F. J. 2009. PARP-1 is involved in autophagy induced by DNA damage. *Autophagy,* 5**,** 61-74.

MUZ, B., KHAN, M. N., KIRIAKIDIS, S. & PALEOLOG, E. M. 2009. Hypoxia. The role of hypoxia and HIF-dependent signalling events in rheumatoid arthritis. *Arthritis Res Ther,* 11**,** 201.

NAGAHIRO, S., UNO, M., SATO, K., GOTO, S., MORIOKA, M. & USHIO, Y. 1998. Pathophysiology and treatment of cerebral ischemia. *J Med Invest,* 45**,** 57-70.

NAKAMURA, M., BHATNAGAR, A. & SADOSHIMA, J. 2012. Overview of pyridine nucleotides review series. *Circ Res,* 111**,** 604-10.

NEUGEBAUER, V. 2001. Metabotropic glutamate receptors: novel targets for pain relief. *Expert Rev Neurother,* 1**,** 207-24.

NIKOLETOPOULOU, V., MARKAKI, M., PALIKARAS, K. & TAVERNARAKIS, N. 2013. Crosstalk between apoptosis, necrosis and autophagy. *Biochim Biophys Acta,* 1833**,** 3448-59.

OKADA, H., SUH, W. K., JIN, J., WOO, M., DU, C., ELIA, A., DUNCAN, G. S., WAKEHAM, A., ITIE, A., LOWE, S. W., WANG, X. & MAK, T. W. 2002. Generation and characterization of Smac/DIABLO-deficient mice. *Mol Cell Biol,* 22**,** 3509-17.

OLNEY, J. W. 1969. Brain lesions, obesity, and other disturbances in mice treated with monosodium glutamate. *science,* 164**,** 719-721.

OLNEY, J. W., RHEE, V. & HO, O. L. 1974. Kainic acid: a powerful neurotoxic analogue of glutamate. *Brain Res,* 77**,** 507-12.

ORELLANA, J. A., SAEZ, P. J., SHOJI, K. F., SCHALPER, K. A., PALACIOS-PRADO, N., VELARDE, V., GIAUME, C., BENNETT, M. V. & SAEZ, J. C. 2009. Modulation of brain hemichannels and gap junction channels by pro-inflammatory agents and their possible role in neurodegeneration. *Antioxid Redox Signal,* 11**,** 369-99.

OZAWA, S., KAMIYA, H. & TSUZUKI, K. 1998. Glutamate receptors in the mammalian central nervous system. *Prog Neurobiol,* 54**,** 581-618.

PACHER, P., BECKMAN, J. S. & LIAUDET, L. 2007. Nitric oxide and peroxynitrite in health and disease. *Physiol Rev,* 87**,** 315-424.

PACHER, P. & SZABO, C. 2008. Role of the peroxynitrite-poly(ADP-ribose) polymerase pathway in human disease. *Am J Pathol,* 173**,** 2-13.

PALMER, M. J., TASCHENBERGER, H., HULL, C., TREMERE, L. & VON GERSDORFF, H. 2003. Synaptic activation of presynaptic glutamate transporter currents in nerve terminals. *J Neurosci,* 23**,** 4831-41.

PENNINGER, J. M. & KROEMER, G. 2003. Mitochondria, AIF and caspases--rivaling for cell death execution. *Nat Cell Biol,* 5**,** 97-9.

PERALTA-LEAL, A., RODRIGUEZ-VARGAS, J. M., AGUILAR-QUESADA, R., RODRIGUEZ, M. I., LINARES, J. L., DE ALMODOVAR, M. R. & OLIVER, F. J. 2009. PARP inhibitors: new partners in the therapy of cancer and inflammatory diseases. *Free Radic Biol Med,* 47**,** 13-26.

PERSKY, R. W., TURTZO, L. C. & MCCULLOUGH, L. D. 2010. Stroke in women: disparities and outcomes. *Curr Cardiol Rep,* 12**,** 6-13.

PIVOVAROVA, N. B., NGUYEN, H. V., WINTERS, C. A., BRANTNER, C. A., SMITH, C. L. & ANDREWS, S. B. 2004. Excitotoxic calcium overload in a subpopulation of mitochondria triggers delayed death in hippocampal neurons. *J Neurosci,* 24**,** 5611-22.

POIRIER, G. G., DE MURCIA, G., JONGSTRA-BILEN, J., NIEDERGANG, C. & MANDEL, P. 1982. Poly(ADP-ribosyl)ation of polynucleosomes causes relaxation of chromatin structure. *Proc Natl Acad Sci U S A,* 79**,** 3423-7.

RAMEAU, G. A., CHIU, L. Y. & ZIFF, E. B. 2003. NMDA receptor regulation of nNOS phosphorylation and induction of neuron death. *Neurobiol Aging,* 24**,** 1123-33.

RAVI, R., MOOKERJEE, B., BHUJWALLA, Z. M., SUTTER, C. H., ARTEMOV, D., ZENG, Q., DILLEHAY, L. E., MADAN, A., SEMENZA, G. L. & BEDI, A. 2000. Regulation of

tumor angiogenesis by p53-induced degradation of hypoxia-inducible factor 1alpha. *Genes Dev,* 14**,** 34-44.

REGULA, K. M., ENS, K. & KIRSHENBAUM, L. A. 2002. Inducible expression of BNIP3 provokes mitochondrial defects and hypoxia-mediated cell death of ventricular myocytes. *Circ Res,* 91**,** 226-31.

REUBOLD, T. F., WOHLGEMUTH, S. & ESCHENBURG, S. 2011. Crystal structure of full-length Apaf-1: how the death signal is relayed in the mitochondrial pathway of apoptosis. *Structure,* 19**,** 1074-83.

RIZZUTO, R. & POZZAN, T. 2006. Microdomains of intracellular Ca2+: molecular determinants and functional consequences. *Physiol Rev,* 86**,** 369-408.

ROMAN, R., BARTKOWSKI, H. & SIMON, R. 1989. The specific NMDA receptor antagonist AP-7 attenuates focal ischemic brain injury. *Neurosci Lett,* 104**,** 19-24.

ROTHWELL, P. M. 2001. The high cost of not funding stroke research: a comparison with heart disease and cancer. *Lancet,* 357**,** 1612-6.

ROULEAU, M., PATEL, A., HENDZEL, M. J., KAUFMANN, S. H. & POIRIER, G. G. 2010. PARP inhibition: PARP1 and beyond. *Nat Rev Cancer,* 10**,** 293-301.

SABIROV, R. Z. & OKADA, Y. 2009. The maxi-anion channel: a classical channel playing novel roles through an unidentified molecular entity. *J Physiol Sci,* 59**,** 3-21.

SANES, J. R. & LICHTMAN, J. W. 1999. Can molecules explain long-term potentiation? *Nat Neurosci,* 2**,** 597-604.

SATTLER, R. & TYMIANSKI, M. 2000. Molecular mechanisms of calcium-dependent excitotoxicity. *J Mol Med (Berl),* 78**,** 3-13.

SAXENA, A., SAFFERY, R., WONG, L. H., KALITSIS, P. & CHOO, K. H. 2002a. Centromere proteins Cenpa, Cenpb, and Bub3 interact with poly(ADP-ribose) polymerase-1 protein and are poly(ADP-ribosyl)ated. *J Biol Chem,* 277**,** 26921-6.

SAXENA, A., WONG, L. H., KALITSIS, P., EARLE, E., SHAFFER, L. G. & CHOO, K. H. 2002b. Poly(ADP-ribose) polymerase 2 localizes to mammalian active centromeres and interacts with PARP-1, Cenpa, Cenpb and Bub3, but not Cenpc. *Hum Mol Genet,* 11**,** 2319-29.

SCHREIBER, V., DANTZER, F., AME, J. C. & DE MURCIA, G. 2006. Poly(ADP-ribose): novel functions for an old molecule. *Nat Rev Mol Cell Biol,* 7**,** 517-28.

SCHULTZ, N., LOPEZ, E., SALEH-GOHARI, N. & HELLEDAY, T. 2003. Poly(ADP-ribose) polymerase (PARP-1) has a controlling role in homologous recombination. *Nucleic Acids Res,* 31**,** 4959-64.

SEMENZA, G. L. 1999. Regulation of mammalian O2 homeostasis by hypoxia-inducible factor 1. *Annu Rev Cell Dev Biol,* 15**,** 551-78.

SERMEUS, A. & MICHIELS, C. 2011. Reciprocal influence of the p53 and the hypoxic pathways. *Cell Death Dis,* 2**,** e164.

SHENG, M. 2001. The postsynaptic NMDA-receptor--PSD-95 signaling complex in excitatory synapses of the brain. *J Cell Sci,* 114**,** 1251.

SHIBATA, A. & JEGGO, P. A. 2014. DNA double-strand break repair in a cellular context. *Clin Oncol (R Coll Radiol),* 26**,** 243-9.

SIEGEL, C., TURTZO, C. & MCCULLOUGH, L. D. 2010. Sex differences in cerebral ischemia: possible molecular mechanisms. *J Neurosci Res,* 88**,** 2765-74.

SIEGEL, C. S. & MCCULLOUGH, L. D. 2013. NAD+ and nicotinamide: sex differences in cerebral ischemia. *Neuroscience,* 237**,** 223-31.

SIMPKINS, J. W., RAJAKUMAR, G., ZHANG, Y. Q., SIMPKINS, C. E., GREENWALD, D., YU, C. J., BODOR, N. & DAY, A. L. 1997. Estrogens may reduce mortality and ischemic damage caused by middle cerebral artery occlusion in the female rat. *J Neurosurg,* 87**,** 724-30.

SIMS, J. L., BERGER, S. J. & BERGER, N. A. 1983. Poly(ADP-ribose) Polymerase inhibitors preserve nicotinamide adenine dinucleotide and adenosine 5'-triphosphate pools in DNA-damaged cells: mechanism of stimulation of unscheduled DNA synthesis. *Biochemistry,* 22**,** 5188-94.

SIMS, N. R. & MUYDERMAN, H. 2010. Mitochondria, oxidative metabolism and cell death in stroke. *Biochim Biophys Acta,* 1802**,** 80-91.

SKAPER, S. D. 2003. Poly(ADP-Ribose) polymerase-1 in acute neuronal death and inflammation: a strategy for neuroprotection. *Ann N Y Acad Sci,* 993**,** 217-28; discussion 287-8.

SMITH, S. 2001. The world according to PARP. *Trends Biochem Sci,* 26**,** 174-9.

SMITH, S., GIRIAT, I., SCHMITT, A. & DE LANGE, T. 1998. Tankyrase, a poly(ADP-ribose) polymerase at human telomeres. *Science,* 282**,** 1484-7.

STEIGERWALD, F., SCHULZ, T. W., SCHENKER, L. T., KENNEDY, M. B., SEEBURG, P. H. & KOHR, G. 2000. C-Terminal truncation of NR2A subunits impairs synaptic but not extrasynaptic localization of NMDA receptors. *J Neurosci,* 20**,** 4573-81.

STEINBERG, G. K., KUNIS, D., DELAPAZ, R. & POLJAK, A. 1993. Neuroprotection following focal cerebral ischaemia with the NMDA antagonist dextromethorphan, has a favourable dose response profile. *Neurol Res,* 15**,** 174-80.

STEINBERG, G. K., SALEH, J., DELAPAZ, R., KUNIS, D. & ZARNEGAR, S. R. 1989. Pretreatment with the NMDA antagonist dextrorphan reduces cerebral injury following transient focal ischemia in rabbits. *Brain Res,* 497**,** 382-6.

STROKA, D. M., BURKHARDT, T., DESBAILLETS, I., WENGER, R. H., NEIL, D. A., BAUER, C., GASSMANN, M. & CANDINAS, D. 2001. HIF-1 is expressed in normoxic tissue and displays an organ-specific regulation under systemic hypoxia. *FASEB J,* 15**,** 2445-53.

SUGIMURA, K., TAKEBAYASHI, S., TAGUCHI, H., TAKEDA, S. & OKUMURA, K. 2008. PARP-1 ensures regulation of replication fork progression by homologous recombination on damaged DNA. *J Cell Biol,* 183**,** 1203-12.

SUSIN, S. A., LORENZO, H. K., ZAMZAMI, N., MARZO, I., SNOW, B. E., BROTHERS, G. M., MANGION, J., JACOTOT, E., COSTANTINI, P., LOEFFLER, M., LAROCHETTE, N., GOODLETT, D. R., AEBERSOLD, R., SIDEROVSKI, D. P., PENNINGER, J. M. & KROEMER, G. 1999. Molecular characterization of mitochondrial apoptosis-inducing factor. *Nature,* 397**,** 441-6.

SUWANWELA, N. & KOROSHETZ, W. J. 2007. Acute ischemic stroke: overview of recent therapeutic developments. *Annu Rev Med,* 58**,** 89-106.

TALLIS, M., MORRA, R., BARKAUSKAITE, E. & AHEL, I. 2014. Poly(ADP-ribosyl)ation in regulation of chromatin structure and the DNA damage response. *Chromosoma,* 123**,** 79-90.

THAYER, S. A. & WANG, G. J. 1995. Glutamate-induced calcium loads: effects on energy metabolism and neuronal viability. *Clin Exp Pharmacol Physiol,* 22**,** 303-4.

TRAN, H., BRUNET, A., GRENIER, J. M., DATTA, S. R., FORNACE, A. J., JR., DISTEFANO, P. S., CHIANG, L. W. & GREENBERG, M. E. 2002. DNA repair pathway stimulated by the forkhead transcription factor FOXO3a through the Gadd45 protein. *Science,* 296**,** 530-4.

TU, J. C., XIAO, B., NAISBITT, S., YUAN, J. P., PETRALIA, R. S., BRAKEMAN, P., DOAN, A., AAKALU, V. K., LANAHAN, A. A., SHENG, M. & WORLEY, P. F. 1999. Coupling of mGluR/Homer and PSD-95 complexes by the Shank family of postsynaptic density proteins. *Neuron,* 23**,** 583-92.

TU, W., XU, X., PENG, L., ZHONG, X., ZHANG, W., SOUNDARAPANDIAN, M. M., BALEL, C., WANG, M., JIA, N., ZHANG, W., LEW, F., CHAN, S. L., CHEN, Y. & LU, Y. 2010. DAPK1 interaction with NMDA receptor NR2B subunits mediates brain damage in stroke. *Cell,* 140**,** 222-34.

TYMIANSKI, M., CHARLTON, M. P., CARLEN, P. L. & TATOR, C. H. 1993. Source specificity of early calcium neurotoxicity in cultured embryonic spinal neurons. *J Neurosci,* 13**,** 2085-104.

VANDE VELDE, C., CIZEAU, J., DUBIK, D., ALIMONTI, J., BROWN, T., ISRAELS, S., HAKEM, R. & GREENBERG, A. H. 2000. BNIP3 and genetic control of necrosis-like cell death through the mitochondrial permeability transition pore. *Mol Cell Biol,* 20**,** 5454-68.

VIRAG, L., ROBASZKIEWICZ, A., RODRIGUEZ-VARGAS, J. M. & OLIVER, F. J. 2013. Poly(ADP-ribose) signaling in cell death. *Mol Aspects Med,* 34**,** 1153-67.

VIRAG, L., SALZMAN, A. L. & SZABO, C. 1998. Poly(ADP-ribose) synthetase activation mediates mitochondrial injury during oxidant-induced cell death. *J Immunol,* 161**,** 3753-9.

WALLS, K. C., GHOSH, A. P., BALLESTAS, M. E., KLOCKE, B. J. & ROTH, K. A. 2009. bcl-2/Adenovirus E1B 19-kd interacting protein 3 (BNIP3) regulates hypoxia-induced neural precursor cell death. *J Neuropathol Exp Neurol,* 68**,** 1326-38.

WANG, G. J. & THAYER, S. A. 1996. Sequestration of glutamate-induced Ca2+ loads by mitochondria in cultured rat hippocampal neurons. *J Neurophysiol,* 76**,** 1611-21.

WANG, Y., DAWSON, V. L. & DAWSON, T. M. 2009. Poly(ADP-ribose) signals to mitochondrial AIF: a key event in parthanatos. *Exp Neurol,* 218**,** 193-202.

WARR, O., TAKAHASHI, M. & ATTWELL, D. 1999. Modulation of extracellular glutamate concentration in rat brain slices by cystine-glutamate exchange. *J Physiol,* 514 (Pt 3)**,** 783-93.

WONG, H. K., LIU, X. B., MATOS, M. F., CHAN, S. F., PEREZ-OTANO, I., BOYSEN, M., CUI, J., NAKANISHI, N., TRIMMER, J. S., JONES, E. G., LIPTON, S. A. & SUCHER, N. J. 2002. Temporal and regional expression of NMDA receptor subunit NR3A in the mammalian brain. *J Comp Neurol,* 450**,** 303-17.

XU, J., KURUP, P., ZHANG, Y., GOEBEL-GOODY, S. M., WU, P. H., HAWASLI, A. H., BAUM, M. L., BIBB, J. A. & LOMBROSO, P. J. 2009. Extrasynaptic NMDA receptors couple preferentially to excitotoxicity via calpain-mediated cleavage of STEP. *J Neurosci,* 29**,** 9330-43.

XU, Y., HUANG, S., LIU, Z. G. & HAN, J. 2006. Poly(ADP-ribose) polymerase-1 signaling to mitochondria in necrotic cell death requires RIP1/TRAF2-mediated JNK1 activation. *J Biol Chem,* 281**,** 8788-95.

YELAMOS, J., FARRES, J., LLACUNA, L., AMPURDANES, C. & MARTIN-CABALLERO, J. 2011. PARP-1 and PARP-2: New players in tumour development. *Am J Cancer Res,* 1**,** 328-346.

YING, W. 2007. NAD+ and NADH in brain functions, brain diseases and brain aging. *Front Biosci,* 12**,** 1863-88.

YING, W., ALANO, C. C., GARNIER, P. & SWANSON, R. A. 2005. NAD+ as a metabolic link between DNA damage and cell death. *J Neurosci Res,* 79**,** 216-23.

YING, W., GARNIER, P. & SWANSON, R. A. 2003. NAD+ repletion prevents PARP-1-induced glycolytic blockade and cell death in cultured mouse astrocytes. *Biochem Biophys Res Commun,* 308**,** 809-13.

YING, W., WEI, G., WANG, D., WANG, Q., TANG, X., SHI, J., ZHANG, P. & LU, H. 2007. Intranasal administration with NAD+ profoundly decreases brain injury in a rat model of transient focal ischemia. *Front Biosci,* 12**,** 2728-34.

YU, S. W., ANDRABI, S. A., WANG, H., KIM, N. S., POIRIER, G. G., DAWSON, T. M. & DAWSON, V. L. 2006. Apoptosis-inducing factor mediates poly(ADP-ribose) (PAR) polymer-induced cell death. *Proc Natl Acad Sci U S A,* 103**,** 18314-9.

YU, S. W., WANG, H., DAWSON, T. M. & DAWSON, V. L. 2003. Poly(ADP-ribose) polymerase-1 and apoptosis inducing factor in neurotoxicity. *Neurobiol Dis,* 14**,** 303-17.

YU, S. W., WANG, H., POITRAS, M. F., COOMBS, C., BOWERS, W. J., FEDEROFF, H. J., POIRIER, G. G., DAWSON, T. M. & DAWSON, V. L. 2002. Mediation of poly(ADP-ribose) polymerase-1-dependent cell death by apoptosis-inducing factor. *Science,* 297**,** 259-63.

YUAN, J., LIPINSKI, M. & DEGTEREV, A. 2003. Diversity in the mechanisms of neuronal cell death. *Neuron,* 40**,** 401-13.

ZARDO, G., REALE, A., PASSANANTI, C., PRADHAN, S., BUONTEMPO, S., DE MATTEIS, G., ADAMS, R. L. & CAIAFA, P. 2002. Inhibition of poly(ADP-

ribosyl)ation induces DNA hypermethylation: a possible molecular mechanism. *FASEB J,* 16**,** 1319-21.

ZHANG, J., DAWSON, V. L., DAWSON, T. M. & SNYDER, S. H. 1994. Nitric oxide activation of poly(ADP-ribose) synthetase in neurotoxicity. *Science,* 263**,** 687-9.

ZHANG, J., YE, J., ALTAFAJ, A., CARDONA, M., BAHI, N., LLOVERA, M., CANAS, X., COOK, S. A., COMELLA, J. X. & SANCHIS, D. 2011a. EndoG links Bnip3-induced mitochondrial damage and caspase-independent DNA fragmentation in ischemic cardiomyocytes. *PLoS One,* 6**,** e17998.

ZHANG, S. J., STEIJAERT, M. N., LAU, D., SCHUTZ, G., DELUCINGE-VIVIER, C., DESCOMBES, P. & BADING, H. 2007a. Decoding NMDA receptor signaling: identification of genomic programs specifying neuronal survival and death. *Neuron,* 53**,** 549-62.

ZHANG, S. J., ZOU, M., LU, L., LAU, D., DITZEL, D. A., DELUCINGE-VIVIER, C., ASO, Y., DESCOMBES, P. & BADING, H. 2009. Nuclear calcium signaling controls expression of a large gene pool: identification of a gene program for acquired neuroprotection induced by synaptic activity. *PLoS Genet,* 5**,** e1000604.

ZHANG, Z., SHI, R., WENG, J., XU, X., LI, X. M., GAO, T. M. & KONG, J. 2011b. The proapoptotic member of the Bcl-2 family Bcl-2 / E1B-19K-interacting protein 3 is a mediator of caspase-independent neuronal death in excitotoxicity. *FEBS J,* 278**,** 134-42.

ZHANG, Z., YANG, X., ZHANG, S., MA, X. & KONG, J. 2007b. BNIP3 upregulation and EndoG translocation in delayed neuronal death in stroke and in hypoxia. *Stroke,* 38**,** 1606-13.

ZHAO, S. T., CHEN, M., LI, S. J., ZHANG, M. H., LI, B. X., DAS, M., BEAN, J. C., KONG, J. M., ZHU, X. H. & GAO, T. M. 2009. Mitochondrial BNIP3 upregulation precedes

endonuclease G translocation in hippocampal neuronal death following oxygen-glucose deprivation. *BMC Neurosci,* 10**,** 113.

ZHARKOV, D. O. 2008. Base excision DNA repair. *Cell Mol Life Sci,* 65**,** 1544-65.

ZINGARELLI, B., O'CONNOR, M., WONG, H., SALZMAN, A. L. & SZABO, C. 1996. Peroxynitrite-mediated DNA strand breakage activates poly-adenosine diphosphate ribosyl synthetase and causes cellular energy depletion in macrophages stimulated with bacterial lipopolysaccharide. *J Immunol,* 156**,** 350-8.

ZONG, W. X., DITSWORTH, D., BAUER, D. E., WANG, Z. Q. & THOMPSON, C. B. 2004. Alkylating DNA damage stimulates a regulated form of necrotic cell death. *Genes Dev,* 18**,** 1272-82.